The molecular mechanism of mitotic telomere deprotection

Diana Romero Zamora

The molecular mechanism of mitotic telomere deprotection

By

Diana Romero Zamora

A dissertation submitted in partial fulfillment of the

requirements for the degree of

Doctor of Philosophy

in

Life Sciences

in the Graduate School of Biostudies

of

Kyoto University

July 2023

Abstract

Telomeres, crucial for genome stability, form a protective T-loop structure. However, during prolonged mitotic arrest, the T-loop can dissolve, leading to mitotic telomere deprotection and cell death. This process mediated by Aurora B kinase serves as an anti-tumor mechanism, eliminating precancerous cells. However, the underlying Aurora B-dependent mechanism of mitotic telomere deprotection remains elusive. Here, an overexpression screening of the RecQ helicase family identified WRN and BLM as suppressor and driver of mitotic telomere deprotection, respectively. WRN was found to suppress mitotic telomere deprotection independently of its enzymatic activities. A specific region within WRN N-terminus, encompassing amino acids 168-333 with a coiled-coil motif, was sufficient for this suppression. The suppressive effect relied on protein levels of TRF2, a T-loop stabilizing protein, indicating mutual dependence between these proteins. Putative Aurora B phosphorylation sites, particularly S282, regulate suppressive activity in WRN. Concurrently, BLM in collaboration with Top3A-RMI1/2 (BTR complex) promotes telomere deprotection during mitotic arrest through interaction with TRF1. Aurora B was found to phosphorylate TRF1 at the T358 site, promoting the recruitment of the components of the Chromosomal Passenger Complex (CPC). These interactions supported mitotic telomere deprotection, especially when TRF1 delocalized from telomeres, potentially transporting complexes along the chromosome axis. In addition, an *in vitro* assay revealed that Aurora B phosphorylates TRF2 at S65 within the basic domain, facilitating the linearization of mitotic chromosome ends through the BTR complex. The roles of WRN and BLM in suppressing and promoting T-loop dissolution, respectively, shed light on the complex interplay between various proteins and phosphorylation events involved in this process. This study represents an important step towards unraveling the intricate mechanisms governing mitotic telomere deprotection.

I dedicate this work to my past self, to the little one that dreamed for studying life and meeting adventures in foreign lands. You did not how resilient and capable you were until now. To my future self reading these lines, remember this journey of knowledge, follow your instincts, refuse to settle for less, do not stay in conformity and above all, continue harvesting passions regardless of the time or obstacles.

Acknowledgement I

This thesis is based on the materials contained in the following scholarly paper:

Romero-Zamora, Diana, and Makoto T. Hayashi. “A Non-Catalytic N-Terminus Domain of WRN Prevents Mitotic Telomere Deprotection.” *Scientific Reports* 13, no. 1 (January 12, 2023): 645.

All of the figures and tables, including the respective legends, were modified from this paper.

Acknowledgement II

In 2009, in a cafe, I heard for the first time about a DNA sequence that shortens with age. With that simple piece of information, I became fascinated and decided to study telomeres. This decision turned into a dream and then into a path full of discoveries, obstacles, lessons, a pandemic, and new passions. But I haven't walked this path alone, and I want to acknowledge the value of each person who has been a fundamental part of this process.

First and foremost, I want to thank my advisor, Makoto Hayashi. There are not enough words to express my gratitude for all his help, support, and immense patience throughout these years of preparation. Truth be told, I feel incredibly fortunate to have been under his guidance, as I learned to do science in a different way and he helped me expand my mind in general.

I want to thank my main collaborators, Tony, Sam, and Ronnie. With them, I had the opportunity to learn how to collaborate remotely and to approach science in a different way. I greatly appreciate the time they dedicated to the project with so much enthusiasm that was truly contagious.

I also want to thank my family, starting with my mother Guillermina, who always cared for me and welcomed me with a warm hug every time I visited my hometown. To my father Ignacio, I am grateful for all his support and for doing everything possible to see each other despite the distance. To my brother Nahúm, for taking care of me, listening to me, and lifting my spirits. I thank Miau, whom I loved dearly, for sitting by my side in the afternoons while I studied my papers. Visiting her and sharing a lot of love helped me recharge my energy to keep fighting for my goals.

To my dear Haru, I am grateful for all the love and support that helped me through the toughest parts of my doctoral journey and helped me grow as a person. There is still much to learn, but I hope we continue doing it together.

I express my deepest gratitude to my dear friend Rodrigo. I never imagined that sharing the bench would bring me the best friend in the world. The experiments, the walks, the summers, and the frolicsome moments are cherished in my heart.

I thank my friend Oliver for being around during my journey with his unconditional friendship. His empathy and care lightened my days.

I was fortunate to meet my friend Andrea, to whom I am grateful for her excellent work in the lab and for being a friend who listens and encourages me.

To Pedro, I thank him for all these years where we shared the ups and downs of our scientific paths.

I value the time and hugs from my friends in Mexico. From a distance, I felt a lot of support and affection that I truly needed. I thank those who crossed paths with me at some point during my journey. I carry the teachings of those who are no longer here, and from a distance, I will be wishing them the best in life.

To my Kendo coach, Monica sensei, and the members of the dojo, I thank them for believing in me during the scholarship process and for teaching me to pursue my dreams despite the obstacles.

Lastly, I am grateful to my professors at UAM Iztapalapa for teaching me so many things. They laid the foundations of my knowledge that I applied in my doctoral studies. My professors have been my great role models, and now it's my turn to share my knowledge as they did.

List of Abbreviations

53BP1 p53-Binding Protein 1

ALT Alternative Lengthening of Telomeres

ATM Ataxia Telangiectasia Mutated

ATP Adenosine triphosphate

ATR Ataxia Telangiectasia and Rad3-Related

AURKB Aurora kinase B

BLM Bloom

bp base pair

BSA Bovine serum albumin

CPC Chromosomal passenger complex

ddH_2O Double-destilled H_2O (water)

D-loop Displacement loop

DDR DNA damage response

dHJ Double Holliday Junction

DNA Deoxyribonucleic acid

DNA-PK DNA-Dependent Protein Kinase

DSB Double-strand break

dsDNA Double-Stranded DNA

HJ Holliday Junction

HR Homologous Recombination

HRDC Helicase and RNaseD C-terminal domain

hTERT Human Telomerase Reverse Transcriptase

INCENP Inner centromere protein

kb kilobase

kD kilodalton

MAD-TIF Mitotic arrest-dependent TIF

MEL Murine erythroleukemia

meta-TIF Telomere dysfunction-induced foci in metaphase

MPS1 Monopolar Spindle 1

MRN Mre11-Rad50-Nbs1 Complex

MYB Myeloblastosis viral oncogene homolog

NHEJ Non-homologous end joining

p53 protein 53

PAGE Polyacrylamide Gel Electrophoresis

PCR Polymerase Chain Reaction

POT1 Protection of Telomeres 1

PTMs Post-Translational Modifications

RAP1 Repressor and activator protein 1

Rb Retinoblastoma protein

RNA Ribonucleic acid

ROS Reactive oxygen species

RPA Replication Protein A

RQC RecQ C-terminal

SAC Spindle assembly checkpoint

SCEs Sister Chromatid Exchanges

SDS Sodium Dodecyl Sulfate

shRNA short hairpin RNA

ssDNA Single-Stranded DNA

T-loop Telomere loop

TIF Telomere dysfunction-induced foci

TIN2 TRF1-interacting nuclear factor

TPP1 POT1-and TIN2-interacting protein

TRF1 Telomere Repeat binding Factor 1

TRF2 Telomere Repeat binding Factor 2

TRFH Telomeric repeat-binding factor homology

TSS Threonine-Serine-Serine

WRN Werner

WS Werner Syndrome

γ-H2AX Phosphorylation of histone H2AX **(**gamma-H2AX)

Table of contents

List of figures and tables

Chapter 1

Chapter 3

Chapter 4

Chapter 1

Introduction

1.1 Telomere function

Telomeres are double stranded DNA repeats in tandem located at the chromosome termini. These sequences are found as 5'-TTAGGG-3' repeats in humans (Moyzis et al., 1988), and play a crucial role in protecting the end of linear chromosomes from genomic instability by preventing the recognition of the end on linear chromosomes as sites of DNA damage. Telomeres are highly conserved across eukaryotic species with differences in sequence and length. For instance, the telomeres of *Tetrahymena and S. cerevisae* are typically 250-350 base pairs long (Blackburn and Chiou, 1981), while human telomeres can reach up to 15 kb in length (Ozturk et al., 2014). Despite their non-coding nature, the evolutionary conservation of telomeric sequences across living organisms highlights their crucial role in maintaining chromosome stability.

Telomeres function as protective caps, preventing degradation, abnormal recombination, and fusion of chromosomes. They also serve as a molecular clock, determining the lifespan of cells and directing them towards replicative senescence or apoptosis (Rodier et al., 2005; Pearce et al., 2022). The gradual shortening of telomeres can contribute to genomic instability and, when coupled with other oncogenic alterations, may potentially trigger the initiation of cancer.

1.2 Telomere structure and shortening

Telomere length and maintenance are gradually affected in each round of cell division. During DNA replication, RNA primers align to the TTAGGG (G-rich) strand and DNA polymerase synthesizes the new strand in fragments whereas primers are removed. However, removal of the last primer at the telomeric 3' end leaves a gap failing to be filled with nucleotides. This results in an incomplete synthesis and produces a G-rich single-stranded DNA overhang. This event is known as the end-replication problem (Watson, 1972; Olovnikov, 1973), which results in a G-rich single stranded DNA (ssDNA) known as G-tail or G-overhang (Makarov et al, 1997). Meanwhile, the CCCTAA (C-rich) strand is continuously replicated but further processed by nucleases resulting in a longer G-overhang (Sampathi and Chai, 2011). This G-overhang produces an invasion into adjacent telomeric double-stranded DNA (dsDNA) repeats creating a displacement loop (D-loop), which forms the telomere loop (T-loop) structure (de Lange, 2004; Griffith et al., 1999) (**Figure 1.1A**).

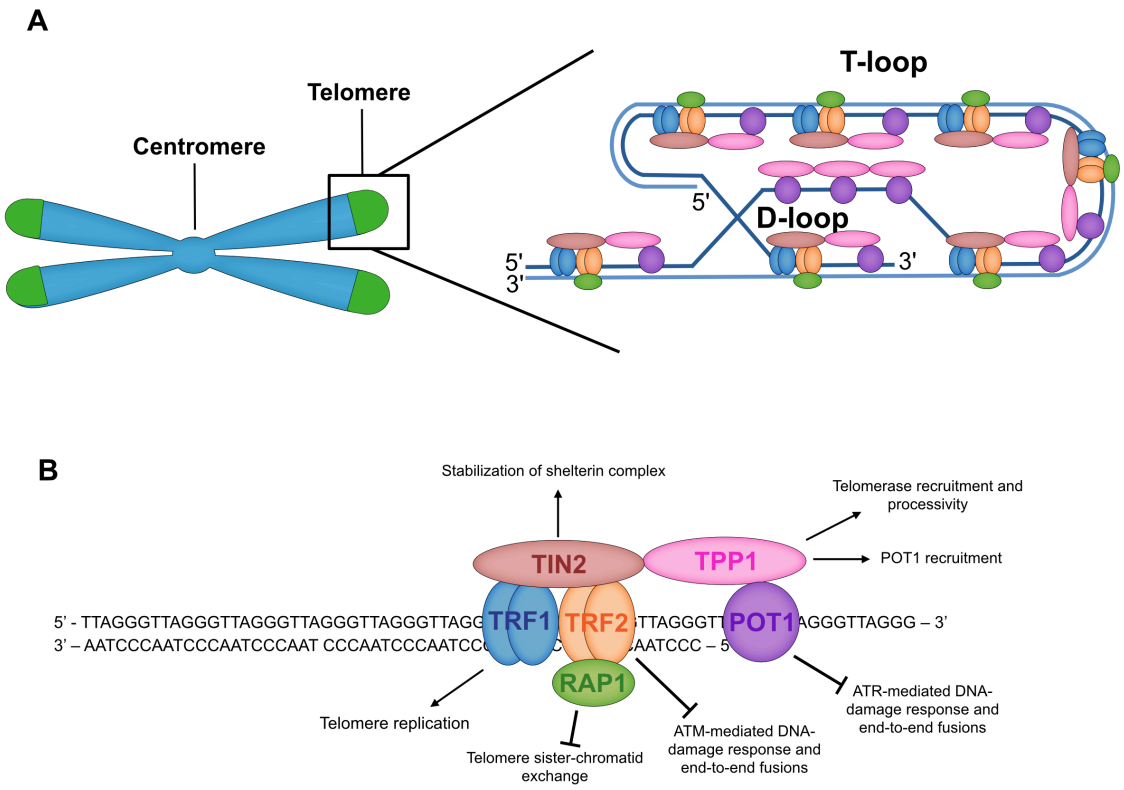

Figure 1.1 Schematic model of telomere structure and shelterin complex.

A) Telomeres are located at the end of the chromosomes serving as capping of repetitive DNA sequences (TTAGGG)n. Telomeres fold back its double stranded DNA by the invasion of the free 3' single-stranded DNA (G-overhang) producing a Displacing loon (D-loop) which is required for completing the formation of the telomere loop (T-loop). **B)** The shelterin complex, conformed by six specific proteins, assembles along the telomere region. Each protein has a characteristic role for telomere maintenance, stabilization and protection (Figure modified from Xu et al., 2013).

Critically shortened telomeres lack of T-loop structure exposing the telomeric DNA as sites of double strand breaks, which results in the activation of the DNA damage response (DDR) factors, such as ataxia telangiectasia mutated protein (ATM) (Reaper et al., 2004). DDR triggers cell cycle arrest allowing time for DNA repair in a p53-dependent manner. Upon DDR activation, DNA repair factors from the Nonhomologous End Joining (NHEJ) repair pathway promote the ligation of lineal telomeres (Doksani and de Lange, 2014). As

a consequence, the fused chromosomes become a challenge for the proper chromosome segregation leading to future genomic aberrations. In the evolutionarily view, T-loop structure is the result of a strategy of the primitive lineal DNA to avoid recircularization of the genome promoted by ligation (Tomaska et al., 2019). Therefore, the T-loop structure is indispensable for the proper functioning of telomeres, as it plays a crucial role in preventing genomic instability and inhibiting unnecessary activation of the DDR pathway.

1.3 Shelterin complex

Telomeres and the protective T-loop caps are stabilized by a complex of six telomere-associated proteins known as the "shelterin complex", consisting of telomeric repeat-binding factor 1 (TRF1), telomeric repeat-binding factor 2 (TRF2), repressor and activator protein 1 (RAP1), TRF1- interacting nuclear protein 2 (TIN2), POT1-and TIN2-interacting protein (TPP1) and protection of telomeres 1 (POT1) (Palm and de Lange, 2008) (**Figure 1.1B**).

The proteins comprising the shelterin complex exhibit direct or indirect biding to telomeres. Specifically, TRF1 and TRF2 directly bind to the double-stranded telomeric repeats, both contributing to telomere protection and regulation. POT1 binds to the single-stranded G-overhang and prevents it from being recognized as DNA damage. Although these proteins are not likely to interact directly, TIN2 acts a bridging protein, linking TRF1 and TRF2, and facilitating the recruitment of TPP1 and POT1, thus stabilizing the complex (Xu et al., 2013). Additionally, RAP1 is recruited to telomeres through direct binding to TRF2, and its function is found to regulate telomere length (Li et al., 2000). Dysfunction in any of the shelterin complex members can lead to several outcomes, such as progressive telomere shortening or failure to maintain T-loop structure (Liu et al., 2019; Bahr et al., 2021).

Super-resolution microscopy has revealed that T-loop formation requires TRF2 to stimulate the 3' telomeric end invasion to the duplex, and stabilize the resulting D-loop structure through its N-terminal basic domain (Doksani et al., 2013; Necasová et al., 2017). Therefore, TRF2 subunit is considered a repressor of the DDR activation by avoiding the exposure of telomere strands (Karlseder et al., 1999). It is estimated that TRF2 can wrap approximately 90 bp of telomeric DNA around its TRF homology (TRFH) domain, which main function is TRF2 dimerization (Benarroch-Popivker et al., 2016). Furthermore, TRFH domain enables TRF2 binding to Holliday Junction (HJs) substrates. This interaction

promotes the condensation of these DNA substrates and effectively protects them from enzymatic cleavage (Nora et al., 2010; Schmutz et al., 2017). The unique property of the TRF2 basic domain, which modifies DNA topology through the aforementioned reactions, could potentially explain its role in stimulating telomere DNA folding. Although both TRF1 and TRF2 share a TRFH domain with similar homology, TRF1 demonstrates less efficient invasion of the telomeric end due to the acidic nature of its N-terminus (Poulet et al., 2012). However, the TRFH domain in TRF1 is essential for regulating protein-protein interactions with the shelterin complex, ensuring proper maintenance of telomeres (Okamoto et al., 2009).

The essential functions of TRF1 and TRF2 in telomeres rely on their MYB domain, which is responsible for recognizing and binding to the double-stranded DNA of telomeric repeats (Broccoli et al., 1997). Deletion of the MYB domain in TRF1 leads to the development of fragile telomeres due to replication problems, whereas absence of MYB domain in TRF2 results in a failure to repress DNA repair pathways, such as NHEJ and Homologous Recombination (HR) (Mao et al., 2007; Yang et al., 2022). These features highlight the crucial role of TRF1 and TRF2 proteins as key components in the maintenance and functionality of telomeres.

1.4 Telomere capping and activation of the DNA damage response

As previously mentioned, the shelterin complex is essential for telomere capping to avoid the activation of the DDR and the subsequent occurrence of detrimental events that can compromise genomic stability. The formation of T-loop, facilitated by the activity of TRF2, leads to a "closed state" of the telomere able to suppress undesired DDR activation and DSB repair (Doksani and de Lange, 2014). However, the loss of T-loop can occur due to various factors, such as a partial depletion of TRF2, which produces an "intermediate-state" (**Figure 1.2**). In this state, telomeres become deprotected and cells become susceptible to DDR activation during G1/S phase. Nevertheless, the activation of DNA damage repair pathways (e.g. NHEJ), is inhibited if cells retain sufficient levels of TRF2 bound to the telomeres (Cesare et al., 2013). Complete removal of TRF2 from telomeres results in the "uncapped-state" of telomeres, causing chromosome end-to-end fusions (Cesare and Karlseder, 2012). Additionally, excessive telomere shortening caused by the end replication problem can further contribute to the uncapped state of telomeres (**Figure**

1.2). Short telomeres retain insufficient levels of TRF2 resulting in chromosome fusion (Bailey and Murnane, 2006). The fused chromosomes subsequently form anaphase bridges of chromatin that are to breakage, resulting in large-scale genomic rearrangements.

Upon telomere deprotection, the activation of the Ataxia Telangiectasia Mutated kinase (ATM), a DDR factor, initiates a series of phosphorylation events and translocation of DNA damage substrates near the exposed telomeric strands (Takai et al., 2003). These dynamic processes occurring at the chromosome termini offer a cytological mean to visualize and detect the loss of T-loops. Specifically, the presence of colocalizations between telomeric DNA or protein DDR factors, such as phosphorylated histone H2AX (γ-H2AX) and p53-Binding Protein 1 (53BP1), serves as a distinct marker (Takai et al., 2003). These regions are referred to as telomere dysfunction-induced foci (TIF) and are highly associated with replicative senescence, which imposes a limit on the number of cell divisions (Takai et al., 2003; Fagagna et al., 2003). TIFs that originate in interphase are unable to recover the capping state and persist into mitosis. The signal from interphase TIFs becomes prominently visible on prometaphase and/or metaphase chromosomes, referred as meta-TIFs. The quantification of these telomeric foci is assessed through a meta-TIF analysis, which also helps to determine the specific position of TIFs on individual chromosome (Cesare et al., 2009).

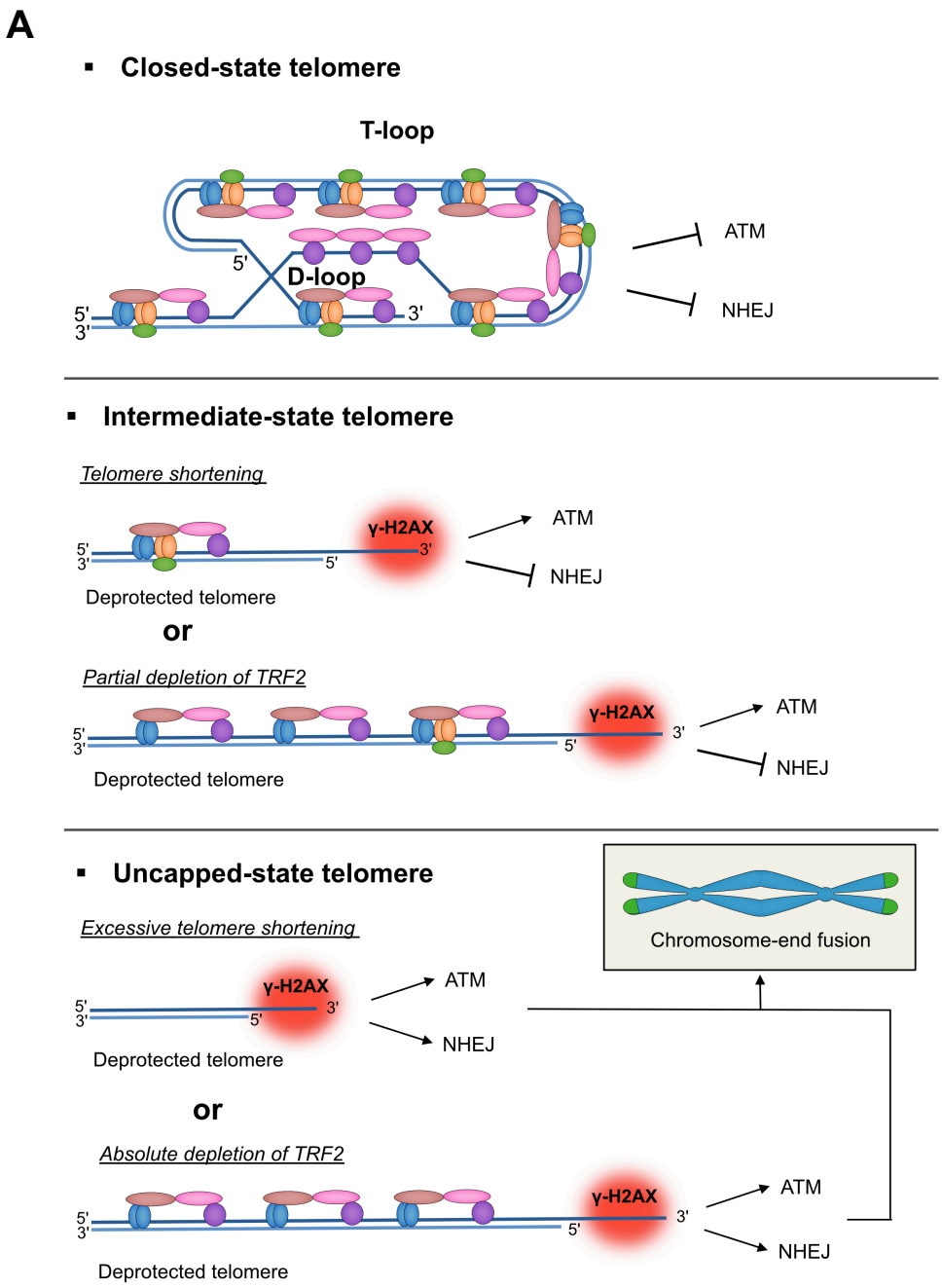

Figure 1.2 Graphical representation of the three-state of the telomere model.

A) The closed-state telomere consists of T-loop which suppresses the activation of DDR factors. Failure to maintain T-loop structure produce an Intermediate-state telomere due to telomere shortening that activates ATM. Presence of sufficient levels of TRF2 at short and long telomeres prevents chromosome fusions caused by an active c-NHEJ pathway. Uncapped-state telomeres result from either excessive telomere shortening lacking of

binding sites for TRF2, or from absolute depletion of TRF2. Maintenance of T-loop and TRF2 levels is essential for telomere protection (Figure modified from Cesare and Karlseder, 2012).

1.5 Spontaneous telomere deprotection drives replicative senescence

The protective T-loop structure is gradually lost as telomeres undergo erosion due to the end-replication problem, a consequence of repeated cell divisions in human somatic cells. Telomere shortening is a problem that can be countered by the expression of the telomerase telomerase ribonucleoprotein. The telomerase reverse transcriptase (TERT, or hTERT in humans) is the catalytic subunit of the telomerase enzyme that promotes the elongation of telomeres by adding TTAGGG sequences to the 3' end of the chromosome termini (Greider and Blackburn, 1975; Weinrich et al., 1997). While telomerase activity is typically suppressed in most somatic cells, it is active in cells with a high proliferation rate, such as stem cells and cancer cells (Daniel et al., 2012). However, mutations in the TERT promoter, which is responsible for regulating the expression of the telomerase gene, can lead to an increase in telomerase expression. This abnormal upregulation of telomerase enables cells with accumulated mutations to maintain unlimited viability, contributing to the development of tumorigenesis (Liu et al., 2016).

Before healthy cells acquire malignant features such as telomere elongation, cells undergo a long process involving several round of divisions that gradually affects the length and configuration of telomeres. The erosion of telomeres with each cell division sets a limit on the number of times that cells divide during their lifespan. Researchers Hayflick and Moorhead discovered that cells in culture undergo 40 to 60 population doublings before entering a state of cell growth arrest known as replicative senescence but referred as mortality stage 1 (M1) (Hayflick and Moorhead, 1961; Hayflick, 1965). This process also known as the "Hayflick effect", which is considered a major contributor to replicative aging, with telomere length playing a critical role in limiting cell division (Wright and Shay, 1992). Cells with critical short telomeres undergo the activation of the tumor suppressor proteins p53 transcription factor and retinoblastoma protein (Rb) that induces cell cycle arrest or apoptosis (Sherr and McCormick, 2002). This state of irreversible growth arrest is referred as "senescence" characterized of impaired cell functions that promote age-related pathologies and the progressive decline of tissue and organ function. Senescent cells

remain viable and metabolically active, but with impaired tissue repair and regeneration capabilities (van Deursen, 2014; Kwon et al., 2019). However, a fraction of senescent cells bypass the cell cycle arrest and resume proliferation (**Figure 1.3**).

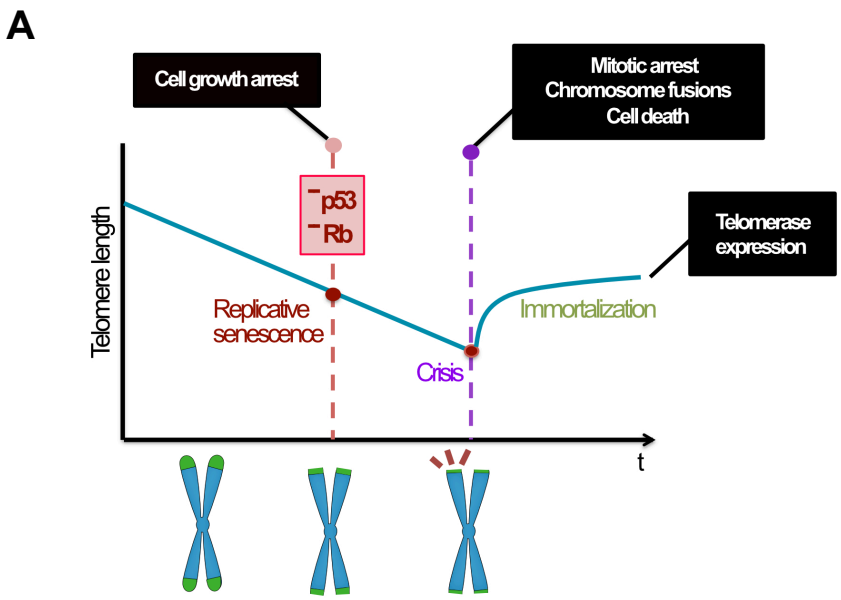

Figure 1.3 Association of telomere length in carcinogenesis.

A) Telomere shortening leads to two main barriers that control proliferation of cells harboring genomic instability to become precancerous. Replicative senescence results from short telomeres that promote irreversible cell growth arrest. Cells bypass senescence in the absence of cell cycle checkpoints (p53 or Rb), and continue proliferating until crisis. Chromosomes with short telomeres in crisis, caused by progressive telomere erosion, experience catastrophic events (e.g. chromosome end fusions), but also mitotic arrest and a consequent massive cell death. However, cell survivors to crisis are immortalized by reactivation of telomerase enzyme which ensures telomere length upon accelerated proliferationion (Wright and Shay, 1992).

Continued cell division results in a progressive erosion of telomeres reaching a length of 2-3 kb long (Capper et al., 2007). At this stage, telomeres become too short to retain shelterin proteins, resulting in structural problems and catastrophic events, including chromosome fusions and extensive cell death. This stage of reduced cell proliferation is known as crisis (M2) (Shay et al., 1991). The mechanism of cell death in crisis is not fully

understood, but recent studies observed that crisis cells undergo an arrest in mitosis, resulting in telomere deprotection and subsequent cell death (Hayashi et al., 2012; Hayashi et al., 2015) (**Figure 1.3)**. Another study suggests that autophagy, mediated by the cGAS-STING pathway, plays a role in the cell death of crisis cells in response to uncapped telomeres (Nassour et al., 2019; Nassour et al., 2023). The death observed during crisis acts as a tumor-suppressive barrier, facilitating the elimination of a significant population of dysfunctional senescent cells that have accumulated gross chromosomal aberrations by this point. Eventually, rare cells manage to escape from DNA instability and death during crisis, leading to the emergence of immortalized cells that acquire the ability to reactivate telomerase for telomere length maintenance, a characteristic from cancer cells. Growing evidence has led to the identification of senescence and crisis processes to be associated with different degrees of telomere deprotection that contributes to the elimination of precancerous cells within the population (Hayashi et al., 2015; Masamsetti et al., 2019; Nassour et al., 2019). However, more studies are needed to elucidate the molecular mechanisms underlying these processes and gain a deeper understanding of carcinogenesis.

1.6 Mitotic telomere deprotection

Telomere deprotection is a process that not only occurs in interphase, but also manifests when cells are unable to progress from metaphase to the next stage of cell division. This mitotic arrest, when prolonged, results in the dissolution of the T-loop structure giving origin to a phenomenon known as mitotic telomere deprotection. Mitotic arrest provides a cascade of events in the cell affecting mitochondria, chromosomal integrity, centrosome, microtubules and telomeres (Lai et al., 2011; Orth et al., 2012; Hayashi et al., 2012; Traversi et al., 2019). Several common factors, such as chromosome segregation errors or DNA replication stress, can induce mitotic arrest in the cells. However, telomere problems are also able to promote an arrest in mitosis. As previously mentioned, crisis cells harboring short telomeres experience chromosome fusions that triggers a DNA damage response, causing cell cycle arrest in mitosis and the loss of telomere caps through an unknown mechanism (Hayashi et al., 2012). Moreover, mitotic arrest can be induced in cell culture by microtubule inhibitors (e.g. colcemid, taxol or nocodazole) which maintains cells in metaphase by preventing spindle formation (Jha et., 1994; ref.). Under this condition, mitotically arrested cells also display the accumulation of deprotected

telomeres despite containing sufficient levels of TRF2 protein (Hayashi et al., 2012).

Since a variety of enzymes are active during mitotic arrest, a screening has been performed by using inhibitors targeting kinases highly required to sustain an arrest in mitosis, such as Aurora A, Aurora B and MPS1. Interestingly, suppression of Aurora B resulted in the absence of meta-TIFs in cells that could be arrested in mitosis by inhibiting the degradation of the anaphase-promoting complex (APC), a process required for mitotic exit (Peters, 2006; Hayashi et al., 2012). This observation suggests that mitotic telomere deprotection requires Aurora B activity in addition to the protective role of TRF2 in T-loops. From this finding, the definition of TIFs has expanded to encompass new concepts distinguishing types of deprotected telomeres: "Interphase-TIFs" for telomeres that lose caps in interphase, likely due to extensive telomere erosion, and mitotic arrest-dependent TIFs or "MAD-TIFs" referring to deprotected telomeres arising exclusively from a prolonged mitotic arrest (Romero-Zamora et al. 2023). Both interphase and MAD-TIFs can be visualized in metaphase spreads and are generally referred to as "meta-TIF" in technical analyses.

1.7 Mitotic checkpoint and its implications

Organisms require cell division to produce genetically identical daughter cells, achieved through genome replication and segregation. Accurate distribution of the replicated genome in mitosis is crucial for generating genetically identical cells, as errors can cause genomic instability and cancer-related abnormalities. Chromosome segregation depends on dynamic connections between chromosomes and spindle microtubules, facilitated by kinetochores, which are large multiprotein complexes assembled on centromeric DNA. To ensure proper chromosome-microtubule attachments, cells employ the Spindle Assembly Checkpoint (SAC) machinery (Lara-Gonzalez et al., 2021). The SAC functions by detecting tension or lack of tension on the kinetochores and subsequently delays the progression from metaphase to anaphase until all kinetochores are correctly attached to the mitotic spindles. In addition to attachment errors, mitotic arrest can also be induced by replication stress occurring in S-phase and persisting until mitotic entry (Masamsetti, et al., 2019). Cell death is the common outcome after a prolonged mitotic arrest enhanced by stressors that arise in perturbed mitosis, such as the accumulation of reactive oxygen species (ROS) and massive mitotic telomere deprotection (Hayashi et al., 2012; Patterson

et al., 2020). Activation of pro-apoptotic signals drives cell death in mitotic arrest, which also occurs in p53-compromised cells (Fragkos and Beard, 2011). In the presence of a weakened mitotic checkpoint, arrested cells commonly undergo mitotic slippage, wherein cells exit mitosis without completing cytokinesis (Brito and Reider; 2006). Consequently, these cells enter interphase with double DNA content and exhibit aberrations. Hence, the spindle checkpoint acts as a surveillance system during mitosis, ensuring the accurate segregation of chromosomes and maintaining genomic integrity.

1.8 CPC complex

The full activation of the SAC triggers a mitotic arrest, providing time for error corrections facilitated by chromosomal passenger complex (CPC), consisting in Aurora B kinase (AURKB), inner centromere protein (INCENP), Survivin (BIRC5) and Borealin (CDCA8) (Carmena et al., 2012). During prometaphase, the CPC concentrates at the inner centromere and ensures proper chromosome alignment by correcting erroneous kinetochore-microtubule attachments. Once mitotic defects are corrected, the CPC promotes the onset of anaphase by inhibiting the activity of SAC responsible for sustaining the mitotic arrest. Phosphorylations on the CPC at centromeres are important as they play a crucial role in regulating its function and activity for correcting mitotic defects (Wang et al, 2011; Tan and Kapoor, 2011). The activation of Aurora B requires direct interaction with the C-terminal region of INCENP, known as the IN-box domain leading to the activation of its kinase activity at low levels. This initial activation enables Aurora B to phosphorylate a Thr-Ser-Ser (TSS) motif located at the C-terminal region of INCENP, as well as Thr232 located in the activation loop of its own kinase domain (Yasui et al., 2004). These phosphorylation events are critical for achieving full activation of Aurora B, which in turn promotes SAC signaling and the production of the mitotic checkpoint complex. In addition, Survivin and Borealin are required to maintain this high kinase activity by binding to the CEN-box of INCENP C-terminus, where both associate with each other through a three-helix bundle (Chen et al. 2003, Jelluma et al., 2018). This bundle is necessary for the CPC to localize correctly at the inner centromere and other regions on the chromosome.

While the CPC is known to localize at inner centromeres, Aurora B is distributed at various locations during distinct mitotic stages. In early prophase, the CPC localizes at chromosomal arms to facilitate sister chromatid resolution (Dai et al., 2006). At anaphase

onset, the CPC translocates to the spindle midzone to regulate the cleavage furrow (Carmena, 2008). Isolation of telomere chromatin from murine erythroleukemia (MEL) cells has identified INCENP, Borealin and Aurora B to associate with the chromosome termini, suggesting their potential regulatory involvement (Ide et al., 2021). Mitotic telomere deprotection is an Aurora B- dependent event that can be inhibited in human cells treated with hesperadin, an ATP-competitive small molecule inhibitor of Aurora B kinase (Hauf S. et al., 2003; Hayashi et al., 2012). Although the functions of Aurora B and the other CPC components in distinct cell compartments have been widely studied, it remains unclear the specific role of Aurora B at telomeres.

Chapter 2

Materials and Methods

2.1 Cell culture

The IMR-90 E6E7 hTERT cell line was produced by infecting normal diploid human fibroblast cells (IMR-90) with a retrovirus carrying HPV16 E6 and E7 oncoproteins (pLXSN3-16E6E7) (Le Poole et al., 1997). These cells were then immortalized by introducing human telomerase (hTERT) expression using a retrovirus carrying wild-type hTert (pWZL-hTERT). The cells were cultured in Dulbecco's Modified Eagle Medium (DMEM) supplemented with 10% fetal bovine serum (FBS) (S1810-500, biowest), 200 mM L-glutamine, 5% NaHCO3, 100 U/mL penicillin, streptomycin, and 5 µg/mL Plasmocin (InvivoGen). Cells were maintained at a temperature of 37°C in 5% CO_2 and 3% O_2. HT1080 cells were culture under same DMEM-FBS media at 37°C in 5% CO_2 and 5% O_2.

2.2 Plasmid construction

Truncation and mutants used in this study were generated by site-directed mutagenesis involving HiFi DNA Assembly (NEB) or DNA synthesis (Integrated NDA Technologies). All cDNAs were cloned in-frame and downstream of puromycin or blasticidin S-resistance gene followed by self-cleaving P2A sequences in a 3rd generation lentiviral plasmid vector. The NLS, FLAG and Myc sequences were inserted between the P2A and peptide sequences by PCR. Complementary DNAs encoding human functional short isoform of TRF2 (XP_005256180.1; missing the first 42 amino acids) (Timashev and de Lange, 2020) and WRN (NP_000544.2) were generously provided by Dr. Jan Karlseder.

Short hairpin RNA against WRN and TRF2 were cloned into pLKO.1 vector by conventional restriction enzyme cloning of annealed oligo nucleotides. The shRNA target sequences were as follows:

Scramble 5’-CCTAAGGTTAAGTCGCCCTCGCTC-3',

WRN 5′-CCTGTTTATGTAGGCAAGATT-3′ (TRCN0000004902)

TRF2 5’-GCGCATGACAATAAGCAGATT-3’ (Cesare et al., 2013)

shRNA-resistant silent mutations were as follows (lower cases are silent mutations):

WRN: 5'-CCa GTa TAc GTt GGg AAa ATc-3'

BLM 5'-c GCt AAc GAt CAa GCc ATt-3'

2.3 Lentivirus production

Lentivirus was produced by following the same protocol for all the constructs in this study. Fresh cultured human embryonic kidney cells (HEK293 FT) were maintained in fully supplemented DMEM medium at 37°C and 5% CO_2. A day before transfection, approximately 500,000 cells were plated in a 10 cm Petri dish. Following 24 hours of incubation, a plasmid mix was prepared by adding 2.6 µg packaging plasmid PCMV, 2.6 µg envelope plasmid PCAG and 4.5 µg target plasmid, and OPTIMEM (Gibco) to complete 400 µl of total volume. After the addition of 1 mg/mL polyethylenimine Max (PEI), the mix was homogenized and and incubated for 30 minutes at room temperature while protecting from light. Afterwards, HEK293 FT cells were transfected by directly adding the mix into the plate and incubated for 24 hours. After the incubation time, the medium was discarded and replaced with fresh DMEM medium. Infectious lentiviral particles were harvested from cell culture 48 and 72 hours post-transfection. For each time point, the virus supernatant was carefully collected and filtered through 0.45 µm filter unit into 10 mL tubes containing polybrane (final 4 µg/mL). The collected lentivirus was aliquoted and stored at -80^{o}C.

2.4 Lentiviral transduction

For the stably expression of target proteins, cells were plated in a 3.5 cm dish and infected with virus supernatant complemented with 8 µg/mL polybrane. After 48 hours of exposure, medium containing virus was discarded and replaced with fresh DMEM containing 10 µg/mL Blasticidin S (Funakoshi) for at least five days. Complete selected cells were either stored at -80^{o}C or kept in culture for downstream experiments. For protein knockdown, cells were infected by following the same method and time points described above However, selection was carried out by using 1 µg/mL puromycin (ChemCruz) for a course of three days before the experimental procedure.

2.5 Cell growth assay

Vector and WT-WRN cells were transduced with an shControl or shWRN by lentiviral infection for 24 hours and subjected to selection with1 µg/mL puromycin for three days.

After the selection period, cells were collected by tripsinization, and 20,000 cells were re-plated in each well of a 24-well plate with 500 µl of fresh medium. Cell viability was measured at day 2 and 4 in culture by counting cells using an automated cell counter (DeNovix CellDrop BF).

2.6 Live-cell imaging

Cells were plated in a 48-well plate 24 hours prior to the initiation of imaging. One hour before imaging, cells were treated with 100 ng/mL colcemid, 500 nM taxol, and 40 nM hesperadin. Time-lapse imaging was conducted using a specialized microscope incubator system (Tokai Hit), which ensured precise control of environmental conditions, including maintenance of cells at a temperature of 37°C and a CO2 concentration of 5%, over a duration of 60 to 72 hours. The BZ-X710 microscope equipped with a 10 × objective lens (Plan Apo 0.45 NA) was employed for observations, with z-stack sections capturing optical sections approximately 0.7 µm in thickness. The determination of mitotic duration and cell fate was performed manually based on cellular morphologies observed from the first frame of mitotic entry (i.e., a sign of nuclear envelope breakdown or cell rounding) until the end of the phase (i.e., a sign of cytokinesis, nuclear blebbing, or cell flattening). The software tools ImageJ and QuickTime Player were utilized for the analysis of movie files.

2.7 Immunofluorescence and telomere FISH on metaphase spreads

IMR-90 E6E7 hTERT cells were cultured into fresh medium and incubated at 37 °C for 24 hours. Then, the cells were exposed to 100 ng/mL colcemid for either 2 or 24 hours to accumulate mitotic cells. For the experiments involving DNA damage induction, 0.2 µg/mL bleomycin was added 2 hours before the completion of the 24-hour colcemid treatment. The cells were treated with a hypotonic solution (0.2% KCl, 0.2% Tri-sodium citrate) at room temperature for 10 minutes after collection and centrifuged at 12,000 rpm for 3 minutes. The solution was discarded and metaphase chromosome spreads were fixated with 4% formaldehyde solution at room temperature for 10 minutes and rinsed the slides with ddH_2O for 5 times. Next, samples were permeabilized with KCM buffer (120 mM KCl, 20 mM NaCl, 10 mM Tris pH 7.5, 0.1% Triton-100X) at room temperature for 10 minutes, and blocked in ABDIL buffer (150 mM NaCl, 20 mM Tris pH 7.4, 0.1% Triton X-100, 2% BSA, 0.2% Fish Gelatin) with 100 µg/mL RNase A at 37 °C for 15 minutes in a wet

chamber. After incubation, primary antibody mouse anti-γ-H2AX p-Ser139 (613,402 Clone 2F3, Biolegend) was added at a dilution of 1:200 in ABDIL buffer and incubation was carried out at room temperature for 1 hour. Slides were washed 3 times for 5 minutes each and then incubated with the secondary antibody Alexa-568-conjugated anti-mouse (A11031, Invitrogen) at a dilution of 1:1,000 in ABDIL at room temperature for 30 minutes. Slides were washed 3 times for 5 minutes each and fixed in 4% formaldehyde at room temperature for 10 minutes. Slides were washed 3 times for 5 minutes and dehydrated with a graded ethanol series [70%, 95%, 100% (vol/vol)]. After air drying the slides, telomere staining was performed by denaturing the slides for 8 minutes at 80°C using the Tel-C FAM-OO-(CCCTTAA)3 PNA probe (Panagene). Following denaturation, hybridization was continued overnight at room temperature in a wet chamber. The slides were washed and dehydrated by the ethanol series [70%, 95%, 100% (vol/vol)] and briefly air-dried before DNA counterstaining and mounting with Vectashield PLUS Antifade medium containing DAPI (H-2000, Vector Laboratories). The images of metaphase spreads were captured using a 100X objective lens (PlanApo/1.45-NA oil) on a BZ-X710 fluorescence microscope (KEYENCE) and analyzed through automated counting using the Hybrid Cell Count and Macro Cell Count software modules (KEYENCE). Outliers in the data sets were excluded from the analysis.

2.8 Cell cycle synchronization

Cell synchronization of cells in mitosis was performed by double-thymidine block. The cells were exposed to a concentration of 2mM thymidine for a duration of 14 hours. Following this incubation period, the cells were subjected to three washes with 1xPBS solution and subsequently cultured in fresh media for an additional 10 hours in fresh media. Subsequently, the cells were treated with a second round of 2 mM thymidine treatment for another 14 hours. After three additional washes with 1xPBS, the cells were released into fresh media, marking the beginning of the experimental timeline (0 hours post-release). After 6 hours of post-release, cells were arrested in mitosis by adding 100 ng/mL colcemid to the culture medium. Mitotic cells were collected by shake-off at 8 and 24 hours post-release (2 and 18 hours colcemid treatment), and used for downstream analysis.

2.9 Western Blot

Cell pellets were washed twice in phosphate buffered saline (PBS), and then incubated in lysis buffer for 1 hour. Lysis buffer consisted of 20 mM Tris-HCl adjusted to pH 8.0, 2.5 mM MgCl2, 150 mM KCl, 0.5% NP40, 1 mM DTT and 0.2 mM PMSF, 1X protease inhibitor (ROCHE) and 1X phosphatase inhibitor (ROCHE). Centrifugation was performed for 10 minutes at 12,000 rpm, and debris was removed. Following isolation of protein, the total protein concentration was measured by spectrometry using a Bio-Rad Protein Assay Dye Reagent (5000006JA, Bio-Rad Laboratories). Approximately 50 µg of cell lysate was loaded into 4–20% Mini-PROTEAN TGX precast gels (Bio-Rad) in Tris-Glycine running buffer followed by electrophoretic separation for 80 minutes hours at 100V. After electrophoresis, proteins were transferred onto a polyvinylidene fluoride (PVDF) membrane (Millipore) with 1x Transfer Buffer (17004274, Bio-Rad), using a Trans-Blot Turbo Transfer System (BioRad). For CBB staining, the gel was incubated for 1 h with CBB Stain One (Nacalai), followed by washes with deionized water. Next, membranes were blocked for 20 minutes at room temperature with Blocking Buffer (Nacalai) with gentle shaking. Membranes were cut to adequate size and primary antibody diluted in the blocking solution was added according to the specified concentrations. Incubation with primary antibody was carried overnight at 4^{o}C with gentle shaking. Membranes were washed 3 times in 1xTris-NaCl-Tween20 (1X TNT) buffer of 5 minutes each with shaking. Secondary antibody was diluted in 1X TNT and incubated the membranes for 1 hour at room temperature according to the indicated dilution. Next, membranes were washed 3 times in 1X TN of 5 minutes each. Antibodies on the membrane were detected by ECL reaction and imaged by LAS-3000 (Fuji). Exposure time and signal intensity were adjusted during image acquisition.

2.10 Antibodies and Concentration for Immunoblotting

Primary antibodies for immunoblotting: rabbit anti-WRN (ab124673, Abcam; 1:500 dilution), mouse anti-FLAG (F1804, Sigma; 1:1000 dilution), mouse anti-GAPDH (MAB374, Millipore; 1:5,000 dilution), RecQ1 (A300-450A-M, Bethyl; 1:1,000 dilution), rabbit anti-RecQ4 (17008-1-AP, ProteinTech; 1:1,000 dilution), mouse anti-RecQ5 (sc-515050, Santa Cruz; 1:1,000 dilution), and rabbit anti-TRF2 (NB110-57130SS, Novus Biologicals; 1:1000 dilution). HRP labeled secondary antibodies: anti-mouse (NA931, GE Healthcare; 1:10,000 dilution) and anti-rabbit (2074, Cell Signaling; 1:10,000 dilution).

2.11 Protein structure prediction and sequence alignment

The protein structure prediction for the $WRN^{168-333}$ fragment was generated by using the ColabFold interface to the AlphaFold 2 pipeline on the Colab platform (AlphaFold2.ipynb) (Jumper et al., 2021; Mirdita et al., 2022). For protein sequence alignment, protein sequences obtained from BLAST were aligned using multiple sequence comparisons by log expectation (MUSCLE) and color-coded using Clustal X in SnapGene software (GSL Biotech) (Myler et al., 2021).

2.12 Statistical analysis

All statistical analyses and graphs were performed using GraphPad Prism software (version 9.0). We did not assume Gaussian distribution and performed two-tailed unpaired non-parametric tests for all quantitative data in this study. Mann–Whitney test was used to compare two samples, while Kruskal–Wallis followed by Dunn's test was used to compare multiple samples. This test was chosen as it assumes equal variances between the two groups. For all the data analyses, a p-value less than 0.05 was considered statistically significant and represented in asterisks (ns: not significant; * $p<0.05$; ** $p<0.01$; *** $p<0.001$; **** $p<0.0001$). The numbers of biological replicates are indicated in the figure legends.

Chapter 3

Screening and identification of RecQ helicases involved in mitotic telomere deprotection.

3.1 Introduction

3.1.1 RecQ helicases: structure and function

RecQ DNA helicases are a conserved protein family that plays a vital role in various DNA processes, such as replication, recombination, and repair. In humans, RecQ family consists of five helicases: RecQ1, BLM, WRN, RecQ4, and RecQ5 (isoforms RecQ5α, RECQ5β) (**Figure 3.1.1A**). This group of helicases is crucial for maintaining genome integrity and stability, considering them to be the "guardians of the genome" (Larsen and Hickson, 2013). Mutations in the genes encoding these enzymes have been linked to several human diseases, including cancer, premature aging syndromes, and chromosomal instability disorders. Therefore, the proper functioning of the RecQ helicases is necessary for removing DNA structures that represent a challenge for the replication of the genome and telomeres.

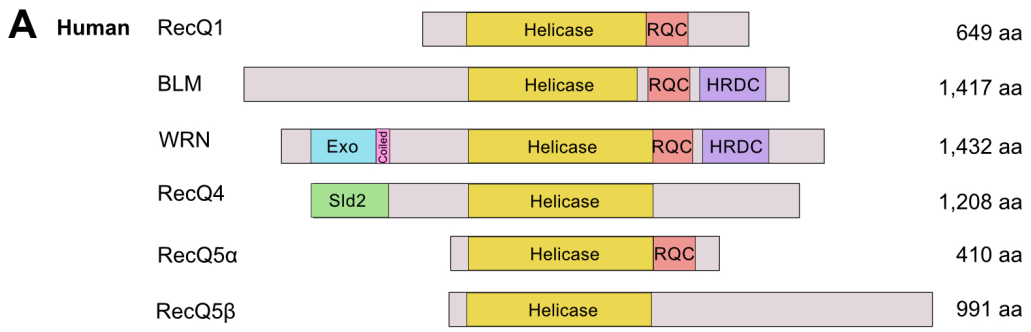

Figure 3.1 Schematic of the RecQ helicase family members.

A) The RecQ helicase family is a group of DNA helicases that play crucial roles in DNA replication, recombination, and repair. This figure illustrates the unique features of each RecQ helicase member: the helicase domain, 3'-5' exonuclease (Exo) domain, multimerization domain (coiled-coil domain), Sld2-like domain, RecQ C-terminal (RQC) domain, and helicase and RNase D C-terminal (HRDC) domain. These domains contribute to the diverse functions of the RecQ helicases, including DNA unwinding, DNA strand annealing, DNA binding, and interactions with other repair proteins.

Most members of the RecQ helicases use energy from ATP hydrolysis to unwind dsDNA in a 3' to 5' directionality (Wu Y., 2012). These helicases share highly conserved domains that enable them to perform enzymatic activities on DNA substrates. The helicase domain is the most conserved elements among all helicase members, whereas the presence of a RecQ C-terminal (RQC) and Helicase and RNase D-like C-terminal (HRDC) domains varies among the helicases (**Figure 3.1.1A**). Additionally, specialized elements, such as the Exonuclease domain in WRN helicase have evolved to confer additional functions for processing specific DNA substrates (Mushegian et al., 1997; Kusano et al., 1999). The helicase domain acts as a DNA translocation module, supporting the primary ATPase activities promoted by the RQC domain, which is responsible for dsDNA binding and unwinding activity (Kitano et al, 2010; Swan et al., 2014). The function of the HRDC domain has been a subject of debate among studies (Newman et al., 2015; Teng et al., 2020). However, crystal structure analyses have identified the HRDC domain in close proximity to the helicase core, suggesting its involvement in ATPase and/or helicase activities (Newman et al., 2015). Furthermore, the HRDC domain exhibits an evolutionary divergence in function among RecQ helicases due to the difference in the surface charges of the protein structure (Kim et al., 2010; Bernstein et al., 2015). In BLM, the HRDC domain plays a critical role in directing DNA strand annealing and the dissolution of double Holliday junctions (dHJ), an activity that cannot be replaced by the HRDC domain of the WRN protein (Wu et al., 2005; Kim et al., 2010). The distinct domain structures and functions of each helicase contribute to their efficiency in unwinding various DNA structures throughout the genome, with a particular emphasis on telomeres. These structures include forked DNA duplexes, D-loops, and G-quadruplexes (Vindigni et al., 2009; Croteau et al., 2014). Cells lacking any of these RecQ proteins display telomere breakage and loss, highlighting their importance in telomere maintenance (Croteau et al., 2014). The interaction of the RecQ helicases with shelterin proteins facilitate their translocation to telomeres and stimulate their helicase activity, leading to an enhanced efficiency to unwind telomere substrates (Opresko et al., 2002; Lillard-Wetherell et al., 2004; Machewe et al., 2004; Ghosh et al., 2012). Moreover, the activity of RecQ helicases is influenced by various factors, including protein-protein interactions, post-translational modifications and oligomeric status (Karmakar et al., 2002; Tripathi et al., 2008; Lu et al., 2017; Croteau et al., 2014). BLM and WRN have been found to form higher order oligomeric states, such as hexamers and tetramers, whereas RecQ1 can be found as

dimers or tetramers (Karow et al., 1999; Lucic et al., 2011). Although oligomerization includes a change of efficiency in DNA-unwinding activities, the monomeric state is sufficient to efficiently unwind DNA, as reported in *in vitro* studies (Muzzolini et al., 2007; Xu et al., 2012).

The key roles of the RecQ helicase members in genome maintenance can confer benefits to cancer cells under conditions of replication stress or DNA damage, promoting the survival and growth of malignant cells. Furthermore, WRN and BLM have shown to be implicated in the alternative lengthening of telomeres (ALT) pathway, which is a telomerase-independent mechanism frequently activated in cancer to facilitate telomere elongation and immortalization (Mendez-Bermudez et al., 2012). Alterations in the expression of the RecQ helicases, particularly overexpression, are found to be associated with increased resistance to anti-cancer drugs, enabling cancer cells to evade cell cycle arrest and apoptosis. Targeting this group of helicases presents an innovative alternative to combat cancer through the development of inhibitors able to efficiently impair helicase activity, reducing cell viability in combination with DNA damage inducers.

Elucidating the diverse roles of RecQ helicases in different stages of carcinogenesis would provide valuable insights for the development of more effective therapeutic strategies. Since telomere maintenance and elongation are crucial events in the promotion of malignant cells, the interaction between RecQ helicases and telomeres in mitotic problems represents a novel context to study that would increase the knowledge into the telomere and cancer fields. Therefore, in this work I aimed to investigate the possible effects of the RecQ proteins in the maintenance o the T-loop structure during a prolonged mitotic arrest.

3.2 Results

3.2.1 A RecQ helicase screening reveals BLM and WRN regulating MAD-TIF formation.

RecQ helicases unwind specific DNA substrates, such as D-loops and HJs in telomeres during replication to facilitate replication fork progression and thus, ensure genomic integrity. To investigate whether proteins with catalytic activities in telomeres participate in the dissolution of T-loops during prolonged mitotic arrest, a screening involving the overexpression of the five RecQ helicases was conducted in search of a phenotype exhibiting reduced or enhanced deprotected telomeres. The experimental study was carried out in a IMR90 E6E7 hTERT cell line, consisting of lung fibroblasts expressing Human Papilloma viral E6 and E7 proteins (IMR90 E6E7), which inhibit p53 and Rb function, respectively. Suppression of both oncoviral proteins provides transformed cells for indefinite divisions without activation of cell cycle checkpoints promoting arrest (Watanabe et al., 1989; Shay et al., 1993). The effects of mitotic arrest in telomeres have been deeply studied and validated in the IMR90 E6E7 cell line (Hayashi et al., 2012), making it an ideal model for exploring the mechanism of telomere deprotection. Cells were subsequently immortalized by expression of human telomerase (hTERT) order to prevent telomere erosion and cell death after prolonged culture (Bodnar et al., 1998). The generated IMR90 E6E7 hTERT cells were then infected with lentivirus carrying constructs for the expression of each RecQ helicase individually, or an empty Vector serving as a control. Following selection with blasticidin marker, after 9 days post-infection, the efficiently transduced cells were collected to determine protein levels (**Figure 3.1A**) and exposed with colcemid, a microtubule inhibitor, for 24 hours to induce a prolonged mitotic arrest. Previous studies have shown that this duration of colcemid treatment in IMR90 E6E7 hTERT is sufficient to promote a significant number of deprotected telomeres (Hayashi et al., 2012). Additionally, a short treatment of 2 hours colcemid was included to arrest cells without inducing telomere deprotection. Deprotected telomeres that arise in interphase (interphase-TIFs) can be passed into mitosis. Therefore, the 2 hours treatment is a helpful control to distinguish deprotected telomeres generated in interphase from the mitotic arrest-dependent TIFs (MAD-TIFs) under experimental conditions. To analyze mitotic telomere deprotection, meta-TIF assay was performed consisting in the collection and cytocentrifuge of treated cells for further immunostaining with γ-H2AX antibody and telomeric DNA probe (Cesare et al., 2015) (**Figure 3.1B**).

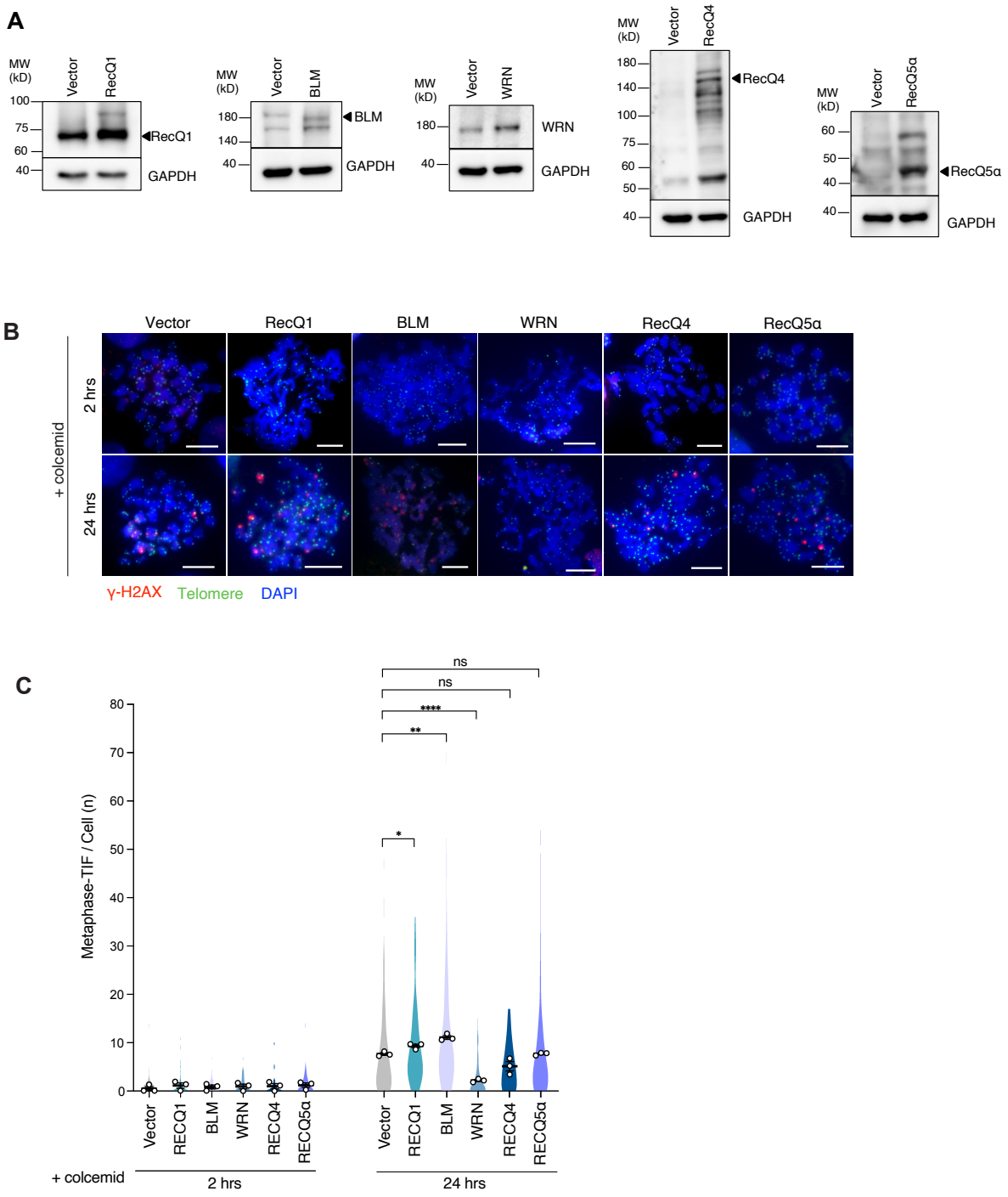

Figure 3.2 - BLM and WRN helicases are involved in the regulation of mitotic telomere deprotection.

A) Immunoblot analysis of the RecQ helicase family members overexpressed in IMR-90 E6E7 hTERT cells. Transduction was performed by lentiviral infection followed by selection with blasticidin for 7 days. Samples were collected at day 12 post-infection for immunoblotting. Protein levels are compared with control cells transduced with an empty Vector construct. Black arrowheads indicate expected protein size: RecQ1 (70 kDa), BLM

(170 kDa), WRN (180 kDa), RecQ4 (150 kDa), RecQ5α (45 kDa). GAPDH serves as a loading control. **B)** Representative images of meta-TIFs (telomeric signals colocalized with γ-H2AX foci) on chromosome spreads from cells treated with 100 ng/ml colcemid for 2 or 24 hours. Scale bar, 10 μm. **C)** Quantification of meta-TIFs per cell upon 100 ng/ml colcemid for the indicated time. Violin plots represent the distribution of all data and averages from three independent experiments (15 metaphases per experiment for 2 hours colcemid; 30 metaphases per experiment for 24 hours colcemid; mean ± s.e.m.; Mann-Whitney test).

Quantification of the total number of γ-H2AX signal colocalizing with the telomeric signal per prometaphase/metaphase spread (metaphase-TIF or meta-TIF) was analyzed and represented in a graph, showing the average meta-TIF count per each replicate of three independent experiments for each experimental group (**Figure 3.1C**). In the analysis, Vector cells treated for 24 hours colcemid exhibited a significant number of deprotected telomeres (~10 in average) induced by an extended time in mitotic arrest, referred to as MAD-TIFs. Interestingly, overexpression of RecQ1, BLM helicases resulted in a significant increase of MAD-TIFs, during a prolonged mitotic arrest without affecting telomeres structure in interphase as observed in 2 hours treatment (**Figure 2.1C**).

However, the most pronounced phenotype between both helicases was observed upon BLM overexpression. In contrast, ectopic expression of WRN led to a suppressed phenotype in mitotic arrested cells. These results from the helicase screening suggest that BLM and WRN are highly involved in the regulation of mitotic telomere deprotection. However, the opposing phenotypes from BLM and WRN overexpression suggest that both helicases engage to T-loop maintenance in a different manner.

According to the obtained data, WRN helicase is a crucial protein that plays a significant role in preventing the formation of MAD-TIFs. While WRN is primarily recognized for its ability to catalyze D-Loops, the findings from this screening suggest the presence of an intriguing yet unknown activity in WRN. This unidentified function appears to confer a protective effect on telomeres instead of promoting their dissolution. Therefore, I consider

essential to investigate the involvement of this helicase in the mechanism of mitotic telomere deprotection.

Chapter 4

A non-catalytic N-terminus domain of WRN prevents mitotic telomere deprotection.

4.1 Introduction

4.1.1 WRN helicase: structure and function.

WRN helicase is the largest member of the RecQ helicase family consisting of 1,432 amino acids and containing multiple functional domains: exonuclease, helicase, RQC and HRDC domains. These domains enable WRN to be involved in DNA repair pathways, particularly in the repair of DSBs (Chen et al., 2003; Lan et al., 2005).

The N-terminal 3'-5' exonuclease domain allows WRN to process a variety of DNA substrates during DNA repair, such as fork-shaped duplexes, dsDNA, D-loops, bubble-structured duplexes, Holliday junctions, and G-quadruplexes (Croteau et al., 2014; Oshima et al., 2017). The conserved RQC domain plays a critical role in WRN by facilitating substrate-specific DNA binding, which initiates the unwinding process. This domain is also involved in the ability of WRN to localize at telomere regions, particularly after oxidative stress (Sun et al., 2017). The HRDC domain of WRN contributes to DNA binding and it is essential for the recruitment of WRN to DSBs (Samanta et al., 2012). Additionally, a small region between the RQC and HRDC domains promotes ssDNA annealing activity and oligomerization (Muftuoglu et al., 2008).

Mutations in the WRN gene lead to Werner syndrome (WS), which is characterized by premature aging symptoms and increased susceptibility to certain cancer types. WS cells exhibit slow replication, an elevated mutation rate, and genomic instability (Fujiwara et al., 1997; Oshima et al., 2017). Unlike Bloom syndrome, WS cells display defects in the HR pathway rather than increased sister chromatid exchanges (SCEs) or excessive homologous recombination (HR). WS patients are predisposed to specific cancer types, including soft-tissue carcinoma, osteosarcoma, and thyroid cancer. WRN expression is regulated in cancer cells, and both silencing and overexpression of WRN can affect genomic stability and cancer cell sensitivity to DNA-damaging agents (Blander et al.,1999; Futami et al., 2007).

The helicase activity of WRN is stimulated by several proteins, including the replication protein A (RPA), the Ku heterodimer, the Mre11-Rad50-Nbs1 (MRN) complex, and TRF2

(Machwe et al., 2004; Lu and Davis, 2012). Notably, binding to multiple RPAs significantly enhances the unwinding activity of WRN, allowing it to unwind duplexes larger than 1 kb in a unidirectional manner (Sommers et al., 2005; Lee et al., 2018). The oligomeric state of WRN also influences its binding preference for specific DNA structures, with WRN dimers binding to fork DNA and tetramers binding to replication forks (Shin et al., 2023). Electron microscopy studies have revealed that oligomerization of WRN results in a strong affinity for the binding to HJs (Compton et al., 2008). Additionally, a small fragment from the WRN N-terminus, encompassing the amino acids 70-240, has shown to form hexamers in the presence of DNA and able to exert exonuclease activities (Xue et al., 2002). However, it remains to be determined whether these oligomeric states affect the efficiency of exonuclease and helicase activities.

4.1.2 WRN in telomere maintenance.

Regarding telomere maintenance, WRN is a critical protein involved in telomere replication and its recruitment to telomeres is enabled by the interaction with shelterin proteins TRF1, TRF2 and POT1. The presence of WRN at telomeres is observed specifically during the S-phase of the cell cycle, as demonstrated by live cell imaging and direct chromatin immunoprecipitation studies (Opresko et al., 2004). WRN interaction with shelterin proteins served multiple purposes, including the resolution of G-quadruplex structures, facilitation of efficient telomere replication, and regulation of the recombinatory ALT pathway (Mohaghegh et al., 2001; Laud et al., 2005; Sidorova et al., 2008; Mukherjee et al., 2018).

Apart from its main role in G-quadruplex dissolution in replication, WRN has not yet been confirmed to be required for T-loop dissolution during telomeric replication. However, WRN has been identified as capable of dissociating telomeric D-loops in *in vitro* studies (Orren et al., 2002; Opresko et al., 2004). Additionally, TRF1 and TRF2 have been found to regulate WRN activities at telomeres (Opresko et al., 2002; Opresko et al., 2004) While these telomere-binding proteins can restrict WRN exonuclease activity on the D-loop, they do not inhibit its helicase activity. This implies that TRF1 and TRF2 play a role in limiting inappropriate processing of telomeric DNA once DNA replication is completed.

4.1.3 WRN activities in mitosis.

Since WRN activities are performed in DNA replication and repair, events that predominantly occur in S-phase, its function during mitosis remains less understood. Depletion of WRN in cancer cells has been associated with certain mitotic defects, such as chromosome bridges and lagging chromosomes (Lieb et al., 2019). However, these signs of genomic instability are a consequence of underlying problems that manifest in cell division. Additionally, limited evidence has suggested that WRN is implicated in mitotic recombination, a process that consists of genetic exchange between homologous chromosomes or sister chromatids during mitosis (Prince et al., 2001). Nevertheless, the direct impact of WRN on the resolution of DNA structures at chromatin or telomeres during mitosis remains unknown, primarily due to the scarcity of studies focused in studying RecQ helicases in distinct cellular contexts. Further research is needed to elucidate the precise functions of WRN during mitotic events and its potential contributions to the maintenance of genome integrity.

4.2 Results

4.2.1 WRN suppresses mitotic telomere deprotection independently of its catalytic activity.

To further understand the role of WRN helicase in mitotic telomere deprotection, the effect of WRN knockdown was examined in IMR90 E6E7 hTERT cells by lentiviral shRNA transduction (**Figure 4.1A**). After 4 days in culture with selection marker, the efficiently transduced cells were treated with colcemid for 2 hours (control) and 24 hours in prior to immunostaining. The decrease in WRN protein levels (**Figure 4.1A**) did not show meta-TIFs after 2 hours of colcemid, but led to an increase in the meta-TIF number in cells treated with colcemid for 24 hours compared to shControl (**Figure 4.1B and C).**

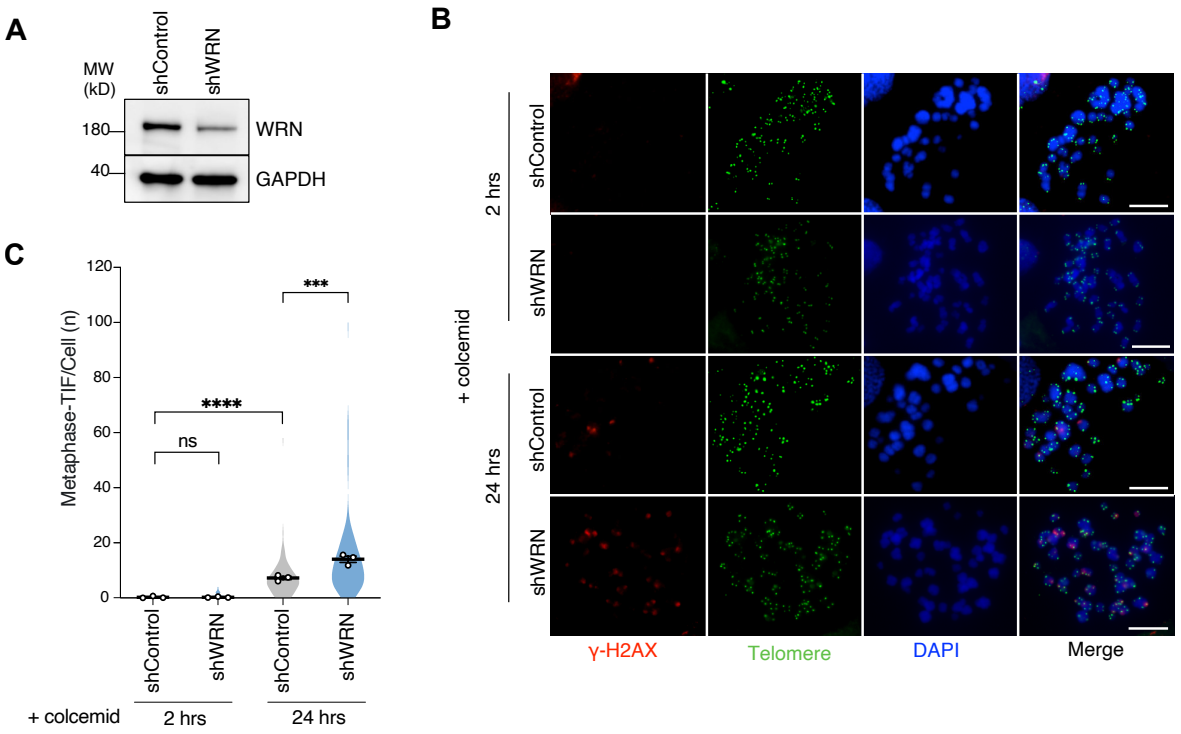

Figure 4.1 WRN depletion exacerbates MAD-TIFs.

A) Immunoblot of IMR-90 E6E7 hTERT cells transduced with shWRN or a non-targeting control short hairpin RNA (shControl) for 5 days. GAPDH serves as a loading control. **B)** Representative images of meta-TIF analysis on mitotic chromosome spreads from WRN knockdown cells after treatment with 100 ng/mL colcemid. Scale bar, 10 μm. **C)** Quantification of telomeric signals colocalized with γ-H2AX foci (metaphase-TIFs or meta-TIFs) per cell in indicated conditions. Violin plots represent the distribution of all data and averages from three independent experiments (15 metaphases per experiment for 2 hrs colcemid; 30 metaphases per experiment for 24 hrs colcemid; mean ± s.e.m.; Kruskal–Wallis followed by Dunn's test).

The exacerbated number of meta-TIF caused by WRN depletion could be rescued by the overexpression of a full-length WRN carrying silent mutations at the shRNA-target sequence (**Figure 4.2A**).

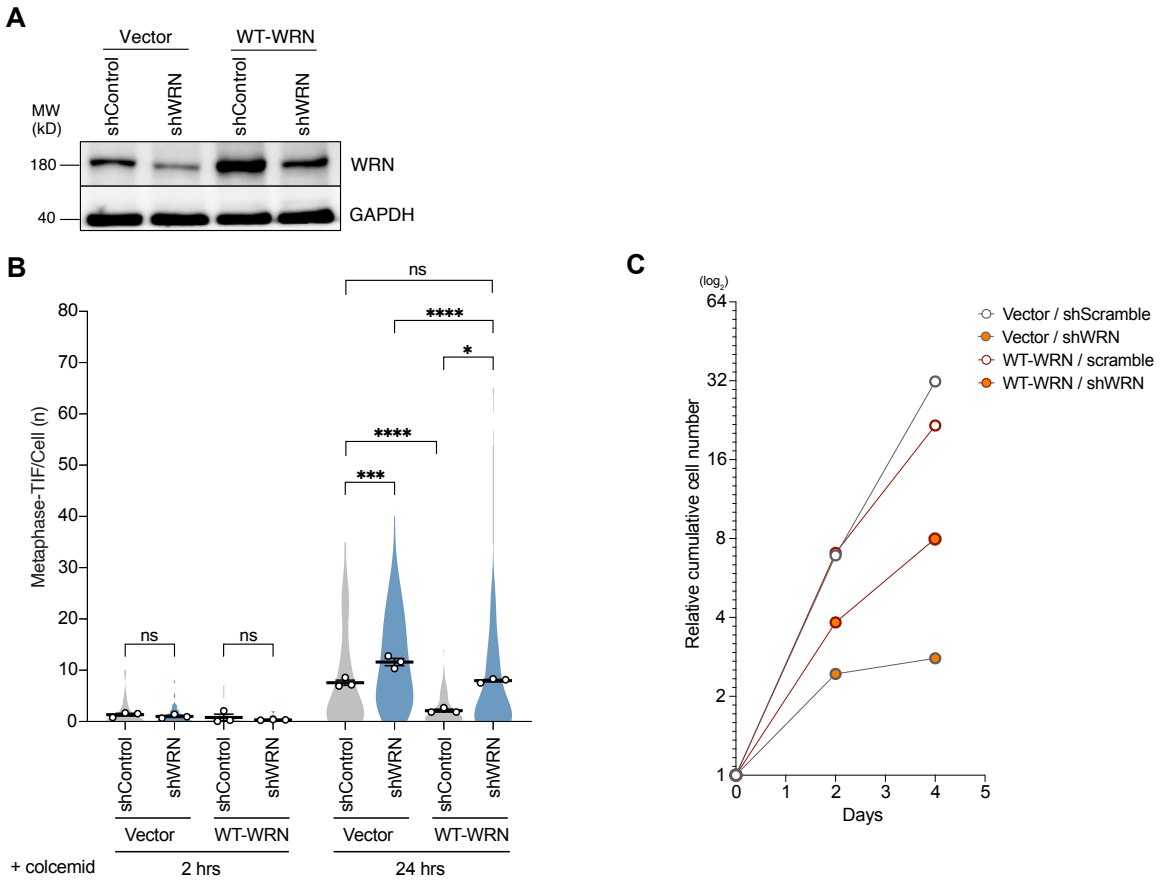

Figure 4.2 Reconstitution of WRN expression rescues cells from excessive telomere deprotection.

A) Immunoblot of IMR-90 E6E7 hTERT cells expressing shRNA-resistant WT-WRN or Vector following transduction with shControl or shWRN for 5 days before analysis. GAPDH serves as a loading control. **B)** Quantification of telomeric signals colocalized with γ-H2AX foci (metaphase-TIF or meta-TIF) from cells treated with 100 ng/mL colcemid at the indicated time points. Violin plots represent the distribution of all data and averages from three independent experiments (15 metaphases per experiment for 2 hrs colcemid; 30 metaphases per experiment for 24 hrs colcemid; mean ± s.e.m.; Kruskal–Wallis followed by Dunn's test). **C)** Growth curve of IMR90 hTERT E6E7 of cells expressing either an empty Vector or WT-WRN, followed by transduction with either shControl or shWRN. After selection, an equal number of cells were seeded in a 24-well plate on day 4 post-infection of shControl and shWRN, and the cell count was assessed on days 2 and 4 after plating to obtain the final cumulative cell number. One data set is represented in the graph.

Interestingly, WT-WRN in an shControl background could suppress completely meta-TIF formation in 24 hours colcemid treatment (**Figure 4.2B**). Moreover, the introduction of exogenous WT-WRN could restore cell growth, which is compromised due to WRN depletion (**Figure 4.2C**). These results demonstrate that the reduction in MAD-TIFs observed in **Figure 4.2B** can be attributed to the expression of a functional WT-WRN protein. Suppression of MAD-TIFs by the overexpression of WT-WRN is not mediated through the regulation of the protein levels of TRF2, a key T-loop protective protein, as I confirmed by an immunoblot showing unchanged TRF2 protein levels in mitotically arrested cells (**Figure 4.3A**). Altogether, these findings suggest that WRN plays a crucial suppressive role in the process of telomere deprotection during mitotic arrest.

Previously, mitotic telomere deprotection has shown to be a time-dependent process that accumulates during mitotic arrest (Hayashi et al., 2012). IMR90 E6E7 cells require to be arrested for a sufficient time for undergoing telomere deprotection, which is achieved by a colcemid treatment longer than 2 hours. Therefore, I aimed to confirm whether depletion or overexpression of WRN affects mitotic duration upon exposure to colcemid. For this purpose, live-cell imaging was performed in cells treated with colcemid for 72 hours. After data collection, the mitotic duration was tracked for all experimental groups (**Figure 4.3B**). Notably, untreated cells exhibited a mitotic duration of less than 2 hours, whereas WRN-depleted cells displayed an extended duration of 3.5 hours (**Figure 4.3C**). Colcemid treatment resulted in a considerable prolongation of mitotic arrest, averaging around 20 hours in both shControl and empty vector cells. WRN-depleted cells exhibited a shorter mitotic duration of 15 hours, whereas WRN-overexpressing cells displayed a mitotic duration similar to that of the vector control. These results suggest that suppression of MAD-TIF formation in cells expressing WT-WRN is not caused by a reduction in the duration of mitotic arrest. Instead, it suggests that the presence of abundant protein levels of WRN impedes mitotic telomere deprotection, thereby exerting its inhibitory effect.

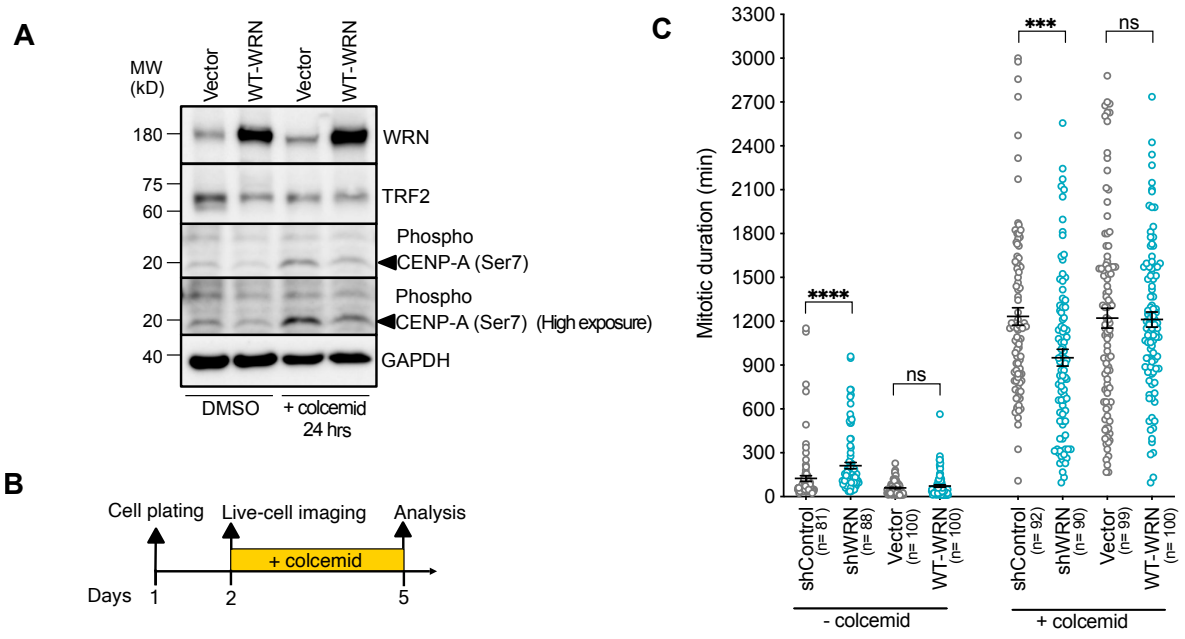

Figure 4.3 TRF2 protein levels and mitotic checkpoint are unaltered upon WRN overexpression.

A) Immunoblot of TRF2 in cells expressing exogenous WT-WRN after 24 hrs exposure to 100 ng/mL colcemid or DMSO for control. Interphase and mitotic cells were collected together. Phospho-CENP-A (Ser7) and GAPDH serves as a mitotic marker and a loading control, respectively. **B)** Schematic of the live-cell imaging. Same number of cells were plated 24 hours before colcemid treatment. After the addition of 100 ng/mL colcemid, imaging of the cell fate was recorded for three days. **C)** Live-cell imaging analysis displaying the distribution of mitotic duration in cells expressing shWRN and ectopic WT-WRN (Median, 25th and 75th percentile; Mann-Whitney test). Cells were either mock-treated or exposed to 100 ng/mL colcemid for mitotic arrest induction. Duration of the mitotic arrest was determined by tracking the morphology of the cells from mitotic entry (from an interphase-flat to a round shape) until the end of mitosis (disappearance of the mitotic round shape).

Since exogenous WRN expression results in suppressed telomere deprotection, I investigated whether this suppression is reliant on the enzymatic activities of WRN. To examine this, WRN defective mutants were used and which contained point mutations at the core domains responsible for unwinding double-stranded DNA substrates (**Figure**

4.4A). One of these mutants carries a Glutamic acid-to-Alanine mutation at the E84 residue located in the exonuclease domain (WRN-E84A) that alters ATPase and 3'-5' exonuclease activities while preserving helicase activity (Huang et al. 1998; Perry et al. 2006). A second mutant with a Lysine-to-Alanine mutation at K577 residue in the helicase domain (WRN-K577M) results in a defective WRN protein with compromised DNA resolution activity (Gray et al., 1997). Both mutants were efficiently expressed and demonstrated the ability to suppress telomere deprotection in mitotically arrested cells, similar to WT-WRN (**Figure 4.4B and C**). The data suggest that suppression of mitotic telomere deprotection by WRN is not dependent on its enzymatic activities.

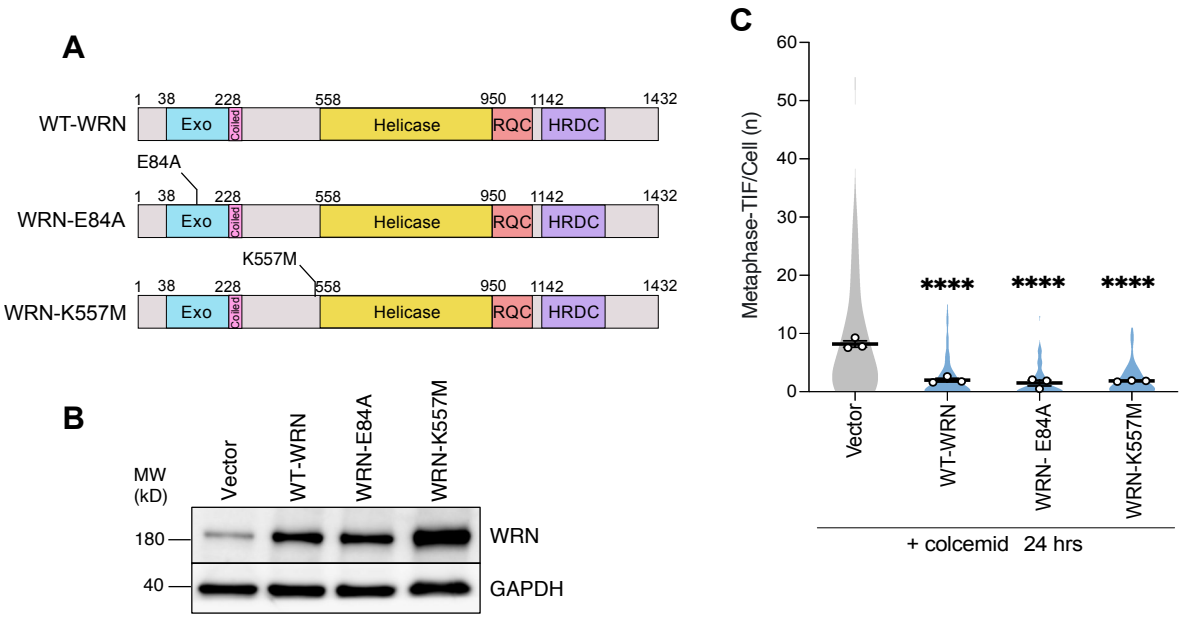

Figure 4.4 WRN suppresses MAD-TIF formation independently from its catalytic activities.

A) Schematic of full-length WRN with location of the point mutations inserted in the Exonuclease and Helicase domains**.** Coiled, coiled-coil motif; Helicase, helicase domain; RQC, RecQ C-terminal DNA-binding domain; HRDC, helicase and RNaseD C-terminal domain. **B)** Immunoblot of WRN in cells expressing exogenous WT-WRN and two WRN mutants (E84A and K557M) with depleted catalytic activities. Transduced cells were harvested on day 10 post-infection. GAPDH serves as a loading control. **C)** Quantification of meta-TIFs (telomeric signals colocalized with γ-H2AX foci) in cells treated with 100 ng/mL colcemid for 24 hours. Data is collected from three independent experiments (30 metaphases per experiment; mean ± s.e.m.; Kruskal–Wallis followed by Dunn's test).

4.2.2 WRN suppressive activity is regulated through the N-terminus 168-333 aa.

To identify the regions of WRN responsible for the suppression of mitotic telomere deprotection, three distinct truncated fragments: WRN^{2-499}, $WRN^{500-946}$, and $WRN^{947-1452}$ were generated. The N-terminus of these fragments was tagged with 4xFlag and NLS peptide to direct their transport into the cell nucleus and localization within the same compartment as an intact full-length WRN protein. The fragments were overexpressed in IMR-90 E6E7 hTERT cells followed by colcemid-induced mitotic arrest (**Figure 4.5A**). All fragments were found to appear with additional bands without affecting the protein levels of endogenous WRN (**Figure 4.5B**). This suggests that each fragment may undergo post-translational modifications (PTMs) of an unknown nature, leading to multimerization of the N-terminus. The meta-TIF analysis revealed that the expression of WRN^{2-499} fragment significantly suppressed mitotic telomere deprotection compared to the vector control and other fragments, $WRN^{500-946}$ and $WRN^{947-1452}$ (**Figure 4.5C**). This result suggests that the suppressive function against mitotic telomere deprotection resides within the N-terminus sequence of WRN.

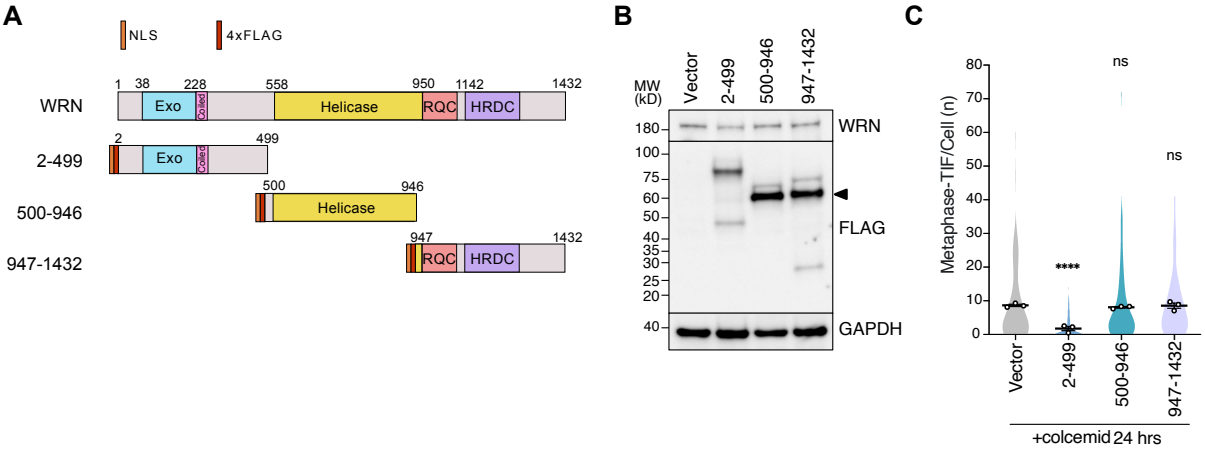

Figure 4.5 N-terminus of WRN is involved in MAD-TIF suppression.

A) Schematic representation of NLS and 4xFLAG tagged WRN fragments derived from full-length WRN. Numbers indicate WRN amino acid coordinate. Exo, exonuclease domain; Coiled, coiled-coil motif; Helicase, helicase domain; RQC, RecQ C-terminal DNA-binding domain; HRDC, helicase and RNaseD C-terminal domain. **B)** Immunoblot of endogenous WRN and WRN fragments in IMR-90 E6E7 hTERT cells expressing indicated

WRN fragments. Transduced cells were analyzed on day 10 post-infection when cells were subjected to experimentation for the meta-TIF assay. Black arrowhead indicates bands of the expected size of 60–70 kDa. GAPDH serves as a loading control. **C)** Quantification of meta-TIFs (telomeric signals colocalized with γ-H2AX foci) in cells treated with 100 ng/mL colcemid for 24 hours. Data is collected from three independent experiments (30 metaphases per experiment; mean ± s.e.m.; Kruskal–Wallis followed by Dunn's test).

Highly stable multimers of WRN have shown to be resistant to SDS denaturation resulting in multiple bands of distinct sizes in a blot (Perry et al., 2010). In order to validate whether the observed modification on WRN^{2-499} in **Figure 4.5B** specifically occurs during mitotic arrest, cells were synchronized by using a double treatment with thymidine followed by the addition of colcemid after 6 hours post-release (**Figure 4.6A**). Arrested cells in mitosis were harvested by shake-off at different time points, showing an accumulation of the higher molecular band in the N-terminal WRN compared to interphase cells (**Figure 4.6B**). As a result, protein levels of endogenous WRN increased in mitosis, but remained unchanged throughout the prolonged mitotic arrest (**Figure 4.6B**). These results suggest that the N-terminus is susceptible to potential PTMs during mitotic arrest.

Next I asked whether the expression of truncated fragments affected the duration of mitosis, since mitotic arrest (>2h) is not sufficient to induce MAD-TIFs. For this purpose, a live cell analysis was performed (**Figure 4.6C**) and the analysis revealed no significant difference in the duration of mitosis among all samples arrested upon colcemid treatment. This observation confirms that the suppressive effect of WRN^{2-499} is not caused by a shortened mitotic arrest.

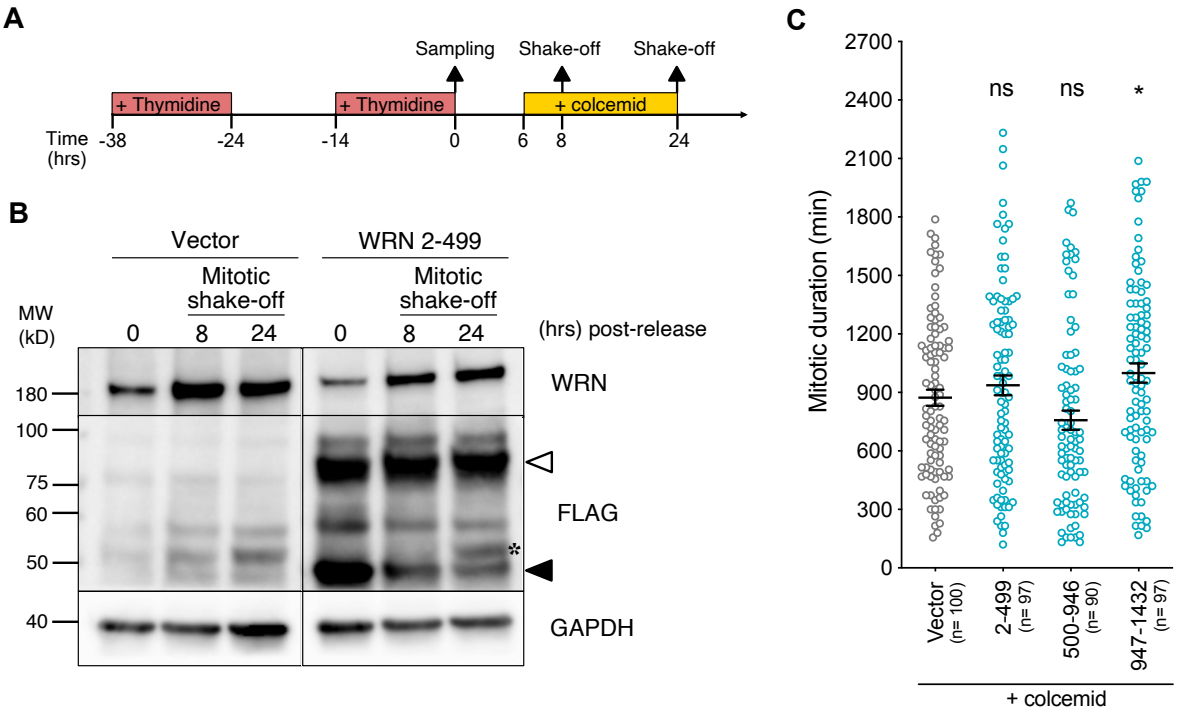

Figure 4.6 WRN N-terminus undergoes modifications upon colcemid treatment without affecting mitotic checkpoint.

A) Timeline for synchronizing cells by double-thymidine block. Samples for Western blotting were collected at 0, 8, and 24 hours after the second release. Mitotic cells were collected by shake-off at 8 and 24 hours.**B)** Immunoblot of endogenous WRN and the 4xFLAG-tagged WRN^{2-499} fragment. The expected band size is indicated by a black arrowhead, and potential complex formation or protein modifications are indicated by a white arrowhead. Asterisk denotes unspecific bands. GAPDH serves as a loading control. **C)** Live-cell imaging analysis displaying the distribution of mitotic duration in cells expressing the indicated WRN fragments (median, 25th, and 75th percentile; Kruskal-Wallis followed by Dunn's test). Cells were exposed to 100 ng/mL colcemid during the three days of data acquisition.

To further identify the specific region of the WRN N-terminus responsible for suppressing MAD-TIF formation, the WRN^{2-499} fragment was separated into three fragments: WRN^{2-167}, $WRN^{168-333}$, $WRN^{334-499}$ (**Figure 4.7A**). These fragments were expressed in IMR-90 E6E7 hTERT cells and immunoblot revealed the appearance of additional bands, different from the expected protein sizes, possibly due to PTMs, cleavage, protein complex formation, or

multimerization (Perry et al., 2010) (**Figure 4.7B and Table 1**). Meta-TIF analysis of colcemid-treated cells for 24 hours revealed that only the WRN$^{168-333}$ fragment effectively abolished mitotic telomere deprotection (**Figure 4.7C and D**). Similar suppression of the WRN$^{168-333}$ fragment was observed in cells with depleted endogenous WRN, indicating its high suppressive function to impair MAD-TIF formation compared to full-length WRN (**Figure 4.7E**).

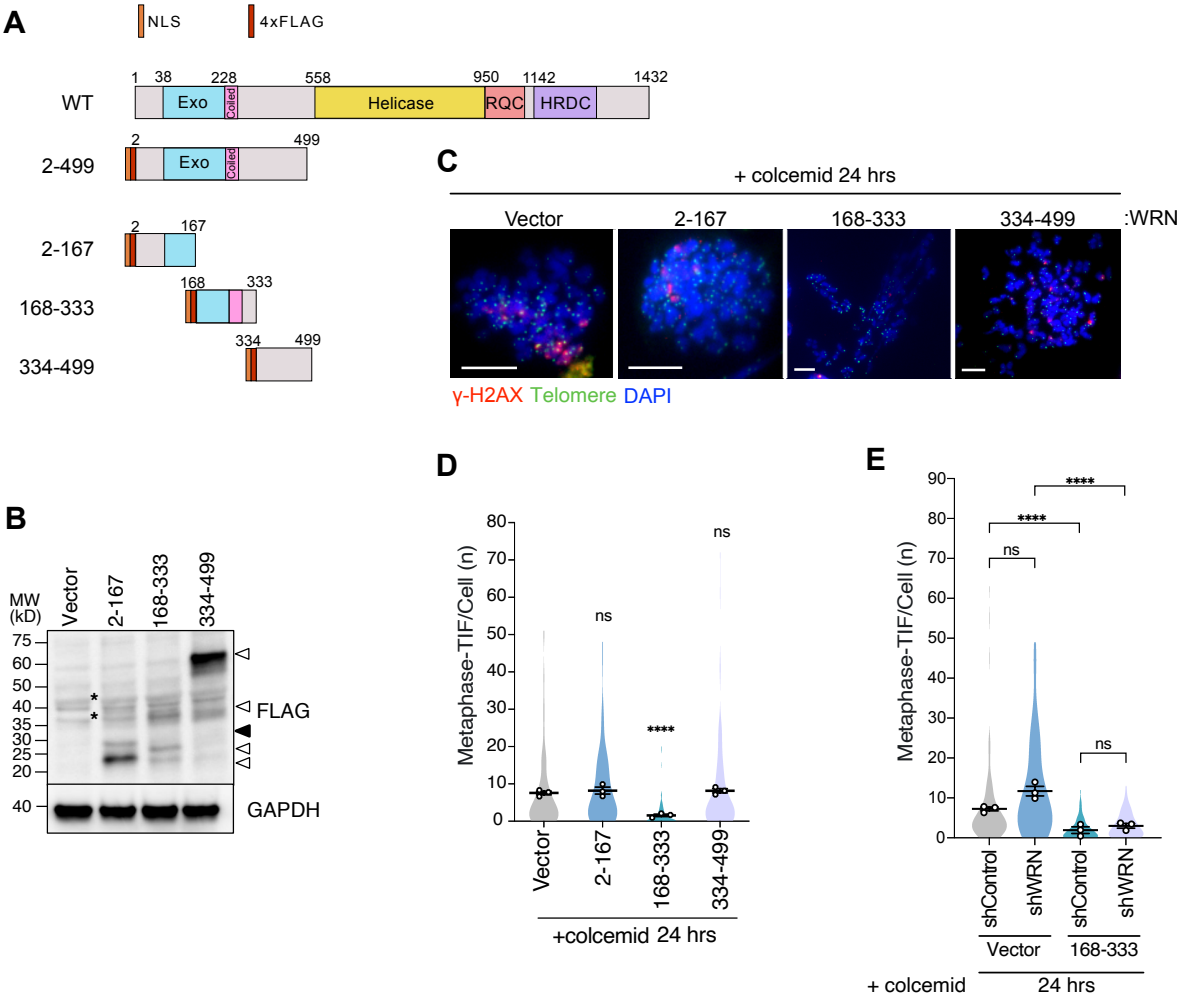

Figure 4.7 WRN N-terminus encompassing 168-333 aa suppresses MAD-TIFs.

A) Schematic representation of WRN sub-fragments derieved from the N-terminus. Numbers indicate WRN amino acid coordinate. **B)** Representative images of the meta-TIF assay from cells expressing indicated WRN fragments after treatment with 100 ng/mL colcemid for 24 hours. Scale bar, 10 μm. **C)** Immunoblot of 4xFLAG tagged WRN fragments expressed in IMR-90 E6E7 hTERT cells. Transduced cells were harvested on

day 12 post-infection for immunoblot and meta-TIF assay, shown in **D**. A black arrowhead indicates the expected fragment size (~ 27 kDa). Potential truncation, complex formation, and post-translational modifications are indictaed with white arrowheads. Asterisks represent unspecific bands from empty Vector. GAPDH serves as a loading control. **D)** Quantification of meta-TIFs (telomeric signals colocalized with γ-H2AX foci) per cell in indicated conditions. Violin plots represent the distribution of all data and averages from three independent experiments (15 metaphases per experiment for 2 hrs colcemid; 30 metaphases per experiment for 24 hrs colcemid; mean ± s.e.m.; Kruskal–Wallis followed by Dunn's test). **E)** Quantification of meta-TIFs (telomeric signals colocalized with γ-H2AX foci) from cells expressing empty Vector or $WRN^{168-333}$ fragment, followed by transduction with shControl or shWRN and treated with 100 ng/mL colcemid for 24 hours. Violin plots represent the distribution of all data and averages from three independent experiments (n=30 per experiment; mean ± s.e.m.; Kruskal-Wallis followed by Dunn's test).

Subsequent cleavage of the $WRN^{168-333}$ produced two fragments: $WRN^{168-205}$ and $WRN^{251-333}$ (**Figure 4.8A**). Among these fragments, $WRN^{251-333}$ appeared as an upper shifted band on SDS-PAGE (**Table 4.1**), and its expression demonstrated a partial ability to suppress mitotic telomere deprotection compared to the complete $WRN^{168-333}$ fragment (**Figure 4.8B and D**). However, the expression of $WRN^{168-250}$ could not be detected by immunoblotting, despite the successful protein separation for this sample, as it was detected by CBB staining of the transferred gel (**Figure 4.8C**). This suggests that this fragment might be prone to protein degradation and, consequently, the average number of meta-TIFs observed was similar to that of the control. Hence, it was not possible to definitively conclude whether $WRN^{168-250}$ also exhibits suppressive effects (**Figure 4.8D**).

Notably, the negative effect $WRN^{168-333}$ expression on MAD-TIFs was further verified in HT1080, a colorectal carcinoma cell line (**Figure 4.9A**). Overexpression of the $WRN^{168-333}$ suppressed MAD-TIFs in mitotic-arrested HT1080 cells, suggesting that WRN is required to impair MAD-TIF formation in cancer-derived cell lines (**Figure 4.9B and C**). Taken together, this data indicates that both WRN^{2-499} and $WRN^{168-333}$ fragments possess a conserved suppressive effect on telomeres during prolonged mitotic arrest (**Table 1**), possibly by inhibiting factors involved in T-loop unwinding.

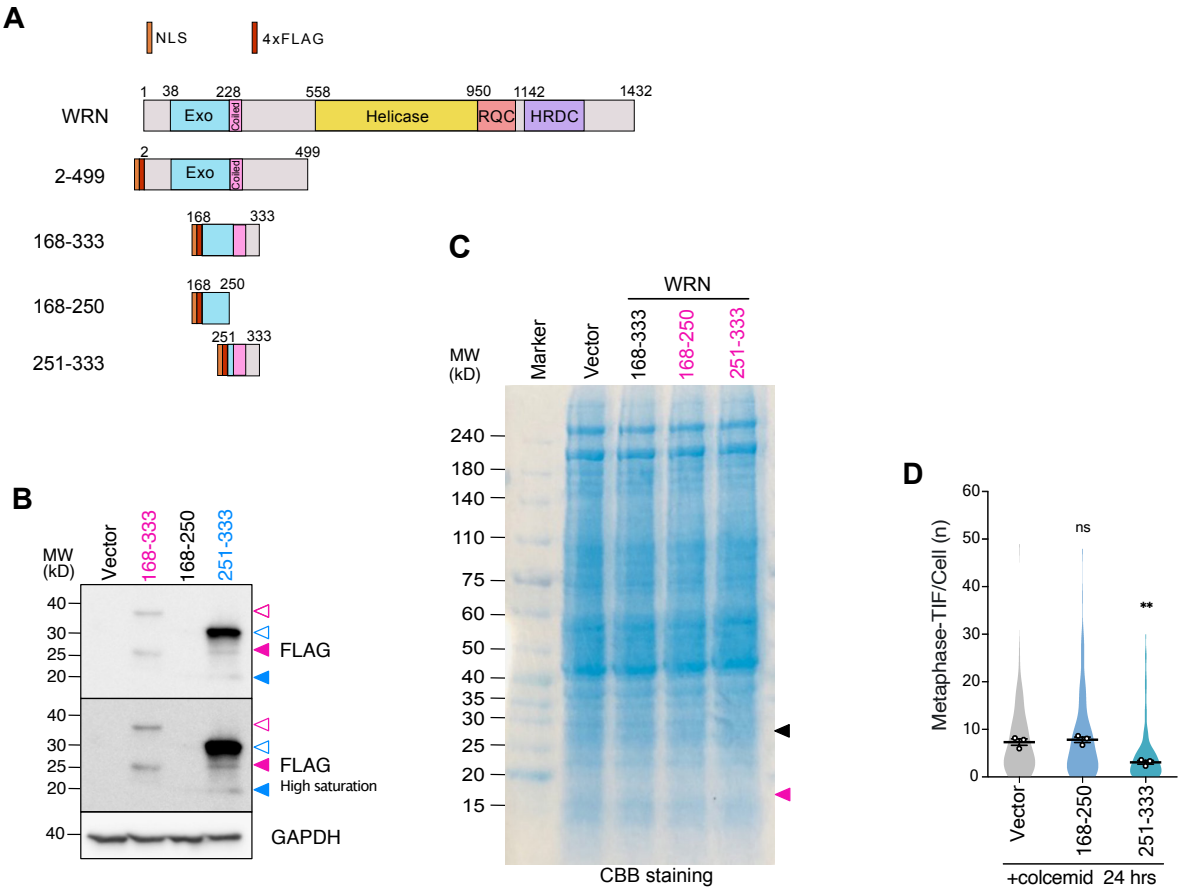

Figure 4.8 WRN coiled-coil domain is sufficient to suppress mitotic telomere deprotection.

A) Schematic representation of WRN fragments derived from WRN $^{168\text{-}333}$ truncated peptide. **B)** Immunoblot of 4xFLAG-WRN fragments in IMR-90 E6E7 hTERT cells harvested on day 12 post-infection. Magenta and blue arrowheads indicate the expected size for the WRN168-333 (~ 27 kDa) and the WRN251-333 (~ 17 kDa) fragments, respectively. White arrowheads with colored lines indicate possible post-translational modifications. **C)** Representative SDS-PAGE gel stained with Coomassie Brilliant Blue (CBB) that corresponds to the blot in **B**. Stained gel confirms successful protein integrity and separation in all lanes. Magenta and Black arrowheads indicate the expected size for the respective fragment. **D)** Quantification of meta-TIFs (telomeric signals colocalized with γ-H2AX foci) in cells treated with 100 ng/mL colcemid for 24 hours. Data is collected from three independent experiments (30 metaphases per experiment; mean ± s.e.m.; Kruskal–Wallis followed by Dunn's test).

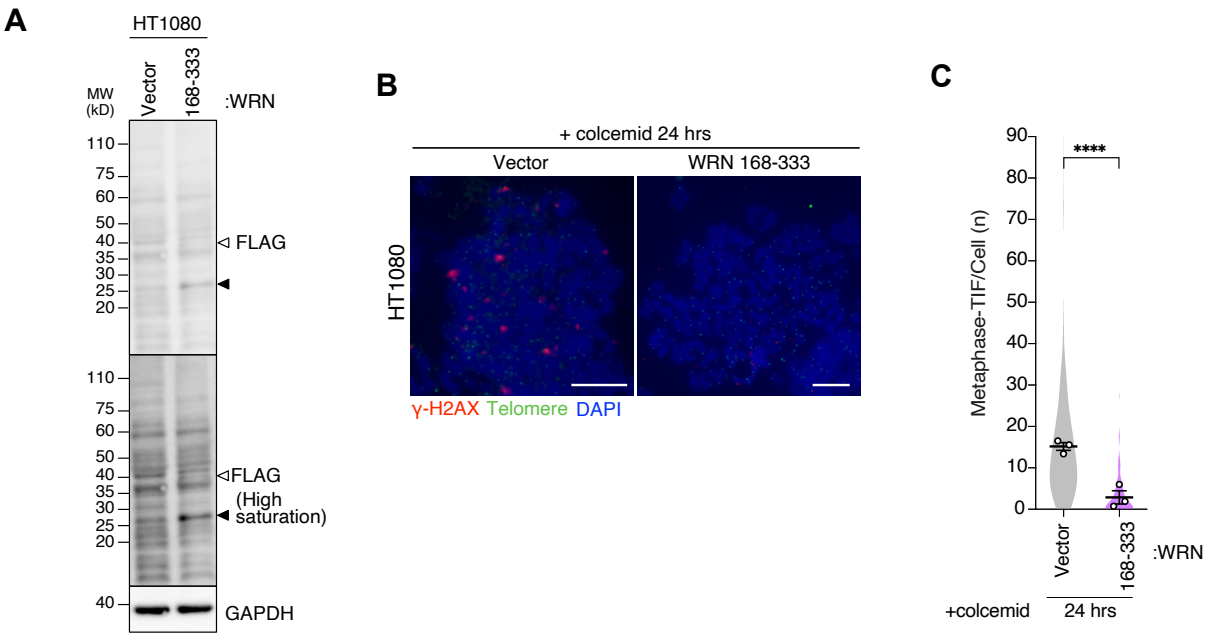

Figure 4.9 WRN (168 - 333 aa) suppresses MAD-TIFs in HT1080 cancer cells.

A) Immunoblot of 4xFLAG-WRN$^{168-333}$ expressed in HT1080 cells. Black and white arrowheads indicate expected size and potentially modified fragment, respectively. GAPDH serves as a loading control. **B)** Representative images of the meta-TIF assay in HT1080 cells expressing WRN$^{168-333}$ fragment after treatment with 100 ng/mL colcemid for 24 hrs. Scale bar, 10 μm. **C)** Quantification of meta-TIFs (telomeric signals colocalized with γ-H2AX foci) in HT1080 cells expressing Vector or WRN$^{168-333}$ fragment and treated with 100 ng/mL colcemid for 24 hours. Data is collected from three independent experiments (30 metaphases per experiment; mean ± s.e.m.; Mann-Whitney test).

4.2.3 WRN overexpression does not affect ATM and Aurora B activities.

In a previous study, Aurora B kinase activity was demonstrated to be required for mitotic telomere deprotection, and its inhibition suppresses this process (Hayashi et al., 2012; Van Ly et al., 2018). Based on this knowledge, I asked whether WRN impairs Aurora B activity, which could explain the absence of MAD-TIF formation observed thus far. To verify this scenario, I exploited a study reporting that Aurora B activity is required for the activation of the SAC machinery in response to microtubule stabilizer taxol, which can induce mitotic arrest (Hauf et al., 2003). As a control, cells expressing empty Vector were

treated with taxol and hesperadin, an Aurora B inhibitor. It is important to note that the 40 nM hesperadin concentration used in this study is low for fully inhibiting Aurora B activity, but it is sufficient to impair MAD-TIF formation and reduce the duration of mitotic arrest (Hayashi et al., 2012). Therefore, live-cell imaging observations revealed a shortened duration of taxol-induced mitotic arrest in vector control cells co-treated with hesperadin (**Figure 4.10A**).

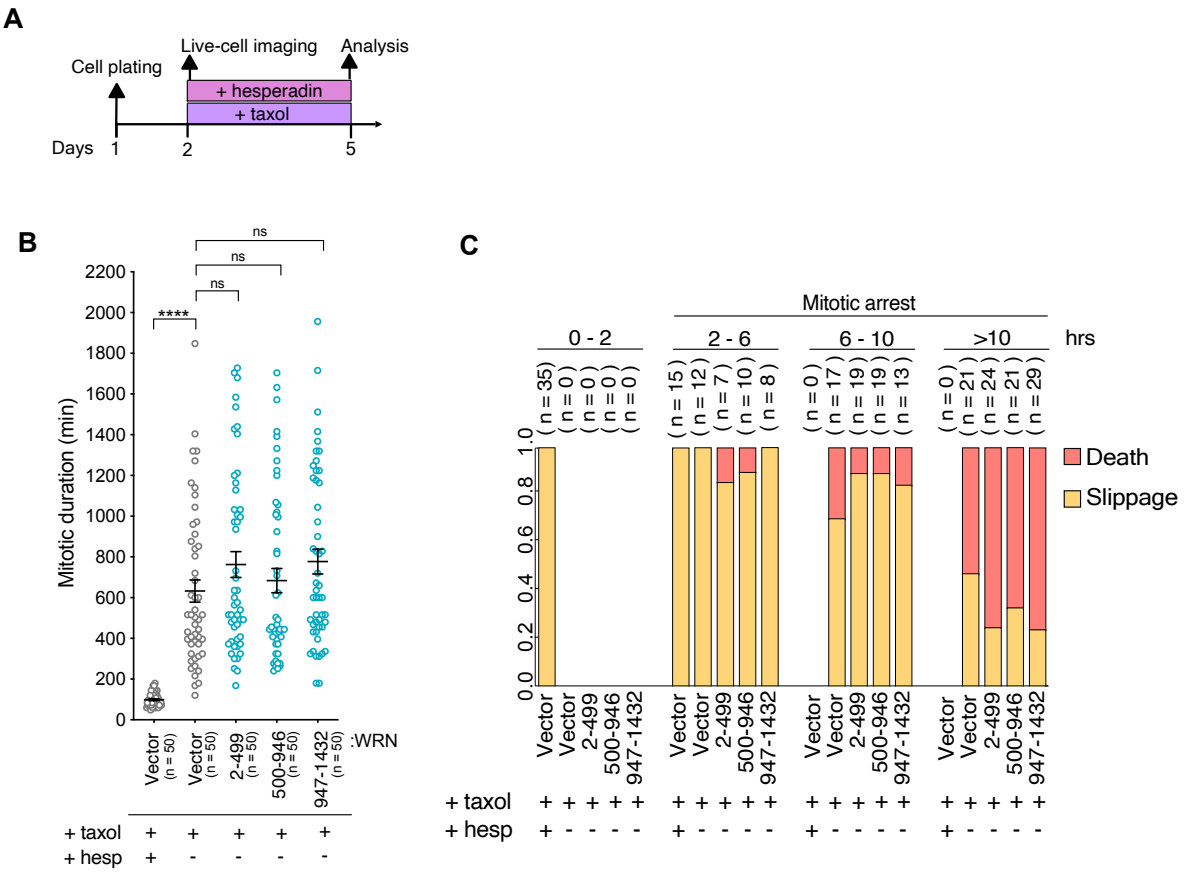

Figure 4.10 WRN N-terminus does not perturb Aurora b kinase activity in mitosis.

A) Timeline of the live-cell imaging. Cells expressing WRN fragments were exposed to 500 nM taxol, a microtubule-stabilizing agent, for three days until the end of data acquisition. Vector cells were co-treated with 40 nM hesperadin, serving as a positive control for inhibition of Aurora B activity, which correlates to a short mitotic duration. **B)** Live-cell imaging analysis displaying the distribution of mitotic duration in cells expressing indicated WRN fragments (Median, 25th, and 75th percentile; Kruskal–Wallis followed by Dunn's test). **C)** The ratio of different cell fates (slippage or cell death) following mitosis was analyzed in the specified cells upon the indicated conditions. The results were categorized

based on the duration of mitotic arrest. Mitosis lasting longer than 2 hours was considered as mitotic arrest.

In contrast, cells expressing different WRN fragments exhibited robust mitotic arrest in response to taxol, similar as vector control cells without hesperadin treatment. Tracking of cell fate after mitotic arrest showed rapid slippage within 2 hours in vector control cells, which is a consequence of Aurora B inhibition (Hauf et al., 2003) (**Figure 4.10B**). However, no significant changes in cell outcome were observed in cells expressing any WRN fragment, which behaved similarly as the untreated vector control cells. These results show that Aurora B activity is maintained in cells expressing WRN^{2-499}, and therefore, the absence of MAD-TIFs cannot be attributed to the inhibition of Aurora B activity or its alterations in mitotic response.

Additionally, ATM kinase is activated in the presence of exposed telomeres recognized as DBSs and depletion of ATM reduces the number of detected TIFs in metaphases (Hayashi et al., 2012). Furthermore, ATM activation has been shown to be regulated by WRN upon DSBs in cells challenged by replication fork collapse during S-phase (Cheng et al., 2008). Considering that ATM is required for the formation of telomeric γ-H2AX foci during mitotic arrest, I questioned whether the absence of MAD-TIF is a result of ATM inhibition by the WRN N-terminal fragment in mitosis. To address this question, cells expressing the WRN^{2-499} fragment were arrested in mitosis with colcemid for 22 hours, followed by a 2 hrs treatment with with 0.2ug/ml bleomycin, a DNA damage inducer, to generate DNA double-strand breaks in mitotic chromosomes (**Figure 4.11A**).

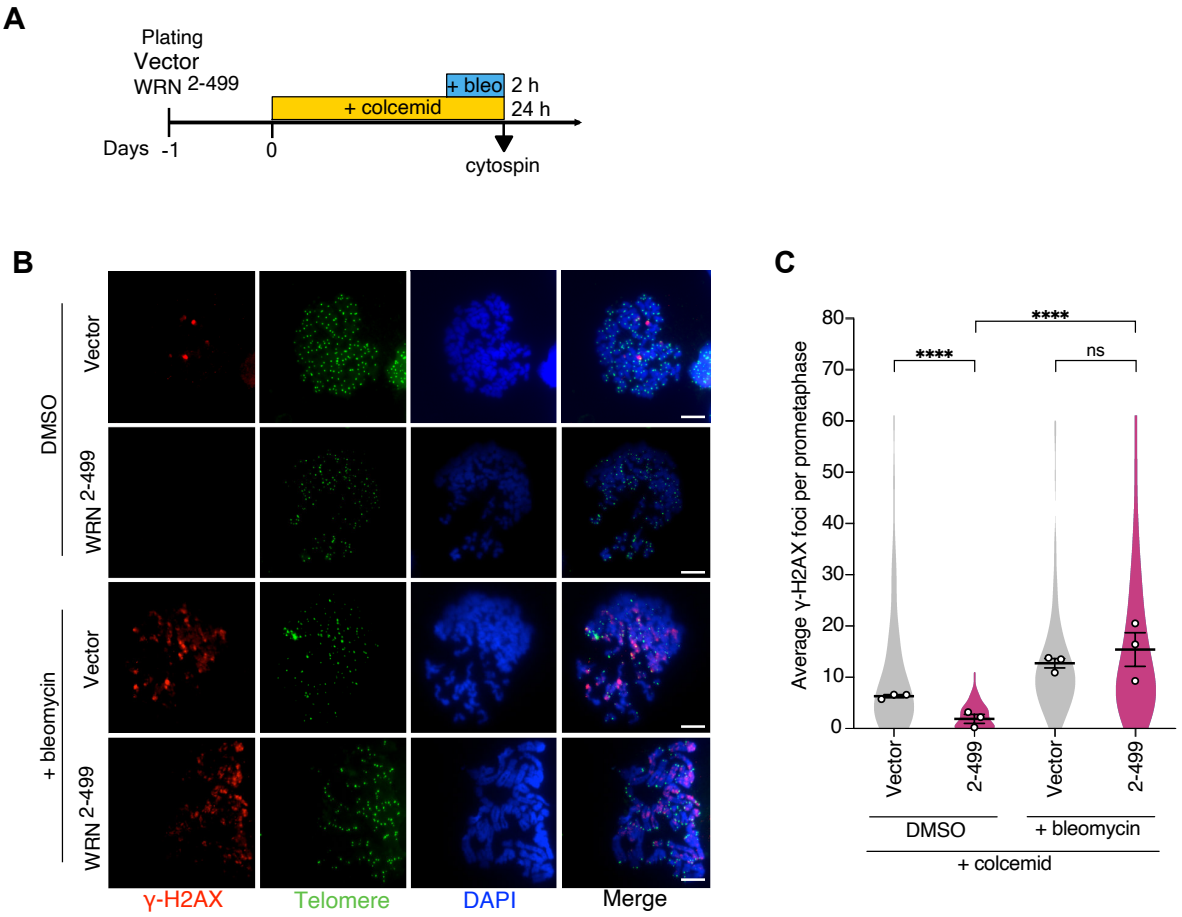

Figure 4.11 Mitotic ATM activity remains intact upon overexpression of WRN N-terminus.

A) Timeline for DNA damage induction on mitotic chromosomes. IMR-90 E6E7 hTERT cells expressing WRN$^{2-499}$ fragment were treated with 100 ng/mL colcemid for 24 hours in which 0.2 µg/ml bleomycin was added two hours before the end of colcemid treatment. Subsequently, cells were harvested and subjected to cytospin for following staining. **B)** Representative images of γ-H2AX foci on mitotic chromosomes in cells treated with colcemid and bleomycin or DMSO, in case of the control. **C)** Quantification of total γ-H2AX foci on mitotic chromosomes from cells expressing Vector or WRN$^{2-499}$ fragment. Violin plots illustrate the distribution of all data and averages from three independent experiments (30 metaphases per experiment; mean ± s.e.m.; Kruskal–Wallis followed by Dunn's test).

Representative images of metaphases showed the distribution of γ-H2AX foci in telomeres and along chromosome arms after bleomycin treatment (**Figure 4.11B**). Quantification of total γ-H2AX foci per metaphase spread indicated that the WRN^{2-499} fragment suppressed the formation of γ-H2AX foci in response to colcemid (**Figure 4.11C**). However, a marked increase in the number of γ-H2AX foci was detected following exposure to bleomycin, comparable to control cells. These results suggest that ATM remains active during mitotic arrest in cells expressing the WRN^{2-499} fragment and effectively responds to the presence of DSBs. Therefore, I can conclude that the N-terminus of WRN suppresses mitotic telomere deprotection in a context where both Aurora B and DDR activities are maintained.

4.2.4 WRN supports the protective function of TRF2 in mitotic telomeres.

TRF2 plays a central role in safeguarding T-loops by tightly binding to the D-loop junction, which maintains the T-loop configuration (Necásova et al., 2017; Timashev and Lange, 2020). WRN possess a strong affinity for Holliday Junctions (HJ), which are structurally similar to the D-loop, in its tetrameric form and participates in the resolution of these structures (Compton et al., 2008). Therefore, I investigated whether WRN can protect telomeres independently of TRF2. For this purpose, cells expressing either the suppressive full-length WT-WRN or distinct suppressive WRN fragments (**Table 1**) were transduced with an shRNA sequence targeting TRF2, which results in TIF formation without leading to end-to-end telomere fusion (Cesare et al., 2013). Knockdown of TRF2 did not alter the protein expression of endogenous and exogenous WRN, as for the N-terminal fragments (**Figure 4.12A**).

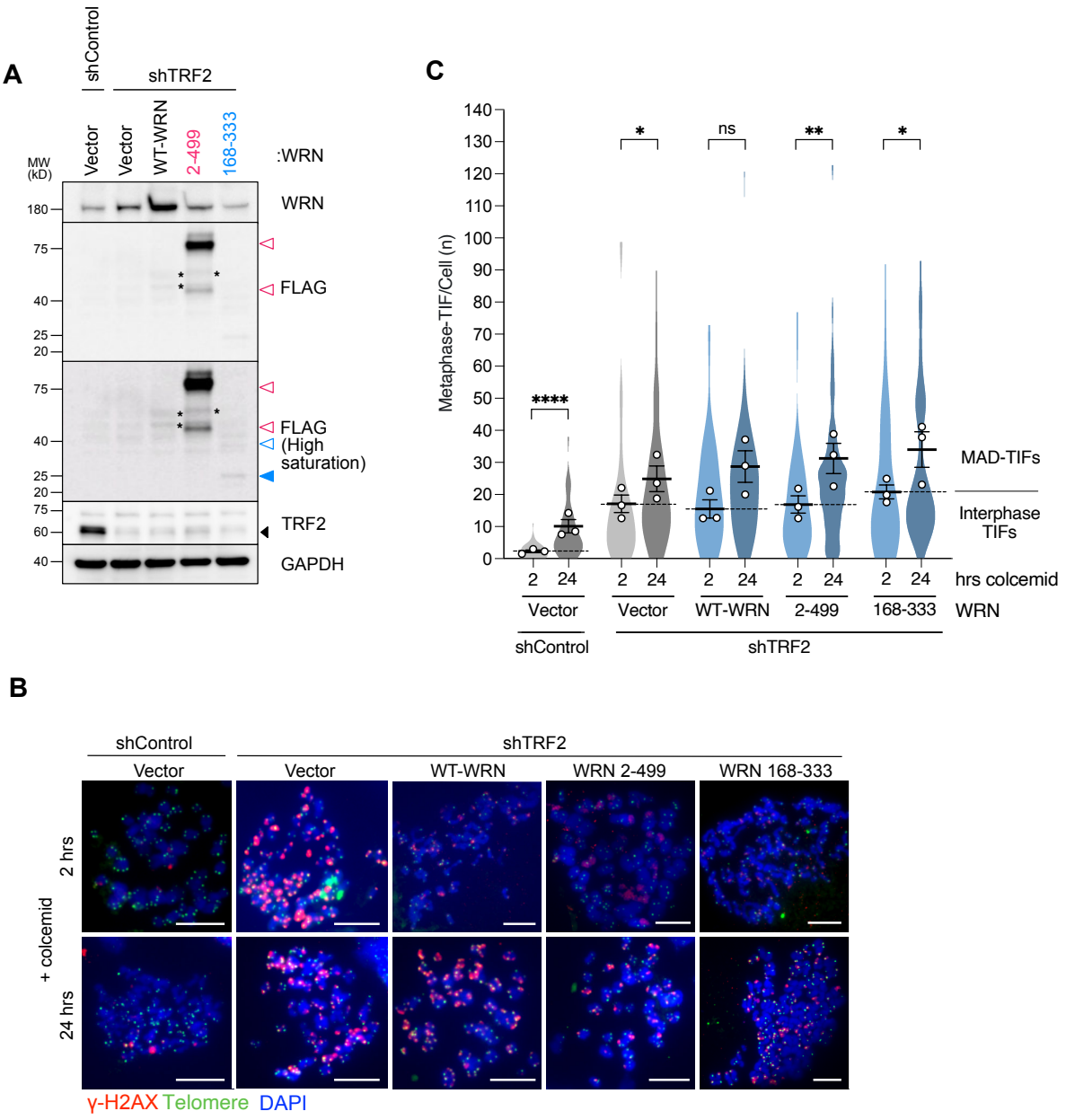

Figure 4.12 WRN requires sufficient TRF2 protein levels to suppress MAD-TIFs.

A) Immunoblot endogenous WRN, 4xFLAG-tagged WRN fragments and TRF2. IMR-90 E6E7 hTERT cells expressing WRN fragments were transduced with an shTRF2 target sequence by lentiviral infection. Cells were collected and lysed at day 7 post-infection. Blue-colored arrowhead indicates the expected size for $WRN^{168-333}$ (~ 27 kDa). White arrowheads (magenta line border for WRN^{2-499} fragment and blue border for $WRN^{168-333}$) indicate possible post-translational modifications or complex formation. GAPDH serves as a loading control. **B)** Representative images of the meta-TIF assay from TRF2 knockdown cells expressing indicated WRN fragments, following treatment with 100 ng/mL colcemid.

Scale bar, 10 μm. **C)** Quantification of meta-TIFs (telomeric signals colocalized with γ-H2AX foci) in cells expressing WRN fragments upon TRF2 knockdown and colcemid treatments. Dashed lines discriminate between the average number of TIFs generated in the interphase (interphase-TIFs) due to shTRF2 (2 hours colcemid) and MAD-TIFs caused by mitotic arrest (24 hours colcemid) (15 metaphases per experiment for 2 hours colcemid; 30 metaphases per experiment for 24 hours colcemid; mean ± s.e.m.; Mann–Whitney test).

However, insufficient levels of TRF2 resulted in a significant arise in the number of TIFs, which originated in interphase but persisted into mitosis, as observed in metaphases from Vector-shTRF2 cells treated with colcemid for 2 hrs (**Figure 4.12B**). Prolonged colcemid treatment for 24 hrs further amplified the number of meta-TIFs in vector cells, indicating the formation of MAD-TIFs that accumulated on metaphase chromosomes, alongside the interphase TIFs generated as a result of TRF2 depletion (Cesare et al., 2013; Hayashi et al., 2015) (**Figure 4.12C**). Both full-length WRN and its N-terminal fragments showed no suppression of the number of meta-TIFs in response to TRF2 knockdown, irrespective of colcemid treatment duration (2 hours or 24 hours) (**Figure 4.12C**). These observations suggest two important points. First, WRN does not play a role in protecting telomeres during interphase when TRF2 levels are depleted. Second, the suppressive function of WRN in mitosis is compromised in the absence of TRF2, despite the high expression of WRN peptides.

Next, I proceeded to test whether TRF2 alone is capable to suppress MAD-TIFs independently of WRN. To examine this, cells were subjected to TRF2 overexpression, which effectively reduced the number of MAD-TIFs in arrested cells transduced with shControl (**Figure 4.13A to C**). However, WRN depletion resulted in a significant number of MAD-TIFs comparable to Vector-shControl cells despite the overexpression of TRF2 (**Figure 4.13B and C**). These findings suggest that WRN supports TRF2 function to maintain the T-loop structure during prolonged mitotic arrest.

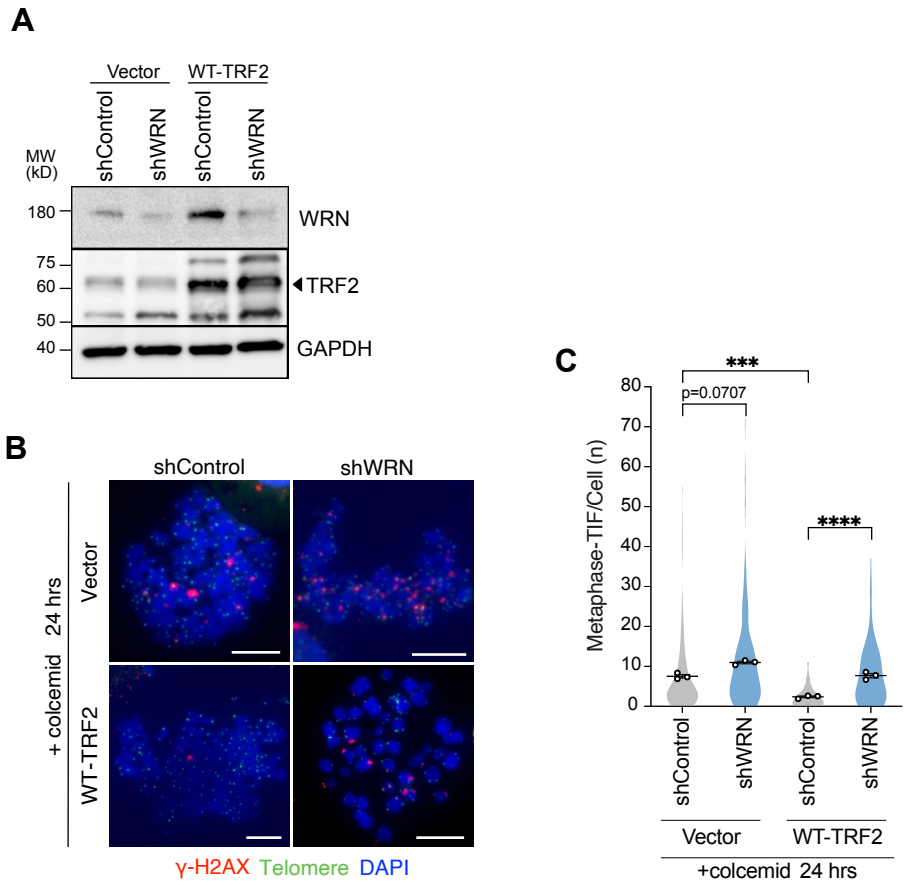

Figure 4.13 WRN supports TRF2 protective function in mitotic telomeres.

A) Immunoblot of endogenous WRN and TRF2. IMR-90 E6E7 hTERT cells expressing exogenous TRF2 were transduced with shWRN by lentiviral infection and analyzed on day 5 post-infection. GAPDH serves as a loading control. **B)** Representative images of meta-TIF assay in indicated cells upon treatment with 100 ng/mL colcemid for 24 hours. **C)** Quantification of meta-TIFs (telomeric signals colocalized with γ-H2AX foci) in cells treated with 100 ng/mL colcemid for 24 hours. Data is collected from three independent experiments (30 metaphases per experiment; mean ± s.e.m.; Kruskal–Wallis followed by Dunn's test).

4.2.5 The suppressive effect of WRN is regulated through Aurora B putative phosphosites.

Post-translational modifications of WRN have been demonstrated to regulate its activity, protein-protein interaction, stability, and subcellular localization (Kusumoto et al., 2007). These observations of the WRN$^{168-333}$ fragment showed the presence of multiple bands

exhibiting different sizes (**Figure 4.7B**). This intriguing finding raises the possibility of kinase-mediated regulation in specific regions of WRN to undergo PTMS particularly in the absence of the remaining domains of WRN, which might hinder the accumulation of such modifications.

By analyzing the sequence of the $WRN^{168-333}$ fragment, a coiled-coil domain was identified comprising amino acid 228-333, which has been previously reported to mediate WRN multimerization (Perry et al., 2010). An *in silico* analysis of the $WRN^{168-333}$ fragment by using the GPS 5.0 software revealed the prediction of an Aurora B consensus phosphorylation site ([R/K]X[S/T][ϕ], where ϕ is hydrophobic residues) (Hengeveld el al., 2012) at position S282 within the coiled-coil domain, as it was determined by Alphafold2 prediction tool (**Figure 4.14A**). Additionally, weak Aurora B putative sites ([R/K]X[S/T]) were predicted at T172, S198, and S312 sites. The observation of a conserved S282 site (RX[ST][ϕ]) across vertebrate species, suggests the relevance of this site to be susceptible to phosphorylation events that likely might regulate specific WRN activities (**Figure 4.14B**). Since Aurora B is required for mitotic telomere deprotection (Hayashi et al., 2012), I aimed to elucidate whether the identified phosphorylation sites are involved in the regulation of the suppressive activity of the N-terminus of WRN. To this end, mutants derived from the $WRN^{168-333}$ fragment were generated in which amino acid substitutions to alanine (phospho-null mutants) or aspartic acid or glutamic acid (phosphomimetic mutants) were introduced at single or multiple Aurora B predicted sites (**Figure 4.14C and Figure 4.15A**). Immunoblot analysis showed a comparable band pattern between the alanine mutants and the original $WRN^{168-333}$ fragment, whereas all phosphomimetic mutants did not show the highest mobility band (**Figure 4.15B**). Importantly, the alanine-mutated fragments could suppress MAD-TIF formation (**Figure 4.15C and D**), whereas the phosphomimetic mutants, failed to suppress MAD-TIFs even in mutants carrying a single modification on S282 (**Figure 4.14C and Figure 4.15D**). Collectively, these findings imply that the protective function of the WRN N-terminus is negatively regulated by phosphorylation at S282.

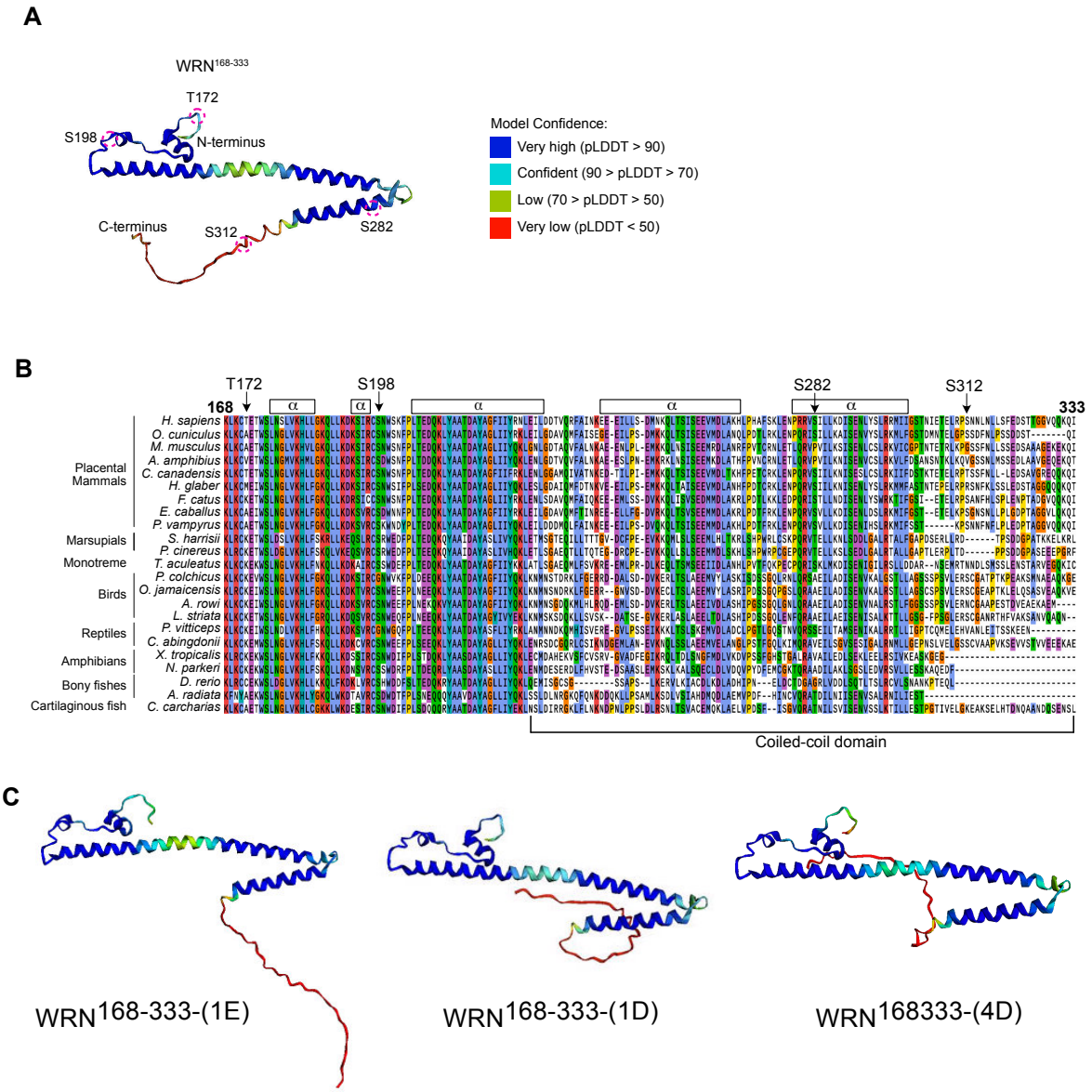

Figure 4.14 The conserved S282 resides in the alpha-helix of the coiled-coil domain.

A) A representative 3D structure of the WRN$^{168-333}$ fragment with a color-coded confidence per-residue (pLDDT) predicted by the AlphaFold2 pipeline. Dashed magenta circles indicate potential Aurora B target sites. **B)** Sequence alignments of human WRN 168-333 aa region with WRN homologs in vertebrate species. Alpha-helices are represented in "α" boxes and positions of the predicted Aurora B sites are shown with arrows. Reported coiled-coil domain is indicated at the bottom (Perry et al., 2010). **C)** Predicted 3D structure of WRN phosphomimetic mutants obtained by AlphaFold2.

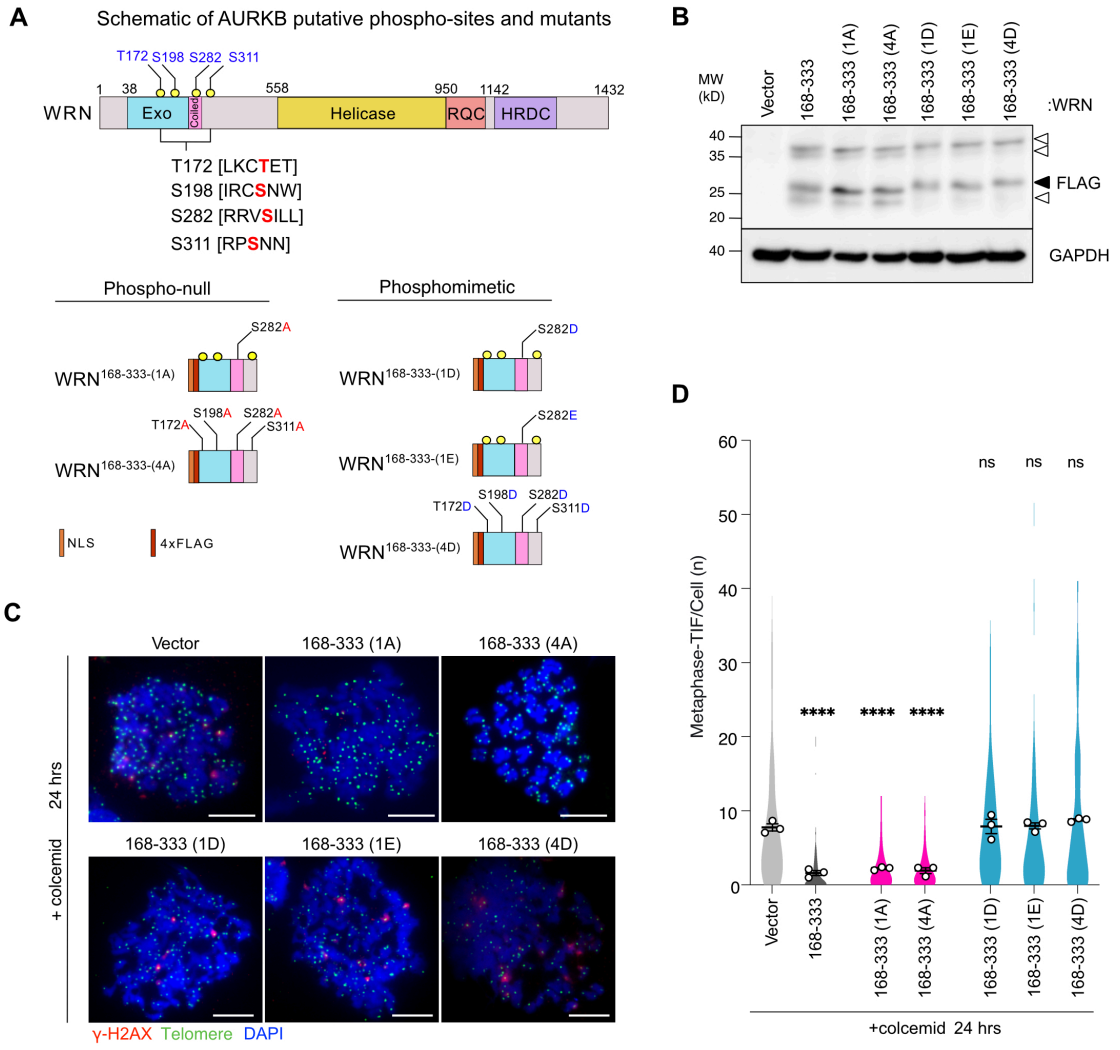

Figure 4.15 Phosphomimetic mutations at S282 in theWRN N-terminus disrupts its suppressive function.

A) Schematic representation of four potential Aurora B sites in the WRN N-terminus (168-333 aa) displaying the sequences of the predicted motif. Aurora B target residues are indicated in bold and red color (Serine (S) or Threonine (T)). Sites of alanine and phosphomimetic mutations on $WRN^{168-333}$ are illustrated. All mutants are tagged with N-terminal NLS and 4xFLAG. **B)** Immunoblot of 4xFLAG-WRN fragments in indicated cells. Transduced cells were harvested on day 12 post-infection. A black arrowhead indicates the expected band size for all the mutants (~ 27 kDa), and white arrowheads indicate additional bands. GAPDH serves as a loading control. **C)** Representative images of meta-TIF assay in cells expressing the mutants indicated in (**A**). Cells were exposed to 100 ng/mL colcemid for 24 hours prior staining. Scale bar, 10 μm. **D)** Quantification of meta-

TIFs (telomeric signals colocalized with γ-H2AX foci) in cells treated with 100 ng/mL colcemid for 24 hours. Data is collected from three independent experiments (30 metaphases per experiment; mean ± s.e.m.; Kruskal–Wallis followed by Dunn's test).

Name	Expected size including NLS-4FL (kD)	Observed band size (kD)	MAD-TIF suppression
WT-WRN	~180	~180	**YES**
WRN^{2-499}	~69	~48, ~80	**YES**
$WRN^{500-946}$	~62	~62,~70	**NO**
$WRN^{947-1432}$	~67	~27,~63,~74	**NO**
WRN^{2-167}	~27	~23,~27	**NO**
$WRN^{168-333}$	~27	~23,~26,~38	**YES**
$WRN^{334-499}$	~27	~23,~62	**NO**
$WRN^{168-250}$	~17	Not expressed	**NO**
$WRN^{251-333}$	~17	~33	**YES** (partial)
$WRN^{168-333}$-1A	~27	~23,~26,~38	**YES**
$WRN^{168-333}$-4A	~27	~23,~26,~38	**YES**
$WRN^{168-333}$-1D	~27	~26,~38	**NO**
$WRN^{168-333}$-1E	~27	~26,~38	**NO**
$WRN^{168-333}$-4D	~27	~26,~38	**NO**

Table 1 Summary of WRN fragments size and phenotypes.

4.3 Discussion

The T-loop capping structure serves to inhibit ATM kinase signaling at the natural ends of chromosomes (Van Ly et al., 2018). One key regulator of T-loop maintenance during the cell cycle is the telomere-binding protein TRF2 (Timashev et al., 2020). Emerging evidence suggests that non-telomeric proteins also play essential roles in T-loop maintenance, particularly in the S-phase (Sarek et al., 2019; Verdun et al., 2006). However, the loss of T-loop in cells undergoing mitotic arrest indicates that the activity of such essential proteins for telomere maintenance is impaired or non-telomeric proteins are able to disrupt the T-loop configuration during various cell cycle stages and cellular conditions.

In this study, the role of WRN helicase in regulating mitotic telomere deprotection was investigated in immortalized fibroblasts and a fibrosarcoma cell line. In a rescue experiment, the findings demonstrated that the number MAD-TIFs is inversely correlated with WRN protein levels (**Figure 4.2A and B**). These observations suggest that variations in WRN protein levels significantly affect the state of the T-loop, and that its depletion might enhance the targeting or activity of enzymes that process T-loops on telomeres. Therefore, WRN can be considered as a critical factor that promotes telomere maintenance by limiting excessive T-loop unwinding. Interestingly, this WRN suppressive function in telomeres is independent of its exonuclease and helicase activities, as observed in cells expressing catalytically inactive mutants that could still suppress MAD-TIFs (**Figure 4.4C**).

Through truncation of WRN, I was able to identify that N-terminal amino acids 168–333 possess a fully repressive effect, but its further truncation into a fragment containing amino acids 251-333 could partially suppress MAD-TIFs (**Figure 4.7D**). An interesting feature that shared all the suppressive N-terminal fragments is the coiled-coil domain (**Table 1**), located within amino acids 228-333, which is required for the multimerization of WRN (Perry et. al., 2010). The N-terminal WRN fragments containing this domain exhibited a higher band shift on SDS-PAGE (**Table 1**). This band shift could be attributed to resistance against SDS-induced denaturation, as previously reported in WRN fragments containing

this coiled-coil domain (Perry et. al., 2010). However, the additional band size does not correspond to the size of multimers, which would be expected to display an apparent molecular weight larger than its monomeric form (Perry et. al., 2010). The presence of PTMs in the oligomers or their cleavage might alter the expected protein size.

The multimerization domain of WRN is known to be involved in the processivity of exonuclease and efficient strand exchange activities (Perry et. al., 2010; Chen et al., 2014). However, the results from this study strongly suggest that the catalytic activity of WRN is not essential for its suppressive function during mitotic arrest. The interaction between multimerized WRN and DNA-dependent protein kinase (DNA-PK) has been found to influence nuclease activity (Perry et. al., 2010). However, it is worth noting that this interaction may not occur or may not be required to activate WRN catalytic activities during mitotic arrest. Although WRN is primarily involved in DNA catalytic activities, it has been reported to possess nonenzymatic functions, such as protecting nascent strands after replication stress without relying on the multimerization domain (Su et al., 2014). Therefore, the findings in this work reveal a novel nonenzymatic function that resides in the multimerization domain of WRN that contributes to the maintenance of mitotic telomere caps.

I found the observation regarding the lack of enzymatic activity of WRN at telomeres during mitosis, particularly in cells overexpressing WT-WRN, to be interesting. Numerous studies have demonstrated the efficacy of WRN in targeting and resolving various DNA substrates present on telomeres, including G-quadruplex and D-loops (Kar et al., 2016; Tomaska et al., 2019). However, the present findings in this studyindicate that WRN is unable to resolve D-loop junction during mitotic arrest, which is proposed to be a structure formed at the T-loop base. This observation suggests that WRN may be enzymatically inactive during mitosis. Alternatively, WRN could still be active, but the T-loop might lack a suitable substrate for WRN. Griffith's group has proposed a hypothesis that challenges the conventional understanding of T-loop remodeling. According to their proposal, T-loops can be formed through telomere transcription, which involves the invasion of blunt-ended telomeric DNA into the transcription bubble (Kar et al., 2016). As a result, the formation of stable junctions, replication forks, or HJs could be generated within the T-loop. The

complexity of these junctions can represent a challenge for WRN activities, except for HJs, which are efficiently processed (Constantinou et al., 2000; Mohaghegh et al., 2001; Nora et al., 2010). Electron microscopy has visualized aggregations of WRN with DNA molecules containing HJs (Compton et al., 2008). However, since the $WRN^{168–333}$ fragment lacks a DNA-binding RQC motif, it is unlikely that the protective function of WRN relies on direct DNA binding activity.

Suppression of MAD-TIFs upon overexpression of WT-WRN or its derived fragments could potentially result from the indirect attenuation of Aurora B or ATM kinase activities during mitotic arrest. Aurora B activity is required to induce mitotic telomere deprotection, while ATM senses exposed telomeric ends and promotes the phosphorylation of histone H2AX (Burma et al., 2001; Guo et al., 2007; Hayashi et al., 2012). Observations from live cell imaging in cells that could sustain mitotic arrest indicated that overexpresion of the $WRN^{168-333}$ fragment containing the multimerization domain did not affect Aurora B (**Figure 4.10B**). Furthermore, the high expression of $WRN^{168-333}$ did not hinder the detection of DNA damages on mitotic chromosomes (**Figure 4.11C**). However, this observation does not definitely confirm that ATM remained active, since other kinases might be responsible for histone H2AX. Nevertheless, the obtained results suggest that multimerization domain of WRN directly influences the state of the T-loop, rather than inhibiting the mitotic checkpoints or DDR upstream signaling. This indicates that the primary function of WRN is focused on protecting chromosome ends during mitotic arrest, possibly by counteracting the activity of enzymes able to disrupt T-loop structure or stabilizing the D-loop junction.

I found that the protective function of the WRN coiled-coil domain is dependent on TRF2 at mitotic telomeres (**Figure 4.12C**). TRF2 has been suggested to be essential for T-loop formation by wrapping approximately 90 bp of DNA, a function that resides in its TRFH domain (Doksani et al., 2013; Benarroch-Popivker et al., 2016). Additionally, TRF2 plays a crucial role in promoting the strand invasion of the telomeric 3' overhang, thus serving as a pivotal protein in the formation and maintenance of the T-loop structure (Timashev et al., 2020). However, the observations on the excessive telomere deprotection observed in WRN knockdown cells (**Figure 4.1C**) suggest that TRF2 alone is not sufficient to provide complete protection to T-loops under specific cellular conditions, such as mitotic arrest. To

stabilize its interaction with telomeric DNA, TRF2 needs to engage with specific protein partners by diffusing along telomeric regions (Lin, et al., 2014). Therefore, I can infer that WRN may enhance the interaction strength between TRF2 with the T-loop base (**Figure 4.3.1A**). Nevertheless, this study uncovers the involvement of WRN, a non-telomeric protein, in supporting the ability of TRF2 to protect the T-loop in mitotically arrested cells.

Next, I speculated that the WRN suppressive region could be regulated during mitotic arrest. Sequence analysis of the $WRN^{168–333}$ fragment, which contains the coiled-coil domain, revealed the presence of four Aurora B consensus sequences (**Figure 4.15A**). This prompted me to investigate whether Aurora B regulates the suppressive effect of the coiled-coil region of WRN through phosphorylations. Amino acid substitutions were inserted at the identified sites and examined the impact on the suppressive activity of the N-terminal fragment of WRN. As a result, phosphomimicking mutants showing loss of suppressive function (**Figure 4.15D**) indicated that phosphorylation might disrupt the ability of WRN to protect the T-loops. However, confirmation of *in-vivo* phosphorylations in WRN during mitotic arrest is needed. Previous studies conducting a phosphoproteomic analysis identified phosphorylation at S282 in cycling cells (Shiromizu et al., 2013; Giansanti et al., 2013), which, in conjunction with this study, suggests that the repressive effect of WRN might be regulated by upstream kinases, such as Aurora B kinase.

The importance of the putative sites of Aurora B might have an impact on the structure and function of the N-terminus of WRN. Phosphorylations have been shown to impact the ability of proteins to form oligomers (Hashimoto et al., 2010). Coiled-coil motifs, which fold into α-helical structures with hydrophobic side chains that facilitate aggregation, can be disrupted by the insertion of negatively charged amino acids or phosphate groups, leading to impaired protein multimerization, aggregation, and localization (Szilák et al., 1997; Groover et al., 2020). Furthermore, phosphorylation of α-helices has been found to strongly inhibit protein aggregate and fibril formation by disrupting the nucleation process (Mishra et al., 2012; Groover et al., 2020). In some proteins, a single phosphorylation event can modify the α-helical conformation (Dorovkov et al., 2011). Therefore, the nonphosphorylatable mutants used in this study might suppress MAD-TIF formation by facilitating multimerization, which subsequently leads to the formation of aggregates

capable of sequestering distinct proteins, including those involved in T-loop unwinding. Disruption of WRN multimerization might be promoted upon Aurora B activity. Phosphorylations by Aurora B might alter the structure of the coiled-coil domain, keeping WRN in a monomeric state unable to inhibit mitotic telomere deprotection (**Figure 4.3.1A**). This model might explain the absence of mitotic telomere deprotection observed upon Aurora B inhibition by hesperadin treatment (Hayashi et al., 2012). Interestingly, the expression of the $WRN^{168–333}$ fragment exhibited a more pronounced suppressive effect compared to the full-length WT-WRN in WRN-depleted cells (**Figure 4.2B and Figure 4.7E**). This suggests that other domains of WRN may influence the coiled-coil property or its PTMs. Although a protein folding prediction tool revealed an unaltered α-helical structure in phosphomimetic mutants (**Figure 4.14C**), the actual structural integrity of all the expressed phospho-mutants utilized in this study remains uncertain. It is crucial to highlight that all the phosphomimetic fragments in this study contain a mutation at S282 within the coiled-coil domain. However, it remains uncertain whether mutations in other serine or threonine residues within the α-helix would yield similar outcomes in terms of the failed suppression of MAD-TIFs. Further studies are needed to determine the specific effects of mutations at different positions within the coiled-coil domain and their impact on the ability to suppress MAD-TIF formation. Nevertheless, at this point the collective findings suggest that the α-helical structure of the WRN N-terminus and its PTMs, especially at S282, likely play a role in safeguarding mitotic telomeres.

As conclusion, a novel function of WRN has been identified involving the multimerization domain that supports TRF2 in maintaining T-loops during prolonged mitotic arrest, an event that occurs in telomere crisis and mitotic drug treatment that can lead to cell death (Hayashi 2012; Hayashi 2015; Masamsetti et al., 2019). The development of inhibitors against WRN helicase activity for clinical purposes has proven valuable in understanding the role of WRN in cells resistant to drug-induced DNA lesions (Aggarwal et al., 2013; Moles et al., 2016; Morales-Juarez and Jackson, 2022). By uncovering WRN function in mitosis, the present study provides new insights into the broader functions of RecQ helicases beyond their well-studied roles in DNA repair and telomere maintenance during the S-phase of the cell cycle that can have an impact in cancer evolution. Therefore, I consider that this study offers valuable perspectives in considering mitotic arrest as a potential alternative to sensitize malignant cells to cell death via regulation of proteins

responsible in telomere maintenance. Importantly, the obtained results also raise the possibility that other enzymes are involved in mitotic telomere deprotection. In Chapter 5 the involvement of additional factors in the T-loop unwinding pathway will be reviewed, providing a comprehensive understanding of the intricate mechanisms underlying telomere dynamics.

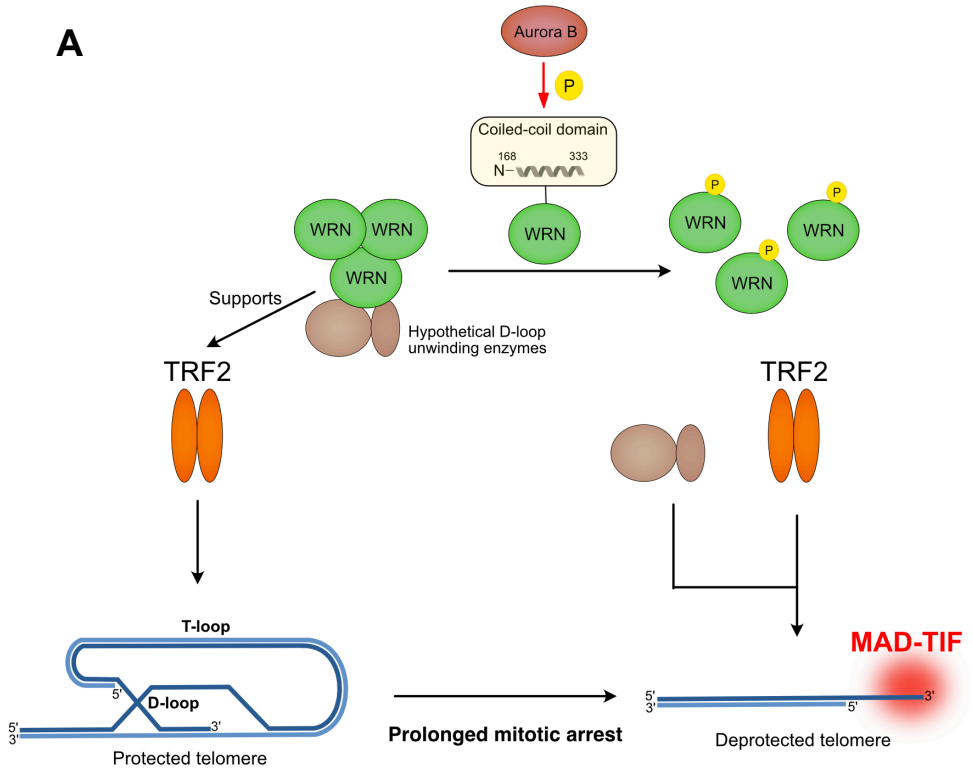

Figure 4.16 Hypothetical model of WRN function in mitotic telomere deprotection.
A) The study also identifies specific regions within the N-terminal fragment of WRN, particularly the coiled-coil domain, that contribute to the suppression of mitotic telomere deprotection. The multimerization domain of WRN is implicated in protecting telomeres by counteracting the activity of enzymes that disrupt the T-loop structure. The study suggests that WRN interacts with telomere-binding protein TRF2 to maintain T-loop integrity during mitotic arrest. Furthermore, the suppressive effect of WRN might be regulated by phosphorylation events mediated by Aurora B kinase, causing the disruption of WRN to multimerize and halts TRF2 protective activity.

References

Aggarwal, Monika, Taraswi Banerjee, Joshua A. Sommers, Chiara Iannascoli, Pietro Pichierri, Robert H. Shoemaker, and Robert M. Brosh. “Werner Syndrome Helicase Has a Critical Role in DNA Damage Responses in the Absence of a Functional Fanconi Anemia Pathway.” *Cancer Research* 73, no. 17 (September 1, 2013): 5497–5507. https://doi.org/10.1158/0008-5472.CAN-12-2975.

Bahr, Anne, Fabienne De Graeve, Claude Kedinger, and Bruno Chatton. “Point Mutations Causing Bloom’s Syndrome Abolish ATPase and DNA Helicase Activities of the BLM Protein.” *Oncogene* 17, no. 20 (November 1998): 2565–71. https://doi.org/10.1038/sj.onc.1202389.

Benarroch-Popivker, Delphine, Sabrina Pisano, Aaron Mendez-Bermudez, Liudmyla Lototska, Parminder Kaur, Serge Bauwens, Nadir Djerbi, et al. “TRF2-Mediated Control of Telomere DNA Topology as a Mechanism for Chromosome-End Protection.” *Molecular Cell* 61, no. 2 (January 21, 2016): 274–86. https://doi.org/10.1016/j.molcel.2015.12.009.

Bernstein, Douglas A., and James L. Keck. “Conferring Substrate Specificity to DNA Helicases: Role of the RecQ HRDC Domain.” *Structure* 13, no. 8 (August 1, 2005): 1173–82. https://doi.org/10.1016/j.str.2005.04.018.

Blackburn, E H, and S S Chiou. “Non-Nucleosomal Packaging of a Tandemly Repeated DNA Sequence at Termini of Extrachromosomal DNA Coding for RRNA in Tetrahymena.” *Proceedings of the National Academy of Sciences of the United States of America* 78, no. 4 (April 1981): 2263–67.

Blander, Gil, Jonathan Kipnis, Juan Fernando Martinez Leal, Chang-En Yu, Gerard D. Schellenberg, and Moshe Oren. “Physical and Functional Interaction between P53 and the Werner’s Syndrome Protein *.” *Journal of Biological Chemistry* 274, no. 41 (October 8, 1999): 29463–69. https://doi.org/10.1074/jbc.274.41.29463.

Bodnar, A. G., M. Ouellette, M. Frolkis, S. E. Holt, C. P. Chiu, G. B. Morin, C. B. Harley, J. W. Shay, S. Lichtsteiner, and W. E. Wright. “Extension of Life-Span by Introduction of Telomerase into Normal Human Cells.” *Science (New York, N.Y.)* 279, no. 5349 (January 16, 1998): 349–52. https://doi.org/10.1126/science.279.5349.349.

Brito, Daniela A., and Conly L. Rieder. “Mitotic Checkpoint Slippage in Humans Occurs via Cyclin B Destruction in the Presence of an Active Checkpoint.” *Current Biology: CB* 16, no. 12 (June 20, 2006): 1194–1200. https://doi.org/10.1016/j.cub.2006.04.043.

Broccoli, Dominique, Agata Smogorzewska, Laura Chong, and Titia de Lange. “Human Telomeres Contain Two Distinct Myb–Related Proteins, TRF1 and TRF2.” *Nature Genetics* 17, no. 2 (October 1997): 231–35. https://doi.org/10.1038/ng1097-231.

Burma, S., B. P. Chen, M. Murphy, A. Kurimasa, and D. J. Chen. “ATM Phosphorylates Histone H2AX in Response to DNA Double-Strand Breaks.” *The Journal of Biological Chemistry* 276, no. 45 (November 9, 2001): 42462–67. https://doi.org/10.1074/jbc.C100466200.

Capper, Rebecca, Bethan Britt-Compton, Maira Tankimanova, Jan Rowson, Boitelo Letsolo, Stephen Man, Michele Haughton, and Duncan M. Baird. “The Nature of Telomere Fusion and a Definition of the Critical Telomere Length in Human Cells.” *Genes & Development* 21, no. 19 (October 1, 2007): 2495–2508. https://doi.org/10.1101/gad.439107.

Carmena, Mar, Michael Wheelock, Hironori Funabiki, and William C. Earnshaw. “The Chromosomal Passenger Complex (CPC): From Easy Rider to the Godfather of Mitosis.” *Nature Reviews Molecular Cell Biology* 13, no. 12 (December 2012): 789–803. https://doi.org/10.1038/nrm3474.

Carmena, Mar. “Cytokinesis: The Final Stop for the Chromosomal Passengers.” *Biochemical Society Transactions* 36, no. Pt 3 (June 2008): 367–70. https://doi.org/10.1042/BST0360367.

Cesare, Anthony J., and Jan Karlseder. “A Three-State Model of Telomere Control over Human Proliferative Boundaries.” *Current Opinion in Cell Biology* 24, no. 6 (December 2012): 731–38. https://doi.org/10.1016/j.ceb.2012.08.007.

Cesare, Anthony J., Christopher M. Heaphy, and Roderick J. O’Sullivan. “Visualization of Telomere Integrity and Function In Vitro and In Vivo Using Immunofluorescence Techniques.” *Current Protocols in Cytometry* 73 (July 1, 2015): 12.40.1-12.40.31. https://doi.org/10.1002/0471142956.cy1240s73.

Cesare, Anthony J., Makoto T. Hayashi, Laure Crabbe, and Jan Karlseder. “The Telomere Deprotection Response Is Functionally Distinct from the Genomic DNA Damage Response.” *Molecular Cell* 51, no. 2 (July 25, 2013): 141–55. https://doi.org/10.1016/j.molcel.2013.06.006.

Chen, Jun, Sha Jin, Stephen K. Tahir, Haichao Zhang, Xuesong Liu, Aparna V. Sarthy, Thomas P. McGonigal, Zhihong Liu, Saul H. Rosenberg, and Shi-Chung Ng. “Survivin Enhances Aurora-B Kinase Activity and Localizes Aurora-B in Human Cells.” *The Journal of Biological Chemistry* 278, no. 1 (January 3, 2003): 486–90. https://doi.org/10.1074/jbc.M211119200.

Cheng, Wen-Hsing, Diana Muftic, Meltem Muftuoglu, Lale Dawut, Christa Morris, Thomas Helleday, Yosef Shiloh, and Vilhelm A. Bohr. “WRN Is Required for ATM Activation and the S-Phase Checkpoint in Response to Interstrand Cross-Link-Induced DNA Double-Strand Breaks.” *Molecular Biology of the Cell* 19, no. 9 (September 2008): 3923–33. https://doi.org/10.1091/mbc.e07-07-0698.

Compton, Sarah A., Gökhan Tolun, Ashwini S. Kamath-Loeb, Lawrence A. Loeb, and Jack D. Griffith. “The Werner Syndrome Protein Binds Replication Fork and Holliday Junction DNAs as an Oligomer.” *The Journal of Biological Chemistry* 283, no. 36 (September 5, 2008): 24478–83. https://doi.org/10.1074/jbc.M803370200.

Constantinou, Angelos, Madalena Tarsounas, Julia K. Karow, Robert M. Brosh, Vilhelm A. Bohr, Ian D. Hickson, and Stephen C. West. “Werner’s Syndrome Protein (WRN) Migrates Holliday Junctions and Co-Localizes with RPA upon Replication Arrest.” *EMBO Reports* 1, no. 1 (July 17, 2000): 80–84. https://doi.org/10.1093/embo-reports/kvd004.

Croteau, Deborah L., Venkateswarlu Popuri, Patricia L. Opresko, and Vilhelm A. Bohr. “Human RecQ Helicases in DNA Repair, Recombination, and Replication.” *Annual Review of Biochemistry* 83 (2014): 519–52. https://doi.org/10.1146/annurev-biochem-060713-035428.

Dai, Jun, Beth A. Sullivan, and Jonathan M. G. Higgins. “Regulation of Mitotic Chromosome Cohesion by Haspin and Aurora B.” *Developmental Cell* 11, no. 5 (November 2006): 741–50. https://doi.org/10.1016/j.devcel.2006.09.018.

Daniel, Michael, Gregory W. Peek, and Trygve O. Tollefsbol. “Regulation of the Human Catalytic Subunit of Telomerase (HTERT).” *Gene* 498, no. 2 (May 1, 2012): 135–46. https://doi.org/10.1016/j.gene.2012.01.095.

Deursen, Jan M. van. “The Role of Senescent Cells in Ageing.” *Nature* 509, no. 7501 (May 22, 2014): 439–46. https://doi.org/10.1038/nature13193.

Doksani, Ylli, and Titia de Lange. “The Role of Double-Strand Break Repair Pathways at Functional and Dysfunctional Telomeres.” *Cold Spring Harbor Perspectives in Biology* 6, no. 12 (September 16, 2014): a016576. https://doi.org/10.1101/cshperspect.a016576.

Doksani, Ylli, John Y. Wu, Titia de Lange, and Xiaowei Zhuang. “Super-Resolution Fluorescence Imaging of Telomeres Reveals TRF2-Dependent t-Loop Formation.” *Cell* 155, no. 2 (October 10, 2013): 345–56. https://doi.org/10.1016/j.cell.2013.09.048.

Dorovkov, Maxim V., Alla S. Kostyukova, and Alexey G. Ryazanov. “Phosphorylation of Annexin A1 by TRPM7 Kinase: A Switch Regulating the Induction of an α-Helix.” *Biochemistry* 50, no. 12 (March 29, 2011): 2187–93. https://doi.org/10.1021/bi101963h.

Fagagna, Fabrizio d’Adda di, Philip M. Reaper, Lorena Clay-Farrace, Heike Fiegler, Philippa Carr, Thomas von Zglinicki, Gabriele Saretzki, Nigel P. Carter, and Stephen P. Jackson. “A DNA Damage Checkpoint Response in Telomere-Initiated Senescence.” *Nature* 426, no. 6963 (November 2003): 194–98. https://doi.org/10.1038/nature02118.

Fragkos, Michalis, and Peter Beard. “Mitotic Catastrophe Occurs in the Absence of Apoptosis in P53-Null Cells with a Defective G1 Checkpoint.” *PloS One* 6, no. 8 (2011): e22946. https://doi.org/10.1371/journal.pone.0022946.

Fujiwara, Y., T. Higashikawa, and M. Tatsumi. “A Retarded Rate of DNA Replication and Normal Level of DNA Repair in Werner’s Syndrome Fibroblasts in Culture.” *Journal of Cellular Physiology* 92, no. 3 (September 1977): 365–74. https://doi.org/10.1002/jcp.1040920305.

Futami, Kazunobu, Motoki Takagi, Akira Shimamoto, Masanobu Sugimoto, and Yasuhiro Furuichi. “Increased Chemotherapeutic Activity of Camptothecin in Cancer Cells by SiRNA-Induced Silencing of WRN Helicase.” *Biological & Pharmaceutical Bulletin* 30, no. 10 (October 2007): 1958–61. https://doi.org/10.1248/bpb.30.1958.

Ghosh, Avik K., Marie L. Rossi, Dharmendra Kumar Singh, Christopher Dunn, Mahesh Ramamoorthy, Deborah L. Croteau, Yie Liu, and Vilhelm A. Bohr. “RECQL4, the Protein Mutated in Rothmund-Thomson Syndrome, Functions in Telomere Maintenance.” *The Journal of Biological Chemistry* 287, no. 1 (January 2, 2012): 196–209. https://doi.org/10.1074/jbc.M111.295063.

Giansanti, Piero, Matthew P. Stokes, Jeffrey C. Silva, Arjen Scholten, and Albert J. R. Heck. “Interrogating CAMP-Dependent Kinase Signaling in Jurkat T Cells via a Protein Kinase A Targeted Immune-Precipitation Phosphoproteomics Approach.” *Molecular & Cellular Proteomics: MCP* 12, no. 11 (November 2013): 3350–59. https://doi.org/10.1074/mcp.O113.028456.

Gray, M. D., J. C. Shen, A. S. Kamath-Loeb, A. Blank, B. L. Sopher, G. M. Martin, J. Oshima, and L. A. Loeb. “The Werner Syndrome Protein Is a DNA Helicase.” *Nature Genetics* 17, no. 1 (September 1997): 100–103. https://doi.org/10.1038/ng0997-100.

Griffith, J. D., L. Comeau, S. Rosenfield, R. M. Stansel, A. Bianchi, H. Moss, and T. de Lange. “Mammalian Telomeres End in a Large Duplex Loop.” *Cell* 97, no. 4 (May 14, 1999): 503–14. https://doi.org/10.1016/s0092-8674(00)80760-6.

Groover, Sharon E., Maryssa Beasley, Visvanathan Ramamurthy, and Justin Legleiter. “Phosphomimetic Mutations Impact Huntingtin Aggregation in the Presence of a Variety of Lipid Systems.” *Biochemistry* 59, no. 49 (December 15, 2020): 4681–93. https://doi.org/10.1021/acs.biochem.0c00788.

Guo, Xiaolan, Yibin Deng, Yahong Lin, Wilfredo Cosme-Blanco, Suzanne Chan, Hua He, Guohua Yuan, Eric J Brown, and Sandy Chang. “Dysfunctional Telomeres Activate an ATM-ATR-Dependent DNA Damage Response to Suppress Tumorigenesis.” *The EMBO Journal* 26, no. 22 (November 14, 2007): 4709–19. https://doi.org/10.1038/sj.emboj.7601893.

Hashimoto, Kosuke, and Anna R. Panchenko. “Mechanisms of Protein Oligomerization, the Critical Role of Insertions and Deletions in Maintaining Different Oligomeric States.” *Proceedings of the National Academy of Sciences of the United States of*

America 107, no. 47 (November 23, 2010): 20352–57. https://doi.org/10.1073/pnas.1012999107.

Hauf, Silke, Richard W. Cole, Sabrina LaTerra, Christine Zimmer, Gisela Schnapp, Rainer Walter, Armin Heckel, Jacques van Meel, Conly L. Rieder, and Jan-Michael Peters. "The Small Molecule Hesperadin Reveals a Role for Aurora B in Correcting Kinetochore-Microtubule Attachment and in Maintaining the Spindle Assembly Checkpoint." *The Journal of Cell Biology* 161, no. 2 (April 28, 2003): 281–94. https://doi.org/10.1083/jcb.200208092.

Hayashi, Makoto T., Anthony J. Cesare, James A. J. Fitzpatrick, Eros Lazzerini-Denchi, and Jan Karlseder. "A Telomere Dependent DNA Damage Checkpoint Induced by Prolonged Mitotic Arrest." *Nature Structural & Molecular Biology* 19, no. 4 (March 11, 2012): 387–94. https://doi.org/10.1038/nsmb.2245.

Hayashi, Makoto T., Anthony J. Cesare, Teresa Rivera, and Jan Karlseder. "Cell Death during Crisis Is Mediated by Mitotic Telomere Deprotection." *Nature* 522, no. 7557 (June 25, 2015): 492–96. https://doi.org/10.1038/nature14513.

Hayflick, L. "The Limited in Vitro Lifetime of Human Diploid Cell Strains." *Experimental Cell Research* 37, no. 3 (March 1, 1965): 614–36. https://doi.org/10.1016/0014-4827(65)90211-9.

Hayflick, L., and P. S. Moorhead. "The Serial Cultivation of Human Diploid Cell Strains." *Experimental Cell Research* 25, no. 3 (December 1, 1961): 585–621. https://doi.org/10.1016/0014-4827(61)90192-6.

Huang, Shurong, Baomin Li, Matthew D. Gray, Junko Oshima, I. Saira Mian, and Judith Campisi. "The Premature Ageing Syndrome Protein, WRN, Is a 3′→5′ Exonuclease." *Nature Genetics* 20, no. 2 (October 1998): 114–16. https://doi.org/10.1038/2410.

Ide, Satoru, Asuka Sasaki, Yusuke Kawamoto, Toshikazu Bando, Hiroshi Sugiyama, and Kazuhiro Maeshima. "Telomere-Specific Chromatin Capture Using a Pyrrole–Imidazole Polyamide Probe for the Identification of Proteins and Non-Coding RNAs." *Epigenetics & Chromatin* 14, no. 1 (October 9, 2021): 46. https://doi.org/10.1186/s13072-021-00421-8.

Jelluma, Nannette, Arjan B. Brenkman, Niels J. F. van den Broek, Carin W. A. Cruijsen, Maria H. J. van Osch, Susanne M. A. Lens, René H. Medema, and Geert J. P. L.

Kops. “Mps1 Phosphorylates Borealin to Control Aurora B Activity and Chromosome Alignment.” *Cell* 132, no. 2 (January 25, 2008): 233–46. https://doi.org/10.1016/j.cell.2007.11.046.

Jumper, John, Richard Evans, Alexander Pritzel, Tim Green, Michael Figurnov, Olaf Ronneberger, Kathryn Tunyasuvunakool, et al. “Highly Accurate Protein Structure Prediction with AlphaFold.” *Nature* 596, no. 7873 (August 2021): 583–89. https://doi.org/10.1038/s41586-021-03819-2.

Kar, Anirban, Smaranda Willcox, and Jack D. Griffith. “Transcription of Telomeric DNA Leads to High Levels of Homologous Recombination and T-Loops.” *Nucleic Acids Research* 44, no. 19 (November 2, 2016): 9369–80. https://doi.org/10.1093/nar/gkw779.

Karlseder, J., D. Broccoli, Y. Dai, S. Hardy, and T. de Lange. “P53- and ATM-Dependent Apoptosis Induced by Telomeres Lacking TRF2.” *Science (New York, N.Y.)* 283, no. 5406 (February 26, 1999): 1321–25. https://doi.org/10.1126/science.283.5406.1321.

Karlseder, Jan, Agata Smogorzewska, and Titia de Lange. “Senescence Induced by Altered Telomere State, Not Telomere Loss.” *Science (New York, N.Y.)* 295, no. 5564 (March 29, 2002): 2446–49. https://doi.org/10.1126/science.1069523.

Karmakar, Parimal, Jason Piotrowski, Robert M. Brosh, Joshua A. Sommers, Susan P. Lees Miller, Wen-Hsing Cheng, Carey M. Snowden, Dale A. Ramsden, and Vilhelm A. Bohr. “Werner Protein Is a Target of DNA-Dependent Protein Kinase in Vivo and in Vitro, and Its Catalytic Activities Are Regulated by Phosphorylation*.” *Journal of Biological Chemistry* 277, no. 21 (May 24, 2002): 18291–302. https://doi.org/10.1074/jbc.M111523200.

Karow, J. K., R. H. Newman, P. S. Freemont, and I. D. Hickson. “Oligomeric Ring Structure of the Bloom’s Syndrome Helicase.” *Current Biology: CB* 9, no. 11 (June 3, 1999): 597–600. https://doi.org/10.1016/s0960-9822(99)80264-4.

Kitano, Ken, Sun-Yong Kim, and Toshio Hakoshima. “Structural Basis for DNA Strand Separation by the Unconventional Winged-Helix Domain of RecQ Helicase WRN.” *Structure (London, England: 1993)* 18, no. 2 (February 10, 2010): 177–87. https://doi.org/10.1016/j.str.2009.12.011.

Kim, Young Mee, and Byong-Seok Choi. “Structure and Function of the Regulatory HRDC Domain from Human Bloom Syndrome Protein.” Nucleic Acids Research 38, no. 21 (November 2010): 7764–77. https://doi.org/10.1093/nar/gkq586.

Kusano, K., M. E. Berres, and W. R. Engels. “Evolution of the RECQ Family of Helicases: A Drosophila Homolog, Dmblm, Is Similar to the Human Bloom Syndrome Gene.” *Genetics* 151, no. 3 (March 1999): 1027–39. https://doi.org/10.1093/genetics/151.3.1027.

Kusumoto, Rika, Meltem Muftuoglu, and Vilhelm A. Bohr. “The Role of WRN in DNA Repair Is Affected by Post-Translational Modifications.” *Mechanisms of Ageing and Development* 128, no. 1 (January 2007): 50–57. https://doi.org/10.1016/j.mad.2006.11.010.

Kwon, So Mee, Sun Mi Hong, Young-Kyoung Lee, Seongki Min, and Gyesoon Yoon. “Metabolic Features and Regulation in Cell Senescence.” *BMB Reports* 52, no. 1 (January 2019): 5–12. https://doi.org/10.5483/BMBRep.2019.52.1.291.

Lai, S-K, C-H Wong, Y-P Lee, and H-Y Li. “Caspase-3-Mediated Degradation of Condensin Cap-H Regulates Mitotic Cell Death.” *Cell Death and Differentiation* 18, no. 6 (June 2011): 996–1004. https://doi.org/10.1038/cdd.2010.165.

Lan, Li, Satoshi Nakajima, Kenshi Komatsu, Andre Nussenzweig, Akira Shimamoto, Junko Oshima, and Akira Yasui. “Accumulation of Werner Protein at DNA Double-Strand Breaks in Human Cells.” *Journal of Cell Science* 118, no. Pt 18 (September 15, 2005): 4153–62. https://doi.org/10.1242/jcs.02544.

Lange, Titia de. “T-Loops and the Origin of Telomeres.” *Nature Reviews Molecular Cell Biology* 5, no. 4 (April 2004): 323–29. https://doi.org/10.1038/nrm1359.

Lara-Gonzalez, Pablo, Jonathon Pines, and Arshad Desai. “Spindle Assembly Checkpoint Activation and Silencing at Kinetochores.” *Seminars in Cell & Developmental Biology* 117 (September 2021): 86–98. https://doi.org/10.1016/j.semcdb.2021.06.009.

Larsen, Nicolai Balle, and Ian D. Hickson. “RecQ Helicases: Conserved Guardians of Genomic Integrity.” *Advances in Experimental Medicine and Biology* 767 (2013): 161–84. https://doi.org/10.1007/978-1-4614-5037-5_8.

Le Poole, I. C., F. M. van den Berg, R. M. van den Wijngaard, D. A. Galloway, P. J. van Amstel, A. A. Buffing, H. L. Smits, W. Westerhof, and P. K. Das. “Generation of a Human Melanocyte Cell Line by Introduction of HPV16 E6 and E7 Genes.” *In Vitro Cellular & Developmental Biology. Animal* 33, no. 1 (January 1997): 42–49. https://doi.org/10.1007/s11626-997-0021-6.

Lee, Mina, Soochul Shin, Heesoo Uhm, Heesun Hong, Jaewon Kirk, Kwangbeom Hyun, Tomasz Kulikowicz, et al. “Multiple RPAs Make WRN Syndrome Protein a Superhelicase.” *Nucleic Acids Research* 46, no. 9 (May 18, 2018): 4689–98. https://doi.org/10.1093/nar/gky272.

Li, B., S. Oestreich, and T. de Lange. “Identification of Human Rap1: Implications for Telomere Evolution.” *Cell* 101, no. 5 (May 26, 2000): 471–83. https://doi.org/10.1016/s0092-8674(00)80858-2.

Lieb, Simone, Silvia Blaha-Ostermann, Elisabeth Kamper, Janine Rippka, Cornelia Schwarz, Katharina Ehrenhöfer-Wölfer, Andreas Schlattl, et al. “Werner Syndrome Helicase Is a Selective Vulnerability of Microsatellite Instability-High Tumor Cells.” *ELife* 8 (n.d.): e43333. https://doi.org/10.7554/eLife.43333.

Lillard-Wetherell, Kate, Amrita Machwe, Gregory T. Langland, Kelly A. Combs, Gregory K. Behbehani, Steven A. Schonberg, James German, John J. Turchi, David K. Orren, and Joanna Groden. “Association and Regulation of the BLM Helicase by the Telomere Proteins TRF1 and TRF2.” *Human Molecular Genetics* 13, no. 17 (September 1, 2004): 1919–32. https://doi.org/10.1093/hmg/ddh193.

Lin, Jiangguo, Preston Countryman, Noah Buncher, Parminder Kaur, Longjiang E, Yiyun Zhang, Greg Gibson, et al. “TRF1 and TRF2 Use Different Mechanisms to Find Telomeric DNA but Share a Novel Mechanism to Search for Protein Partners at Telomeres.” *Nucleic Acids Research* 42, no. 4 (February 2014): 2493–2504. https://doi.org/10.1093/nar/gkt1132.

Liu, Tiantian, Xiaotian Yuan, and Dawei Xu. “Cancer-Specific Telomerase Reverse Transcriptase (TERT) Promoter Mutations: Biological and Clinical Implications.” *Genes* 7, no. 7 (July 18, 2016): 38. https://doi.org/10.3390/genes7070038.

Liu, Yu, Samuel I. Bloom, and Anthony J. Donato. “The Role of Senescence, Telomere Dysfunction and Shelterin in Vascular Aging.” *Microcirculation (New York, N.Y. : 1994)* 26, no. 2 (February 2019): e12487. https://doi.org/10.1111/micc.12487.

Lu, Huiming, Raghavendra A. Shamanna, Jessica K. de Freitas, Mustafa Okur, Prabhat Khadka, Tomasz Kulikowicz, Priscella P. Holland, et al. “Cell Cycle-Dependent Phosphorylation Regulates RECQL4 Pathway Choice and Ubiquitination in DNA Double-Strand Break Repair.” *Nature Communications* 8, no. 1 (December 11, 2017): 2039. https://doi.org/10.1038/s41467-017-02146-3.

Lucic, Bojana, Ying Zhang, Oliver King, Ramiro Mendoza-Maldonado, Matteo Berti, Frank H. Niesen, Nicola A. Burgess-Brown, et al. “A Prominent β-Hairpin Structure in the Winged-Helix Domain of RECQ1 Is Required for DNA Unwinding and Oligomer Formation.” *Nucleic Acids Research* 39, no. 5 (March 2011): 1703–17. https://doi.org/10.1093/nar/gkq1031.

Machwe, Amrita, Liren Xiao, and David K. Orren. “TRF2 Recruits the Werner Syndrome (WRN) Exonuclease for Processing of Telomeric DNA.” *Oncogene* 23, no. 1 (January 2004): 149–56. https://doi.org/10.1038/sj.onc.1206906.

Makarov, V. L., Y. Hirose, and J. P. Langmore. “Long G Tails at Both Ends of Human Chromosomes Suggest a C Strand Degradation Mechanism for Telomere Shortening.” *Cell* 88, no. 5 (March 7, 1997): 657–66. https://doi.org/10.1016/s0092-8674(00)81908-x.

Mao, Zhiyong, Andrei Seluanov, Ying Jiang, and Vera Gorbunova. “TRF2 Is Required for Repair of Nontelomeric DNA Double-Strand Breaks by Homologous Recombination.” *Proceedings of the National Academy of Sciences* 104, no. 32 (August 7, 2007): 13068–73. https://doi.org/10.1073/pnas.0702410104.

Masamsetti, V. Pragathi, Ronnie Ren Jie Low, Ka Sin Mak, Aisling O’Connor, Chris D. Riffkin, Noa Lamm, Laure Crabbe, et al. “Replication Stress Induces Mitotic Death through Parallel Pathways Regulated by WAPL and Telomere Deprotection.” *Nature Communications* 10, no. 1 (September 17, 2019): 4224. https://doi.org/10.1038/s41467-019-12255-w.

Mendez-Bermudez, Aaron, Alberto Hidalgo-Bravo, Victoria E. Cotton, Athanasia Gravani, Jennie N. Jeyapalan, and Nicola J. Royle. “The Roles of WRN and BLM RecQ

Helicases in the Alternative Lengthening of Telomeres." *Nucleic Acids Research* 40, no. 21 (November 2012): 10809–20. https://doi.org/10.1093/nar/gks862.

Mirdita, Milot, Konstantin Schütze, Yoshitaka Moriwaki, Lim Heo, Sergey Ovchinnikov, and Martin Steinegger. "ColabFold: Making Protein Folding Accessible to All." *Nature Methods* 19, no. 6 (June 2022): 679–82. https://doi.org/10.1038/s41592-022-01488-1.

Mishra, Rakesh, Cody L. Hoop, Ravindra Kodali, Bankanidhi Sahoo, Patrick C. A. van der Wel, and Ronald Wetzel. "Serine Phosphorylation Suppresses Huntingtin Amyloid Accumulation by Altering Protein Aggregation Properties." *Journal of Molecular Biology* 424, no. 1–2 (November 23, 2012): 1–14. https://doi.org/10.1016/j.jmb.2012.09.011.

Mohaghegh, Payam, Julia K. Karow, Robert M. Brosh Jr, Vilhelm A. Bohr, and Ian D. Hickson. "The Bloom's and Werner's Syndrome Proteins Are DNA Structure-Specific Helicases." *Nucleic Acids Research* 29, no. 13 (July 1, 2001): 2843–49.

Moles, R., X. T. Bai, H. Chaib-Mezrag, and C. Nicot. "WRN-Targeted Therapy Using Inhibitors NSC 19630 and NSC 617145 Induce Apoptosis in HTLV-1-Transformed Adult T-Cell Leukemia Cells." *Journal of Hematology & Oncology* 9 (November 9, 2016): 121. https://doi.org/10.1186/s13045-016-0352-4.

Moyzis, R. K., J. M. Buckingham, L. S. Cram, M. Dani, L. L. Deaven, M. D. Jones, J. Meyne, R. L. Ratliff, and J. R. Wu. "A Highly Conserved Repetitive DNA Sequence, (TTAGGG)n, Present at the Telomeres of Human Chromosomes." *Proceedings of the National Academy of Sciences of the United States of America* 85, no. 18 (September 1988): 6622–26. https://doi.org/10.1073/pnas.85.18.6622.

Muftuoglu, Meltem, Tomasz Kulikowicz, Gad Beck, Jae Wan Lee, Jason Piotrowski, and Vilhelm A. Bohr. "Intrinsic SsDNA Annealing Activity in the C-Terminal Region of WRN." *Biochemistry* 47, no. 39 (September 30, 2008): 10247–54. https://doi.org/10.1021/bi800807n.

Mushegian, A. R., D. E. Bassett, M. S. Boguski, P. Bork, and E. V. Koonin. "Positionally Cloned Human Disease Genes: Patterns of Evolutionary Conservation and Functional Motifs." *Proceedings of the National Academy of Sciences of the United States of America* 94, no. 11 (May 27, 1997): 5831–36. https://doi.org/10.1073/pnas.94.11.5831.

Myler, Logan R., Charles G. Kinzig, Nanda K. Sasi, George Zakusilo, Sarah W. Cai, and Titia de Lange. “The Evolution of Metazoan Shelterin.” *Genes & Development* 35, no. 23–24 (December 1, 2021): 1625–41. https://doi.org/10.1101/gad.348835.121.

Nassour, Joe, Lucia Gutierrez Aguiar, Adriana Correia, Tobias T. Schmidt, Laura Mainz, Sara Przetocka, Candy Haggblom, et al. “Telomere-to-Mitochondria Signalling by ZBP1 Mediates Replicative Crisis.” *Nature* 614, no. 7949 (February 2023): 767–73. https://doi.org/10.1038/s41586-023-05710-8.

Nassour, Joe, Robert Radford, Adriana Correia, Javier Miralles Fusté, Brigitte Schoell, Anna Jauch, Reuben J. Shaw, and Jan Karlseder. “Autophagic Cell Death Restricts Chromosomal Instability during Replicative Crisis.” *Nature* 565, no. 7741 (January 2019): 659–63. https://doi.org/10.1038/s41586-019-0885-0.

Necasová, Ivona, Eliška Janoušková, Tomáš Klumpler, and Ctirad Hofr. “Basic Domain of Telomere Guardian TRF2 Reduces D-Loop Unwinding Whereas Rap1 Restores It.” *Nucleic Acids Research* 45, no. 21 (December 1, 2017): 12170–80. https://doi.org/10.1093/nar/gkx812.

Newman, Joseph A., Pavel Savitsky, Charles K. Allerston, Anna H. Bizard, Özgün Özer, Kata Sarlós, Ying Liu, et al. “Crystal Structure of the Bloom’s Syndrome Helicase Indicates a Role for the HRDC Domain in Conformational Changes.” *Nucleic Acids Research* 43, no. 10 (May 26, 2015): 5221–35. https://doi.org/10.1093/nar/gkv373.

Nora, Gerald J., Noah A. Buncher, and Patricia L. Opresko. “Telomeric Protein TRF2 Protects Holliday Junctions with Telomeric Arms from Displacement by the Werner Syndrome Helicase.” *Nucleic Acids Research* 38, no. 12 (July 2010): 3984–98. https://doi.org/10.1093/nar/gkq144.

Okamoto, Keiji, and Yoichi Shinkai. “TRFH Domain Is Critical for TRF1-Mediated Telomere Stabilization.” *Cell Structure and Function* 34, no. 2 (2009): 71–76. https://doi.org/10.1247/csf.09007.

Olovnikov, A. M. “A Theory of Marginotomy. The Incomplete Copying of Template Margin in Enzymic Synthesis of Polynucleotides and Biological Significance of the Phenomenon.” *Journal of Theoretical Biology* 41, no. 1 (September 14, 1973): 181–90. https://doi.org/10.1016/0022-5193(73)90198-7.

Opresko, Patricia L., Cayetano von Kobbe, Jean-Philippe Laine, Jeanine Harrigan, Ian D. Hickson, and Vilhelm A. Bohr. “Telomere-Binding Protein TRF2 Binds to and Stimulates the Werner and Bloom Syndrome Helicases.” *The Journal of Biological Chemistry* 277, no. 43 (October 25, 2002): 41110–19. https://doi.org/10.1074/jbc.M205396200.

Opresko, Patricia L., Marit Otterlei, Jesper Graakjaer, Per Bruheim, Lale Dawut, Steen Kølvraa, Alfred May, Michael M. Seidman, and Vilhem A. Bohr. “The Werner Syndrome Helicase and Exonuclease Cooperate to Resolve Telomeric D Loops in a Manner Regulated by TRF1 and TRF2.” *Molecular Cell* 14, no. 6 (June 18, 2004): 763–74. https://doi.org/10.1016/j.molcel.2004.05.023.

Orren, David K., Shaji Theodore, and Amrita Machwe. “The Werner Syndrome Helicase/Exonuclease (WRN) Disrupts and Degrades D-Loops in Vitro.” *Biochemistry* 41, no. 46 (November 19, 2002): 13483–88. https://doi.org/10.1021/bi0266986.

Orth, James D., Alexander Loewer, Galit Lahav, and Timothy J. Mitchison. “Prolonged Mitotic Arrest Triggers Partial Activation of Apoptosis, Resulting in DNA Damage and P53 Induction.” *Molecular Biology of the Cell* 23, no. 4 (February 15, 2012): 567–76. https://doi.org/10.1091/mbc.E11-09-0781.

Oshima, Junko, Julia M. Sidorova, and Raymond J. Monnat. “Werner Syndrome: Clinical Features, Pathogenesis and Potential Therapeutic Interventions.” *Ageing Research Reviews* 33 (January 2017): 105–14. https://doi.org/10.1016/j.arr.2016.03.002.

Ozturk, Saffet, Berna Sozen, and Necdet Demir. “Telomere Length and Telomerase Activity during Oocyte Maturation and Early Embryo Development in Mammalian Species.” *Molecular Human Reproduction* 20, no. 1 (January 2014): 15–30. https://doi.org/10.1093/molehr/gat055.

Pearce, Emily E., Rotana Alsaggaf, Shilpa Katta, Casey Dagnall, Geraldine Aubert, Belynda D. Hicks, Stephen R. Spellman, Sharon A. Savage, Steve Horvath, and Shahinaz M. Gadalla. “Telomere Length and Epigenetic Clocks as Markers of Cellular Aging: A Comparative Study.” *GeroScience* 44, no. 3 (May 18, 2022): 1861–69. https://doi.org/10.1007/s11357-022-00586-4.

Perry, J. Jefferson P., Steven M. Yannone, Lauren G. Holden, Chiharu Hitomi, Aroumougame Asaithamby, Seungil Han, Priscilla K. Cooper, David J. Chen, and John A. Tainer. “WRN Exonuclease Structure and Molecular Mechanism Imply an Editing Role in DNA End Processing.” *Nature Structural & Molecular Biology* 13, no. 5 (May 2006): 414–22. https://doi.org/10.1038/nsmb1088.

Peters, Jan-Michael. “The Anaphase Promoting Complex/Cyclosome: A Machine Designed to Destroy.” *Nature Reviews Molecular Cell Biology* 7, no. 9 (September 2006): 644–56. https://doi.org/10.1038/nrm1988.

Poulet, Anaïs, Sabrina Pisano, Cendrine Faivre-Moskalenko, Bei Pei, Yannick Tauran, Zofia Haftek-Terreau, Frédéric Brunet, et al. “The N-Terminal Domains of TRF1 and TRF2 Regulate Their Ability to Condense Telomeric DNA.” *Nucleic Acids Research* 40, no. 6 (March 2012): 2566–76. https://doi.org/10.1093/nar/gkr1116.

Prince, P. R., M. J. Emond, and R. J. Monnat. “Loss of Werner Syndrome Protein Function Promotes Aberrant Mitotic Recombination.” *Genes & Development* 15, no. 8 (April 15, 2001): 933–38. https://doi.org/10.1101/gad.877001.

Reaper, Philip M., Fabrizio d’Adda di Fagagna, and Stephen P. Jackson. “Activation of the DNA Damage Response by Telomere Attrition: A Passage to Cellular Senescence.” *Cell Cycle (Georgetown, Tex.)* 3, no. 5 (May 2004): 543–46.

Rodier, Francis, Sahn-Ho Kim, Tarlochan Nijjar, Paul Yaswen, and Judith Campisi. “Cancer and Aging: The Importance of Telomeres in Genome Maintenance.” *The International Journal of Biochemistry & Cell Biology* 37, no. 5 (May 2005): 977–90. https://doi.org/10.1016/j.biocel.2004.10.012.

Romero-Zamora, Diana, and Makoto T. Hayashi. “A Non-Catalytic N-Terminus Domain of WRN Prevents Mitotic Telomere Deprotection.” *Scientific Reports* 13, no. 1 (January 12, 2023): 645. https://doi.org/10.1038/s41598-023-27598-0.

Samanta, Saheli, and Parimal Karmakar. “Recruitment of HRDC Domain of WRN and BLM to the Sites of DNA Damage Induced by Mitomycin C and Methyl Methanesulfonate.” *Cell Biology International* 36, no. 10 (October 1, 2012): 873–81. https://doi.org/10.1042/CBI20110510.

Sampathi, Shilpa, and Weihang Chai. “Telomere Replication: Poised but Puzzling.” *Journal of Cellular and Molecular Medicine* 15, no. 1 (January 2011): 3–13. https://doi.org/10.1111/j.1582-4934.2010.01220.x.

Sarek, Grzegorz, Panagiotis Kotsantis, Phil Ruis, David Van Ly, Pol Margalef, Valerie Borel, Xiao-Feng Zheng, et al. “CDK Phosphorylation of TRF2 Controls T-Loop Dynamics during the Cell Cycle.” *Nature* 575, no. 7783 (November 2019): 523–27. https://doi.org/10.1038/s41586-019-1744-8.

Schmutz, Isabelle, Leonid Timashev, Wei Xie, Dinshaw J. Patel, and Titia de Lange. “TRF2 Binds Branched DNA to Safeguard Telomere Integrity.” *Nature Structural & Molecular Biology* 24, no. 9 (September 2017): 734–42. https://doi.org/10.1038/nsmb.3451.

Shay, J. W., W. E. Wright, and H. Werbin. “Defining the Molecular Mechanisms of Human Cell Immortalization.” *Biochimica Et Biophysica Acta* 1072, no. 1 (April 16, 1991): 1–7. https://doi.org/10.1016/0304-419x(91)90003-4.

Shay, J. W., W. E. Wright, D. Brasiskyte, and B. A. Van der Haegen. “E6 of Human Papillomavirus Type 16 Can Overcome the M1 Stage of Immortalization in Human Mammary Epithelial Cells but Not in Human Fibroblasts.” *Oncogene* 8, no. 6 (June 1993): 1407–13.

Sherr, Charles J., and Frank McCormick. “The RB and P53 Pathways in Cancer.” *Cancer Cell* 2, no. 2 (August 2002): 103–12. https://doi.org/10.1016/s1535-6108(02)00102-2.

Shin, Soochul, Kwangbeom Hyun, Jinwoo Lee, Dongwon Joo, Tomasz Kulikowicz, Vilhelm A. Bohr, Jaehoon Kim, and Sungchul Hohng. “Werner Syndrome Protein Works as a Dimer for Unwinding and Replication Fork Regression.” *Nucleic Acids Research* 51, no. 1 (January 11, 2023): 337–48. https://doi.org/10.1093/nar/gkac1200.

Shiromizu, Takashi, Jun Adachi, Shio Watanabe, Tatsuo Murakami, Takahisa Kuga, Satoshi Muraoka, and Takeshi Tomonaga. “Identification of Missing Proteins in the NeXtProt Database and Unregistered Phosphopeptides in the PhosphoSitePlus Database as Part of the Chromosome-Centric Human Proteome Project.” *Journal of Proteome Research* 12, no. 6 (June 7, 2013): 2414–21. https://doi.org/10.1021/pr300825v.

Sommers, Joshua A., Sudha Sharma, Kevin M. Doherty, Parimal Karmakar, Qin Yang, Mark K. Kenny, Curtis C. Harris, and Robert M. Brosh. “P53 Modulates RPA-Dependent and RPA-Independent WRN Helicase Activity.” *Cancer Research* 65, no. 4 (February 15, 2005): 1223–33. https://doi.org/10.1158/0008-5472.CAN-03-0231.

Su, Fengtao, Shibani Mukherjee, Yanyong Yang, Eiichiro Mori, Souparno Bhattacharya, Junya Kobayashi, Steven M. Yannone, David J. Chen, and Aroumougame Asaithamby. “Non-Enzymatic Role for WRN in Preserving Nascent DNA Strands after Replication Stress.” *Cell Reports* 9, no. 4 (November 20, 2014): 1387–1401. https://doi.org/10.1016/j.celrep.2014.10.025.

Sun, Luxi, Satoshi Nakajima, Yaqun Teng, Hao Chen, Lu Yang, Xiukai Chen, Boya Gao, Arthur S. Levine, and Li Lan. “WRN Is Recruited to Damaged Telomeres via Its RQC Domain and Tankyrase1-Mediated Poly-ADP-Ribosylation of TRF1.” *Nucleic Acids Research* 45, no. 7 (April 20, 2017): 3844–59. https://doi.org/10.1093/nar/gkx065.

Swan, Michael K., Valerie Legris, Adam Tanner, Philip M. Reaper, Sarah Vial, Rebecca Bordas, John R. Pollard, Peter A. Charlton, Julian M. C. Golec, and Jay A. Bertrand. “Structure of Human Bloom’s Syndrome Helicase in Complex with ADP and Duplex DNA.” *Acta Crystallographica. Section D, Biological Crystallography* 70, no. Pt 5 (May 2014): 1465–75. https://doi.org/10.1107/S139900471400501X.

Szilák, L., J. Moitra, D. Krylov, and C. Vinson. “Phosphorylation Destabilizes Alpha-Helices.” *Nature Structural Biology* 4, no. 2 (February 1997): 112–14. https://doi.org/10.1038/nsb0297-112.

Takai, Hiroyuki, Agata Smogorzewska, and Titia de Lange. “DNA Damage Foci at Dysfunctional Telomeres.” *Current Biology: CB* 13, no. 17 (September 2, 2003): 1549–56. https://doi.org/10.1016/s0960-9822(03)00542-6.

Teng, Fang-Yuan, Ting-Ting Wang, Hai-Lei Guo, Ben-Ge Xin, Bo Sun, Shuo-Xing Dou, Xu-Guang Xi, and Xi-Miao Hou. “The HRDC Domain Oppositely Modulates the Unwinding Activity of E. Coli RecQ Helicase on Duplex DNA and G-Quadruplex.” *The Journal of Biological Chemistry* 295, no. 51 (December 18, 2020): 17646–58. https://doi.org/10.1074/jbc.RA120.015492.

Timashev LA, De Lange T. “Characterization of t-loop formation by TRF2”. *Nucleus*. (December 2020); 11(1):164-177. https://doi.org/10.1080/19491034.2020.1783782.

Tomaska, Lubomir, Jozef Nosek, Anirban Kar, Smaranda Willcox, and Jack D. Griffith. “A New View of the T-Loop Junction: Implications for Self-Primed Telomere Extension, Expansion of Disease-Related Nucleotide Repeat Blocks, and Telomere Evolution.” *Frontiers in Genetics* 10 (2019). https://www.frontiersin.org/articles/10.3389/fgene.2019.00792.

Traversi, Gianandrea, David Sasah Staid, Mario Fiore, Zulema Percario, Daniela Trisciuoglio, Roberto Antonioletti, Veronica Morea, Francesca Degrassi, and Renata Cozzi. “A Novel Resveratrol Derivative Induces Mitotic Arrest, Centrosome Fragmentation and Cancer Cell Death by Inhibiting γ-Tubulin.” *Cell Division* 14, no. 1 (April 10, 2019): 3. https://doi.org/10.1186/s13008-019-0046-8.

Tripathi, Vivek, Sarabpreet Kaur, and Sagar Sengupta. “Phosphorylation-Dependent Interactions of BLM and 53BP1 Are Required for Their Anti-Recombinogenic Roles during Homologous Recombination.” *Carcinogenesis* 29, no. 1 (January 2008): 52–61. https://doi.org/10.1093/carcin/bgm238.

Van Ly, David, Ronnie Ren Jie Low, Sonja Frölich, Tara K. Bartolec, Georgia R. Kafer, Hilda A. Pickett, Katharina Gaus, and Anthony J. Cesare. “Telomere Loop Dynamics in Chromosome End Protection.” *Molecular Cell* 71, no. 4 (August 16, 2018): 510-525.e6. https://doi.org/10.1016/j.molcel.2018.06.025.

Verdun, Ramiro E., and Jan Karlseder. “The DNA Damage Machinery and Homologous Recombination Pathway Act Consecutively to Protect Human Telomeres.” *Cell* 127, no. 4 (November 17, 2006): 709–20. https://doi.org/10.1016/j.cell.2006.09.034.

Vindigni, Alessandro, and Ian D. Hickson. “RecQ Helicases: Multiple Structures for Multiple Functions?” *HFSP Journal* 3, no. 3 (June 2009): 153–64. https://doi.org/10.2976/1.3079540.

Wang, Jiadong, Junjie Chen, and Zihua Gong. “TopBP1 Controls BLM Protein Level to Maintain Genome Stability.” *Molecular Cell* 52, no. 5 (December 12, 2013): 10.1016/j.molcel.2013.10.012. https://doi.org/10.1016/j.molcel.2013.10.012.

Watanabe, S, T Kanda, and K Yoshiike. “Human Papillomavirus Type 16 Transformation of Primary Human Embryonic Fibroblasts Requires Expression of Open Reading Frames E6 and E7.” *Journal of Virology* 63, no. 2 (February 1989): 965–69.

Watson, J. D. “Origin of Concatemeric T7 DNA.” *Nature: New Biology* 239, no. 94 (October 18, 1972): 197–201. https://doi.org/10.1038/newbio239197a0.

Weinrich, S. L., R. Pruzan, L. Ma, M. Ouellette, V. M. Tesmer, S. E. Holt, A. G. Bodnar, et al. “Reconstitution of Human Telomerase with the Template RNA Component HTR and the Catalytic Protein Subunit HTRT.” *Nature Genetics* 17, no. 4 (December 1997): 498–502. https://doi.org/10.1038/ng1297-498.

Wright, W. E., and J. W. Shay. “The Two-Stage Mechanism Controlling Cellular Senescence and Immortalization.” *Experimental Gerontology* 27, no. 4 (1992): 383–89. https://doi.org/10.1016/0531-5565(92)90069-c.

Wu, Yuliang. “Unwinding and Rewinding: Double Faces of Helicase?” *Journal of Nucleic Acids* 2012 (2012): 140601. https://doi.org/10.1155/2012/140601.

Xu, Lifeng, Shang Li, and Bradley A. Stohr. “The Role of Telomere Biology in Cancer.” *Annual Review of Pathology: Mechanisms of Disease* 8, no. 1 (2013): 49–78. https://doi.org/10.1146/annurev-pathol-020712-164030.

Xue, Yu, Glenn C. Ratcliff, Hong Wang, Paula R. Davis-Searles, Matthew D. Gray, Dorothy A. Erie, and Matthew R. Redinbo. “A Minimal Exonuclease Domain of WRN Forms a Hexamer on DNA and Possesses Both 3’- 5’ Exonuclease and 5’-Protruding Strand Endonuclease Activities.” *Biochemistry* 41, no. 9 (March 5, 2002): 2901–12. https://doi.org/10.1021/bi0157161.

Yang, Zhe, Keshav Sharma, and Titia de Lange. “TRF1 Uses a Noncanonical Function of TFIIH to Promote Telomere Replication.” *Genes & Development* 36, no. 17–18 (September 1, 2022): 956–69. https://doi.org/10.1101/gad.349975.122.

Yasui, Yoshihiro, Takeshi Urano, Aie Kawajiri, Koh-ichi Nagata, Masaaki Tatsuka, Hideyuki Saya, Koichi Furukawa, Toshitada Takahashi, Ichiro Izawa, and Masaki Inagaki. “Autophosphorylation of a Newly Identified Site of Aurora-B Is Indispensable for Cytokinesis.” *The Journal of Biological Chemistry* 279, no. 13 (March 26, 2004): 12997–3. https://doi.org/10.1074/jbc.M311128200.